

Kinetics and Thermodynamics of (1+2) Cycloadditions of Transient  
Diphenylgermylene with Alkenes

Kinetics and Thermodynamics of (1+2) Cycloadditions of Transient  
Diphenylgermylene with Alkenes

By

Yaser Saeidi Hayeniaz, M.Sc.

A Thesis

Submitted to the School of Graduate Studies

In Partial Fulfillment of the Requirements

for the Degree

Master of Science

McMaster University

© Yaser Saeidi Hayeniaz, August 2012

Master of Science (2012)  
(Chemistry)

McMaster University  
Hamilton, Ontario

TITLE: Kinetics and Thermodynamics of (1+2) Cycloadditions  
of Transient Diphenylgermylene with Alkenes

AUTHOR: Yaser Saeidi Hayeniaz, M.Sc  
Kharazmi University, Tehran, Iran

SUPERVISOR: Professor William. J. Leigh

NUMBER OF PAGES: xvii, 98

## Abstract

1,1-Dimethyl-3-phenyl-1-germacyclopent-3-ene (**32**) was synthesized and it was used for the study of the reactivity of diphenylgermylene ( $\text{GePh}_2$ ) toward alkenes using steady state and nanosecond laser flash photolysis technique (nLFP) in hexanes solution.

The reactivity of  $\text{GePh}_2$  toward several alkenes including 1-hexene, cis-2-hexene, trans-3-hexene, cyclopentene, cyclohexene, cis-cyclooctene, methylcyclohexene, 2-methyl-2-pentene, 2-methyl-1-pentene and trans-3-methyl-2-pentene has been investigated by nLFP method. In all cases, the equilibrium constant was measured and it was found that there is a direct correlation between the Gibbs free energy of the reaction ( $\Delta G_r$ ) and the ionization potential (IP) of the involved alkene. This indicates that alkenes with higher IP, electron poor alkenes, should lead to more stable germiranes and consequently installation of electron withdrawing groups on alkenes should stabilize the resulting germirane. This is the first time such a quantitative predictor is reported.

Steady state photolysis methods have been used to investigate same aspects of germirane reactivity. Photolysis of **32** in the presence of acrylonitrile and methanol in one experiment, and 3,3-dimethyl-1-pentene and methanol in another experiment, has provided more evidence for the presence of the corresponding germiranes which were trapped by methanol.

Finally, the (1+2) cycloaddition reactions of  $\text{GeH}_2$ ,  $\text{GeMe}_2$  and  $\text{GePh}_2$  with a selection of alkenes were investigated computationally using different DFT methods and 6-311+G(d,p) as the basis set. The results show that the reaction becomes less exergonic

moving from  $\text{GeH}_2$  to  $\text{GeMe}_2$  and then to  $\text{GePh}_2$ . In addition, plots of calculated  $\Delta G_r$  against the experimental IP of the involved alkene reproduced the observed experimental correlation from the laser studies. It was also concluded that  $\omega\text{B97XD}$  and  $\text{mPW1PW91}$  are the most reliable of the DFT methods that were investigated.

## **Acknowledgments**

Deciding to attend graduate studies 10000 km away from home in another country was a very difficult decision. Since I have arrived in Hamilton, I have been through an amazing journey and I feel quite lucky to get the chance of doing my graduate studies at McMaster University. There are many people who have made work pleasant over the past two years and this thesis would not have been possible without them.

First and foremost, I owe my most sincere gratitude to my supervisor, Professor William. J. Leigh, for his support, guidance and kindness through my Master studies. I am also very grateful to my supervisory committee member, Dr Vargas-Baca, who has helped me with his suggestions and insightful comments.

I would like to thank the chemistry staff who made research in McMaster University much easier and enjoyable.

I also thank all past and present members of WJL group that I have worked with, especially Ian Duffy and Svetlana Kostina.

Finally, I would like to express my deepest gratitude to my wonderful parents, Ahmad and Saba Saeidi Hayeniaz, who I dedicate this thesis to. They have done nothing but loving and supporting me through all difficult times, even with a 10000 km geographical separation.

## Table of Contents

<u>Abstract</u> .....	iv
<u>Acknowledgments</u> .....	vi
List of Figures .....	xi
List of Tables.....	xvi
Chapter 1 - Introduction .....	1
1.1. Thesis Overview .....	1
1.2. Nomenclature .....	1
1.3. Electronic Structure and Thermodynamics of Germylenes.....	2
1.4. Generation of Germylenes.....	5
1.4.1. Thermal Generation of Germylenes .....	5
1.4.2. Photolytic Generation of Germylenes .....	5
1.5. Germylene Reactivity .....	7
1.5.1. Insertion into OH Bonds.....	8
1.5.2. (1+4) Cycloaddition Reactions.....	10
1.5.3. (1+2) Cycloaddition.....	12
1.6. Stability of Metalliranes, Steric vs. Electronic Effects .....	15
1.7. Previous Studies of the Reaction of GePh <sub>2</sub> with alkenes in Dr. Leigh's group .....	16
1.8. Applications of Metallylene Chemistry .....	18

1.9. Goals of This Work .....	19
1.10. References .....	20
Chapter 2 – Reaction of Diphenylgermylene with Alkenes .....	24
2.1 Overview.....	24
2.2 Kinetic Measurements by Laser Flash Photolysis .....	25
2.2.1 Photochemistry of Precursor .....	25
2.2.2. Transient UV-Vis Absorption Spectra of the Precursor.....	25
2.2.3. Data Analysis.....	27
2.2.4. Alkenes for Study .....	29
2.2.5. Results.....	29
2.2.6. Discussion .....	37
2.3. Steady-State Photolysis Studies of the Reactions of GePh <sub>2</sub> with Acrylonitrile and 4,4-Dimethyl-1-Pentene (DMP) .....	40
2.3.1. Overview.....	40
2.3.2. Steady-State Photolysis Study of the Reaction of GePh <sub>2</sub> with Acrylonitrile .....	44
2.3.4. Steady-State Photolysis Studies of the Reaction of GePh <sub>2</sub> with Acrylonitrile in the Presence of Methanol.....	47
2.3.5. Steady-State Photolysis Studies of the Reaction of GePh <sub>2</sub> with 4,4- Dimethyl-1-Pentene (DMP) in the Presence of Methanol (MeOH) .....	55
2.3.6. Conclusion.....	62



2.3.7. References .....	63
Chapter 3 – Computational Studies of the Reaction of Germylenes with Alkenes.....	65
3.1 Introduction.....	65
3.2 General Method.....	66
3.3. Geometry Optimization and Thermochemistry .....	66
3.4. Discussion .....	75
3.5. Summary .....	81
3.6. References: .....	81
Chapter 4 –Future Direction.....	82
References .....	84
Chapter 5 - Experimental .....	85
5.1. Synthesis .....	85
5.1.1. Chemicals.....	85
5.1.2. Solvents.....	85
5.1.3. Equipment .....	86
5.1.4. Synthesis of 3,4-dimethyl-1,1-diphenyl-1-germacyclopent-3-ene (32).....	86
5.1.5. Synthesis of 1,1-dimethyl-3-phenyl-1-germacyclopent-3-ene (61) : .....	88
5.2. Nanosecond Laser Flash Photolysis (LFP):.....	93
5.2.1. Chemicals.....	93

5.2.2. System Design .....	93
5.2.3. Experimental Set up for the Determination of Rate/Equilibrium Constants .....	95
5.3. Steady State Photolysis Experiments.....	97
5.3.1. Chemicals.....	97
5.3.2. General Procedure .....	98
5.4. References .....	98

## List of Figures

- Figure 1.1.** General scheme of singlet and triplet states of divalent Group 14 compounds. **2**
- Figure 1.2.** Gibbs free energy of reaction vs Ionization potential of alkenes from the photolysis of **32** in the presence of different alkenes (S.S.Chitnis, unpublished). **17**
- Figure 2.1.** Transient absorption spectra recorded 480-1120 ns (○) and 8.32-9.28 μs (●) after the laser pulse, by laser flash photolysis of a solution of **32** in deoxygenated, anhydrous hexanes; the inset shows transient growth/decay profiles recorded at 440 and 500 nm, with the time windows represented by the two spectra indicated by solid bars. **26**
- Figure 2.2.** (a) Plot of  $k_{\text{decay}}$  vs concentration of 1-hexene from laser flash photolysis of a deoxygenated solution of compound **32** in the presence of 1-hexene (b) plot of  $\Delta A_0/\Delta A_{\text{res}}$  vs concentration of 1-hexene from the same experiment. **30**
- Figure 2.3.** Corrected transient decay traces recorded at 500 nm by laser flash photolysis of a deoxygenated hexanes solution of compound **32** in the presence of various concentrations of 1-hexene. at 25 °C. **30**
- Figure 2.4.** (a) Corrected transient decay traces recorded at 500 nm by laser flash photolysis of a deoxygenated hexanes solution of compound **32** in the presence of various concentrations of cyclohexene at 25 °C; (b) plot of  $\Delta A_0/\Delta A_{\text{res}}$  vs concentration of cyclohexene from the same experiment. Error is reported as  $\pm 2\sigma$ . **31**
- Figure 2.5.** Corrected transient decay traces recorded at 500 nm by laser flash photolysis of a deoxygenated hexanes solution of compound **32** in the presence of various concentrations of methylcyclohexene at 25 °C; (b) plot of  $\Delta A_0/\Delta A_{\text{res}}$  vs concentration of methylcyclohexene from the same experiment. Error is reported as  $\pm 2\sigma$ . **32**
- Figure 2.6.** (a) Corrected transient decay traces recorded at 500 nm by laser flash photolysis of a deoxygenated hexanes solution of compound **32** in the presence of various concentrations of 2-methyl-2-pentene at 25 °C; (b) plot of  $\Delta A_0/\Delta A_{\text{res}}$  vs concentration of 2-methyl-2-pentene from the same experiment. Error is reported as  $\pm 2\sigma$ . **32**
- Figure 2.7.** (a) Corrected transient decay traces recorded at 500 nm by laser flash photolysis of a deoxygenated hexanes solution of compound **32** in the presence of various concentrations of cyclopentene at 25 °C; (b) plot of  $\Delta A_0/\Delta A_{\text{res}}$  vs concentration of cyclopentene from the same experiment. Error is reported as  $\pm 2\sigma$ . **33**

**Figure 2.8.** (a) Corrected transient decay traces recorded at 500 nm by laser flash photolysis of a deoxygenated hexanes solution of compound **32** in the presence of various concentrations of cis-cyclooctene at 25 °C; (b) plot of  $\Delta A_0/\Delta A_{res}$  vs concentration of cis-cyclooctene from the same experiment. Error is reported as  $\pm 2\sigma$ . 33

**Figure 2.9.** (a) Corrected transient decay traces recorded at 500 nm by laser flash photolysis of a deoxygenated hexanes solution of compound **32** in the presence of various concentrations of cis-2-hexene at 25 °C; (b) plot of  $\Delta A_0/\Delta A_{res}$  vs concentration of cis-2-hexene from the same experiment. Error is reported as  $\pm 2\sigma$ . 34

**Figure 2.10.** (a) Corrected transient decay traces recorded at 500 nm by laser flash photolysis of a deoxygenated hexanes solution of compound **32** in the presence of various concentrations of trans-3-hexene at 25 °C; (b) plot of  $\Delta A_0/\Delta A_{res}$  vs concentration of trans-3-hexene from the same experiment. Error is reported as  $\pm 2\sigma$ . 34

**Figure 2.11.** (a) Corrected transient decay traces recorded at 500nm by laser flash photolysis of a deoxygenated hexanes solution of compound **32** in the presence of various concentrations of 2-methyl-1-pentene at 25 °C; (b) plot of  $\Delta A_0/\Delta A_{res}$  vs concentration of 2-methyl-1-pentene from the same experiment. Error is reported as  $\pm 2\sigma$ . 35

**Figure 2.12.** (a) Corrected transient decay traces recorded at 500 nm by laser flash photolysis of a deoxygenated hexanes solution of compound **32** in the presence of various concentrations of trans-3-methyl-2-pentene at 25 °C; (b) plot of  $\Delta A_0/\Delta A_{res}$  vs concentration of trans-3-methyl-2-pentene from the same experiment. Error is reported as  $\pm 2\sigma$ . 35

**Figure 2.13.** Gibbs free energy of reaction vs ionization potential of alkenes from the photolysis of **32** in the presence of different alkenes (Table 2.1 in addition to unpublished results of S.S.Chitnis). 39

**Figure 2.14.** (a) Transient decay traces recorded at 500 nm by laser flash photolysis of a deoxygenated hexanes solution of compound **32** in the presence of various concentrations of acrylonitrile at 25 °C (b) Plot of  $k_{decay}$  vs concentration of acrylonitrile from the same experiment. Error is reported as  $\pm 2\sigma$ . 41

**Figure 2.15.** (a) Transient UV-vis absorption spectra recorded with a ca. 0.003 M solution of **32** in deoxygenated hexanes containing 3.0 mM acrylonitrile, 170-176 ns (○), 1.71-1.73  $\mu$ s (□) after the laser pulse; the inset shows absorbance-time profiles recorded at 300, 440, and 500 nm. (S. S. Chitnis; unpublished) (b) Transient absorption spectra recorded 130-200 ns(○) and 3.38-4.38  $\mu$ s(●) after the laser pulse, by laser flash photolysis of **32** in deoxygenated, anhydrous hexanes containing 40 mM butyronitrile,; the inset shows transient growth/decay profiles recorded at 340 and 440 nm. (S. S. Chitnis; unpublished). 41

- Figure 2.16.** (a) Transient absorption spectra recorded 320-576 ns( $\circ$ ) and 8.77-9.15  $\mu$ s( $\bullet$ ) after the laser pulse, by laser flash photolysis of a deoxygenated hexanes solution of 1,1-bis-(4-methylphenyl)-3,4-dimethyl-1-germacyclopent-3-ene; the inset shows transient growth/decay profiles recorded at 440 and 500 nm. (b) Transient absorption spectra recorded 208-272 ns( $\circ$ ) and 1.87-1.97  $\mu$ s( $\bullet$ ) after the laser pulse, by laser flash photolysis of a deoxygenated hexanes solution of 1,1-bis-(4-methylphenyl)-3,4-dimethyl-1-germacyclopent-3-ene containing 5.5 mM of acrylonitrile; the inset shows transient growth/decay profiles recorded at 300, 380 and 440 nm (offset). **43**
- Figure 2.17.** Photolysis of an argon-saturated cyclohexane-d<sub>12</sub> solution of **32** (0.055 M) with four low-pressure mercury lamps (254 nm) in the presence of acrylonitrile (0.087 M) (A) before irradiation (B) after irradiation for 16 minutes. **46**
- Figure 2.18.** Concentration vs. time plot from irradiation of an argon-saturated cyclohexane-d<sub>12</sub> solution of the **32** (0.055 M) with four low-pressure mercury lamps in the presence of acrylonitrile (0.087 M). Precursor **32** ( $\circ$ ), slope:  $-0.00063 \pm 0.00004$ ; DMB ( $\Delta$ ), slope:  $+0.00085 \pm 0.00007$ ; Acrylonitrile ( $\square$ ), slope:  $-0.0048 \pm 0.0007$ . **47**
- Figure 2.19.** Photolysis of an argon-saturated cyclohexane-d<sub>12</sub> solution of **32** (0.05 M) with four low-pressure mercury lamps (254 nm) in the presence of acrylonitrile (0.07 M) and MeOH (0.02 M) a- before irradiation b-after 14 min irradiation. **49**
- Figure 2.20.** Concentration vs. time plot from irradiation of an argon-saturated cyclohexane-d<sub>12</sub> solution of **32** (0.05 M) with four low-pressure mercury lamps in the presence of acrylonitrile (0.07 M) and MeOH (0.02 M) after 14 min irradiation. **50**
- Figure 2.21.** Photolysis of an argon-saturated cyclohexane-d<sub>12</sub> solution of **32** (0.05 M) with four low-pressure mercury lamps (254 nm) in the presence of acrylonitrile (0.06 M) and MeOH (0.04 M). a- before irradiation; b-after 30 min irradiation; c- after leaving the sample for 48 hours in dark. **53**
- Figure 2.22.** Photolysis of an argon-saturated cyclohexane-d<sub>12</sub> solution of **32** (0.055 M) with four low-pressure mercury lamps (254 nm) in the presence of acrylonitrile (0.082 M) and MeOH (0.03 M). a- before irradiation; b-after 30 min irradiation; c- after removing volatile components. **55**
- Figure 2.23.** Photolysis of an argon-saturated cyclohexane-d<sub>12</sub> solution of **32** (0.058 M) with two low-pressure mercury lamps (254 nm) in the presence of DMP (0.49 M) and MeOH (0.024 M). a- before irradiation; b- after 24 min irradiation. **59**
- Figure 2.24.** Concentration versus. time plots from irradiation of an argon-saturated cyclohexane-d<sub>12</sub> solution of **32** (0.058 M) with two low-pressure mercury lamps in the presence of DMP (0.49 M) and MeOH (0.024M). **60**
- Figure 2.25.** Photolysis of an argon-saturated cyclohexane-d<sub>12</sub> solution of **32** **61**

(0.047 M) with two low-pressure mercury lamps (254 nm) in the presence of DMP (0.46 M) and MeOH (0.0078 M). a- before irradiation; b- after 24 min irradiation; c- after leaving the sample for 48 hours in dark d- after removing volatile components.

**Figure 2.26.** Concentration versus. time plots from irradiation of an argon-saturated cyclohexane-d<sub>12</sub> solution of **32** (0.047 M) with two low-pressure mercury lamps in the presence of DMP (0.46 M) and MeOH (0.0078M). **62**

**Figure 3.1.** Alkenes selected for the computational studies in this thesis. **68**

**Figure 3.2.** Germiranes studied computationally in this thesis. **68**

**Figure 3.3.** Structures of diphenylgermylene, 2-methyl-2-butene (**f**) and three germiranes resulting from (1+2) cycloaddition of GeH<sub>2</sub>, GeMe<sub>2</sub> and GePh<sub>2</sub> with alkene **f**. All the structures were optimized at the PBEPBE/6-311+G(d,p) level of theory. **69**

**Figure 3.4.** Calculated reaction Gibbs free energies employing three DFT methods versus the experimental ionization potential of the alkenes for the reaction of GeH<sub>2</sub> with alkenes **a**, **d** and **f** (Table 3.4). The 6-311G+(d,p) basis set was employed in all cases. **77**

**Figure 3.5.** Calculated reaction Gibbs free energies employing several DFT methods versus the experimental ionization potential of the examined alkenes for the reaction of GeMe<sub>2</sub> with alkenes **a**, **d** and **f** (Table 3.6). The 6-311G+(d,p) basis set was employed in all cases. **77**

**Figure 3.6.** Calculated reaction Gibbs free energies employing several DFT methods versus the experimental ionization potential of the examined alkenes for the reaction of GePh<sub>2</sub> with alkenes **a-g** (Table 3.9). The 6-31G+(d,p) basis set was employed in all cases. **78**

**Figure 3.7.** Calculated reaction Gibbs free energies using G4 and several DFT methods versus the experimental ionization potential of the examined alkenes for the reaction of GeMe<sub>2</sub> with alkenes (eq 3.1). The 6-311G+(d,p) basis set was employed in all cases. **79**

**Figure 3.8.** Comparison between experimental and calculated  $\Delta G^\circ$  of the reactions versus experimental ionization potential of the involved alkene on the reaction of GePh<sub>2</sub> with alkenes. The 6-311G+(d,p) basis set was employed in all cases. **80**

**Figure 5.1.** Overall scheme for the synthesis of 3,4-dimethyl-1,1-diphenyl-1-gemacyclopent-3-ene. **88**

**Figure 5.2.** Synthetic scheme for the synthesis of 1,1-dimethyl-3-phenyl-1- **92**

germacyclopent-3-ene.

**Figure 5.3.** nLFP system set up. **94**

**Figure 5.4.** UV-visible spectrum of a 0.2 M cyclohexene stock solution before and after purification by distillation over maleic anhydride and passing through a silica column. **97**

## List of Tables

<b>Table 1.1.</b> Common names of some Group 14 compounds.	<b>2</b>
<b>Table 1.2.</b> Calculated singlet-triplet energy gap ( $\Delta E_{ST}$ ) and Divalent state stabilization energies (DSSE) of $CH_2$ and parent metallylenes.	<b>4</b>
<b>Table 1.3.</b> Experimental equilibrium constants and Gibbs free energies of the reactions of $GePh_2$ with alkenes in deoxygenated hexane solution at 25 °C.	<b>18</b>
<b>Table 2.1.</b> Parameters from the laser experiment studies of the reaction of $GePh_2$ with alkenes <b>a-j</b> , including the concentration range of the alkenes used in the experiments and the absorbance of the alkene solution at 248 nm. Slope, Y-intercept and $r^2$ values are obtained from the linear regression analysis of the plots of $\Delta A_0/\Delta A_{res}$ versus concentration of alkene in each experiment.	<b>36</b>
<b>Table 2.2.</b> Experimental equilibrium constants and Gibbs free energy for the reactions of $GePh_2$ with alkenes in deoxygenated hexane solution at 25 °C along with the ionization potential of the involved alkene.	<b>37</b>
<b>Table 3.1.</b> Summary of selected bond lengths (Å) and angles (°) from the geometry optimized structures of alkenes <b>a-h</b> and their corresponding germiranes at the PBEPBE/6-311+G(d,p) level of theory.	<b>70</b>
<b>Table 3.2.</b> Summary of selected bond lengths (Å) and angles (°) from the geometry optimized structures of germylenes at the PBEPBE/6-311+G(d,p) level of theory. Numbers in parenthesis are from reference 2 (PW91/TZ2P/ZORA).	<b>70</b>
<b>Table 3.3.</b> Effect of DFT method on calculated structural parameters. Selected bond lengths (Å) and angles (°) from the geometry of three germiranes, optimized with different DFT methods using 6-311+G(d,p) basis set.	<b>71</b>
<b>Table 3.4.</b> Calculated reaction energies, zero-point corrected energies, enthalpies and Gibbs free energies of the (1+2) cycloaddition reaction of $GeH_2$ with alkenes <b>a, d</b> and <b>f</b> (eq 3.2) using the 6-311G+(d,p) basis set.	<b>72</b>
<b>Table 3.5.</b> Calculated reaction energies and zero-point corrected energies of the (1+2) cycloaddition reaction of $GeMe_2$ with alkenes <b>a, d</b> and <b>f</b> (eq 3.2) using the 6-311G+(d,p) basis set.	<b>72</b>
<b>Table 3.6.</b> Calculated reaction enthalpies and Gibbs free energies of the (1+2) cycloaddition reaction of $GeMe_2$ with alkenes <b>a, d</b> and <b>f</b> (eq 3.2) using the 6-311G+(d,p) basis set.	<b>73</b>



- Table 3.7.** Calculated reaction energies and zero-point corrected energies of the (1+2) cycloaddition reaction of  $\text{GePh}_2$  with alkenes **a-g** (eq 3.2) using the 6-311G+(d,p) basis set. **73**
- Table 3.8.** Calculated reaction enthalpies of the (1+2) cycloaddition reaction of  $\text{GePh}_2$  with alkenes **a-g** (eq 3.2) using the 6-311G+(d,p) basis set. **74**
- Table 3.9.** Calculated reaction Gibbs free energies of the (1+2) cycloaddition reaction of  $\text{GePh}_2$  with alkenes **a-g** (eq 3.2) using the 6-311G+(d,p) basis set. **74**
- Table 3.10.** Calculated reaction enthalpies and Gibbs free energies of the (1+2) cycloaddition reactions of  $\text{GeH}_2$ ,  $\text{GeMe}_2$  and  $\text{GePh}_2$  with alkenes **a**, **d** and **f** (eq 3.2) at the PBEPBE/6-311G+(d,p) level of theory. **76**

## Chapter 1 - Introduction

### 1.1. Thesis Overview

Germynes, the germanium analogues of carbenes, are typically short-lived reactive species having the general formula  $\text{GeR}_2$  (R = alkyl group, aryl group, halogen, hydrogen, etc). In the absence of a reactive substrate, they undergo dimerization to form digermenes of general formula  $\text{R}_2\text{Ge}=\text{GeR}_2$  which subsequently oligomerize when R is an unhindered substituent such as hydrogen or methyl.<sup>1</sup> In the presence of alkenes and alkynes however, cycloaddition reactions effectively compete with dimerization, forming the corresponding three membered germacycle (germirane).<sup>2</sup> The lifetimes of the germynes, digermenes and germiranes of interest to our group are within the range of microseconds to milliseconds, so a fast time-resolved spectroscopic technique needs to be employed in order to study their chemistry. This thesis presents the results of kinetic studies of the reaction of diphenylgermylene ( $\text{GePh}_2$ ) with various alkenes along with a computational investigation of this reaction. The results provide an experimental and computational predictor for the effect of alkene substitution on the stability of germiranes.

### 1.2. Nomenclature

The common name given to the Group 14 heavy analogues of carbenes ( $\text{MR}_2$ , M = Si, Ge, Sn) is metallylenes.<sup>3</sup> Similarly, the compounds containing carbon-metal and metal-metal double bonds,  $\text{R}_2\text{M}=\text{CR}_2$  and  $\text{R}_2\text{M}=\text{MR}_2$  (M = Si, Ge, Sn), are known as metallenes and dimetallenes respectively.<sup>4</sup> Another less common nomenclature for

Group 14 divalent M(II) compounds (M = Si, Ge, Sn) is tetrellylene,<sup>5,6</sup> which originated from the generic word for the Group 14 elements, tetrel.<sup>6</sup> Table 1.1. lists some common terms given to compounds incorporating the Group 14 elements.<sup>7</sup>

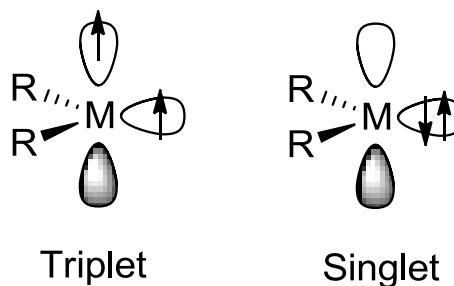
Table 1.1. Common names of some Group 14 compounds

M	Metallylene MR <sub>2</sub>	Metallene R <sub>2</sub> C=MR <sub>2</sub>	Dimetallene R <sub>2</sub> M=MR <sub>2</sub>	Metallane MR <sub>4</sub>
Si	Silylene	Silene	Disilene	Silane
Ge	Germylene	Germene	Digermene	Germane
Sn	Stannylene	Stannene	Distannene	Stannane

### 1.3. Electronic Structure and Thermodynamics of Germylenes

There are two possible ground-state electronic configurations for germylenes due to the existence of a non-bonding pair of electrons: the triplet (two nonbonding electrons are unpaired and are in two different orbitals) and the singlet (two nonbonding electrons are paired in one orbital with high s-character, and the other p orbital is empty) (Figure 1.1).<sup>3</sup>

Figure 1.1. General scheme of singlet and triplet states of divalent Group 14 compounds.



In diaryl- and dialkylcarbenes, the energy difference between the lowest singlet and triplet configurations ( $\Delta E_{ST} = E_{\text{triplet}} - E_{\text{singlet}}$ ) is typically very small and is influenced by

substituent electronic and steric effects,<sup>8</sup> as well as the solvent.<sup>9</sup> Tomioka argued that in bent carbenes, the two p orbitals are not degenerate, and one of them gains s character and becomes stabilized.<sup>8</sup> This separation of energy, which is sensitive to the steric and electronic effects of the substituents, plays the main role in determining ground-state multiplicity. That is, a separation barrier to relieve Coulomb repulsion is required for a triplet ground state configuration. As this energy separation increases, the barrier becomes large enough to compensate the repulsion energy. Electron donors lead to an increase in the energy separation; therefore halocarbenes tend to be ground state singlets. Substituents that favour conjugation, however lower the energy barrier and, as a result, most diarylcarbenes are ground state triplets. Steric effects of substituents on  $\Delta E_{ST}$  depend on the carbon-carbon bond angle. Steric hindrance increases the angle and consequently increases the energy barrier.<sup>8</sup>

Table 1.2 summarizes the calculated  $\Delta E_{ST}$  values of the parent metallylenes ( $MH_2$ ,  $M = Si, Ge, Sn$ ), which shows that the singlet-triplet energy difference ( $\Delta E_{ST}$ ) of the divalent Group 14 elements becomes more positive, meaning the singlet configuration becomes increasingly more favourable than the triplet (Table 1.2), as one proceeds down the group. The increasing  $\Delta E_{ST}$  also indicates that the singlet state is more favourable for stannylenes than germlylenes and silylenes with the same substituents. As a result, other than a few notable exceptions for silylenes,<sup>10,11,12</sup> metallylenes are found as ground state singlets. Apeloig et al. provided an explanation by comparing the singlet and triplet energies of  $CH_2$  and  $SiH_2$ .<sup>13</sup> This computational study suggests that roughly 60% of the energy difference in the singlet-triplet splitting may be attributed to the reduced electron - electron repulsion between the two frontier

electrons due to the increasing size of orbitals. The remaining 40% could be assigned to a complex balance of electron-nuclear attraction, kinetic energy and repulsion of other electrons.<sup>13</sup>

The divalent state stabilization energy (DSSE) is a thermodynamic term to describe the stability of divalent species.<sup>14,15</sup> It is defined as the difference in homolytic bond dissociation enthalpies ( $\Delta H^\circ$ ) of  $MX_4$  and radical  $MX_3$  (equation 1.1).<sup>16</sup> As the divalent species become more stable, it will have lower dissociation enthalpies which lead to higher DSSE values. The DSSE increases down Group 14 because the valence shell s electrons of the heavy element are getting increasingly lower in energy than the p electrons (Table 1.2).<sup>16</sup>

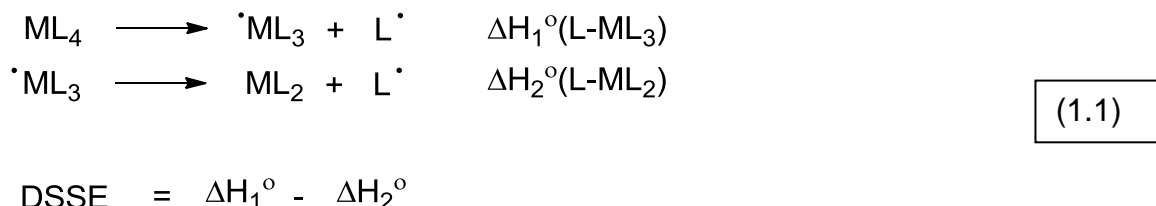


Table 1.2. Calculated singlet-triplet energy gap ( $\Delta E_{ST}$ ) and Divalent state stabilization energies (DSSE) of  $CH_2$  and parent metallylenes.<sup>7</sup> Units: kcal/mol

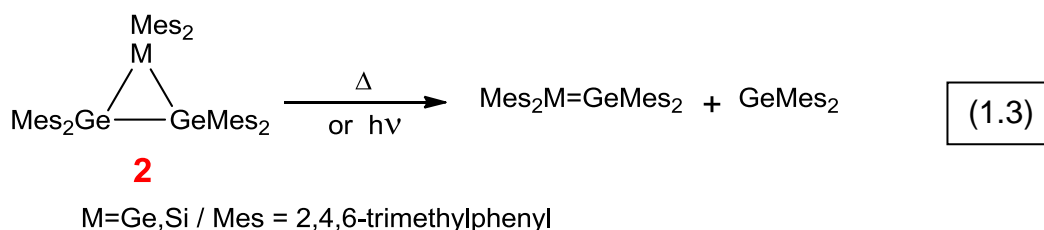
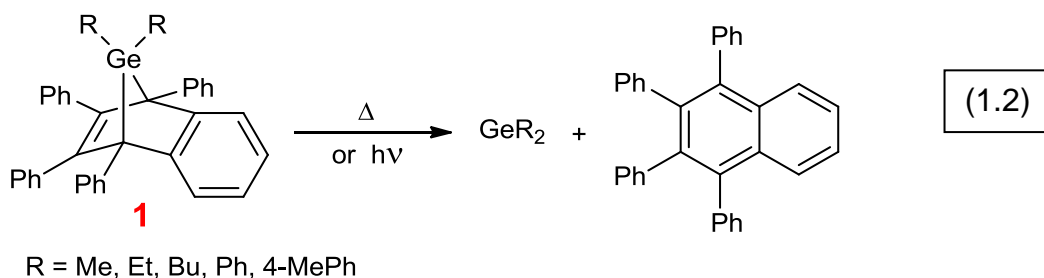
	$\Delta E_{ST}^a$	DSSE
<b>CH<sub>2</sub></b>	-10.4 ( <sup>1</sup> A <sub>1</sub> )	-12 ( <sup>1</sup> A <sub>1</sub> ) <sup>b</sup> , -6 ( <sup>3</sup> B <sub>1</sub> ) <sup>b</sup>
<b>SiH<sub>2</sub></b>	+20.0	+19 <sup>c</sup>
<b>GeH<sub>2</sub></b>	+22.0	+26 <sup>d</sup>
<b>SnH<sub>2</sub></b>	+23.4	+26 <sup>e</sup>

a. CCSD(T)/EC, Reference17; b. MP4SDTQ(FC)/6-311G\*\*//MP2(FU)/6-31G\*, Reference18; c. Experimental, Reference19; d. Experimental, Reference 20; e. BAC-MP4(298K), Reference 21.

## 1.4. Generation of Germylenes

### 1.4.1. Thermal Generation of Germylenes

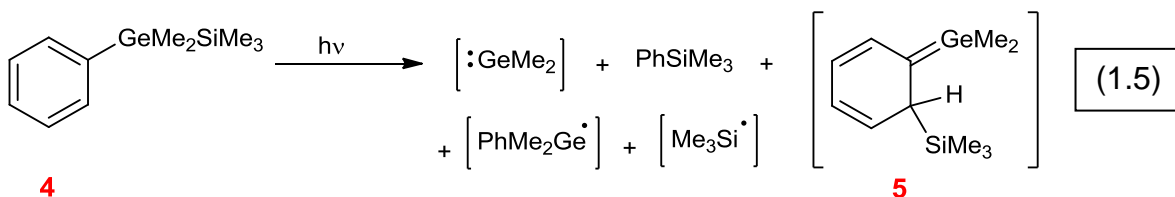
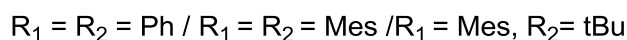
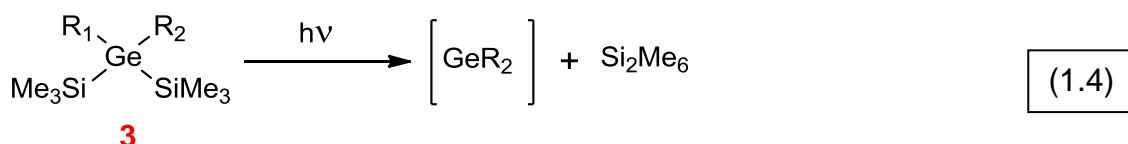
Compound **(1)** has been widely used for the generation of germylenes bearing different alkyl and aryl substituents. It has been shown that the photo- or pyrolytic cycloreversion of this compound generates free germylene and tetraphenylnaphthalene (eq 1.2).<sup>1,22</sup> Moreover, the pyrolysis and photolysis of compounds of general structure **2** yield free germylene and the corresponding digermene or germasilene (eq 1.3). Evidence for the intermediacy of the germylene was obtained from trapping experiments with methanol and 2,3-dimethyl-1,3-butadiene.<sup>23,24</sup>



### 1.4.2. Photolytic Generation of Germylenes

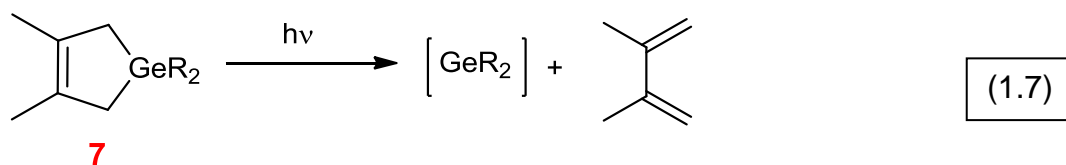
In addition to the examples discussed above, other compounds have been employed to generate germylenes photolytically. Bis(trialkylsilyl)germanes **(3)**, for

example, yield free germylene and hexamethyldisilane upon irradiation with UV light at 254 nm (eq 1.4).<sup>25</sup> The existence of the free germylene is supported by the corresponding transient UV spectrum in a hydrocarbon matrix at 77K<sup>26,27</sup> as well as in hexanes solution at 23 °C.<sup>28</sup> However, it should be noted that interpretation of this reaction is not always straightforward, particularly with phenylated compounds, which undergo competing photorearrangements. For instance, a transient species observed from the photolysis of dimethylphenyl(trimethylsilyl)germane (**4**) was originally assigned to GeMe<sub>2</sub>, however it was later revealed that the transient is in fact germene **5**, the product of [1,3]-silyl migration into the ortho position of the phenyl ring in **4** (eq 1.5).<sup>29</sup>



Diazidogermanes such as (**6**) yield the corresponding germylene and nitrogen gas upon irradiation with 254 nm or 248 nm light. The dissociation of a stable leaving group, N<sub>2</sub>, is suggested to be the driving force for the reaction; however the observed yield of the reaction is low (ca. 30%) (eq 1.6).<sup>30</sup> On the other hand, the photoreaction of germyl azides are reported not to be as clean as diazidogermanes, producing several compounds and in some cases different transient products than germylenes.<sup>31,32</sup>

Germacyclopentenes (**7**) undergo clean photolysis upon irradiation to yield the corresponding germylene and 2,3-dimethyl-1,3-butadiene (DMB) (eq 1.7).<sup>33</sup> This reaction is particularly well suited for time resolved spectroscopic studies due to its high chemical and quantum yield.<sup>2,33</sup>

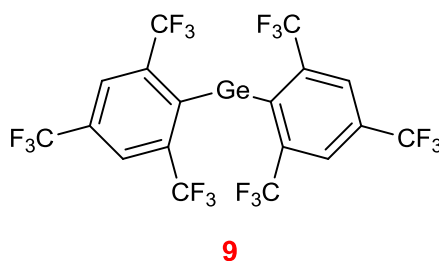
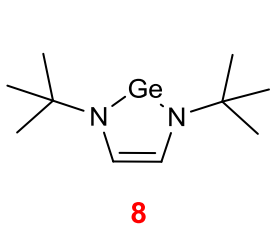


R = H, Me, Ph, Mes

### 1.5. Germylene Reactivity

The common fate of simple germylenes is dimerization to form digermenes, which oligomerize further to yield polygermanes  $(\text{GeR}_2)_n$ .<sup>1</sup> The installation of bulky substituents on germylenes introduces kinetic stabilization due to a reduction in the polymerization rate. For example, the polymerization of bis(2,6-diethylphenyl)germylene stops at the dimer<sup>34</sup> and  $\text{Ge}(\text{CH}(\text{SiMe}_3)_2)_2$  exists in equilibrium with its dimer in solution.<sup>35</sup> It was shown that the introduction of thermodynamic stabilization in addition to the kinetic stabilization can completely prevent the polymerization of germylenes. For instance, both compound (**8**)<sup>36</sup> and (**9**)<sup>37</sup> are reported to be stable crystalline compounds at 25 °C under inert gas, and their crystal structures have been obtained by x-ray crystallography.

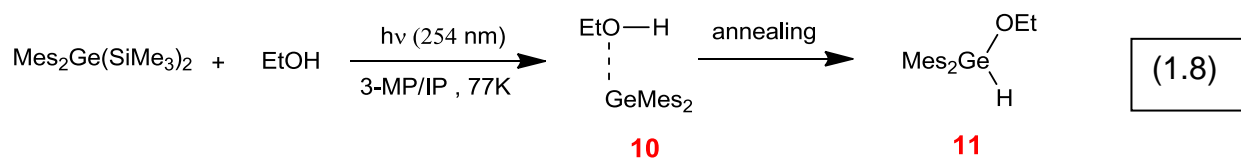




Reactions of germylenes can be classified in the following general categories: a. complexation with Lewis bases, b. halogen atom abstraction, c. insertion into  $\sigma$  bonds, d. addition to  $\pi$ -bonds.<sup>1,3</sup> The reactions studied in this thesis are discussed in more detail in the following sections.

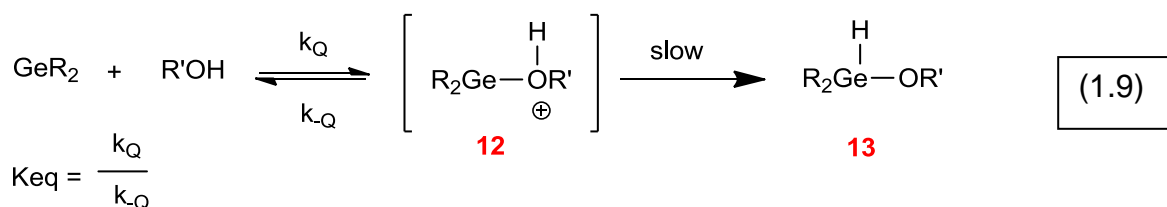
### 1.5.1. Insertion into OH Bonds

Insertion into the OH bonds of alcohols and acetic acid is one of the most common trapping reactions of germylenes.<sup>1,38,39</sup> Early evidence of the insertion product was obtained by the photolysis of bis(trimethylsilyl)germanes at 77 K in a hydrocarbon matrix containing methanol (eq 1.8). The reaction was proposed to proceed via a germylene-alcohol complex (**10**) to justify an observed absorption band at 330 nm in the acquired UV spectrum.<sup>27</sup>



Detailed kinetic studies of the reaction of dialkyl- and diarylgermylenes ( $\text{GePh}_2$ ,  $\text{GeMe}_2$ , and  $\text{GeMes}_2$ ) with alcohols (MeOH, t-BuOH) provided further evidence for a stepwise mechanism for the formation of the corresponding OH insertion product (**13**). It

requires the initial formation of a Lewis acid-base complex (**12**) in a rapid and reversible reaction (eq 1.9). The complexes have been detected as discrete transients which show absorption maxima in the 290 nm - 360 nm region. The second step is a proton transfer from oxygen to germanium, which was proposed to proceed by a catalytic mechanism involving proton transfer and a second molecule of alcohol as the catalyst.<sup>40</sup> The forward rate and equilibrium constants for the complexation step of the reaction of GePh<sub>2</sub> with methanol (MeOH) were reported to be ca.  $4 \times 10^9 \text{ M}^{-1} \text{ s}^{-1}$  and ca.  $2000 \text{ M}^{-1}$  in hexanes at 25 °C, respectively, and the rate constant of the proton transfer step was estimated to be at least 2 orders of magnitude slower than complexation.<sup>40</sup>

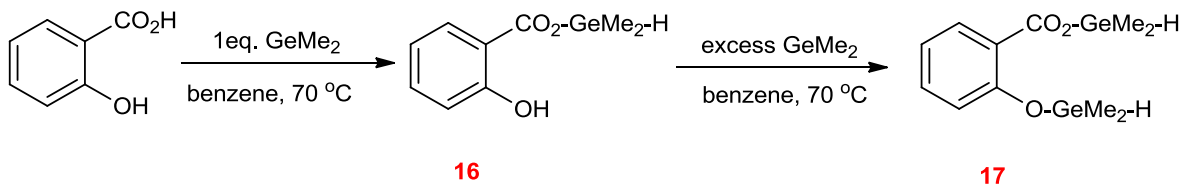


Insertions of germylenes into more acidic OH bonds (e.g. carboxylic acids) have also been studied. The insertion products of the reactions of GeMe<sub>2</sub> with benzoic and cyclohexanecarboxylic acid (**15**) were isolated as stable colorless oils (eq 1.10).<sup>41</sup> Neumann and coworkers observed that with hydroxy-substituted carboxylic acids, insertion into the more acidic OH bond gives the more favored product. For instance, the reaction of GeMe<sub>2</sub> with one equivalent of salicylic acid yields solely the insertion into the carboxylic group (**16**) and reaction with phenolic OH group proceeds only when GeMe<sub>2</sub> is in excess (eq. 1.11).<sup>41</sup>



(R = Cyclohexyl , Ph)

(1.11)



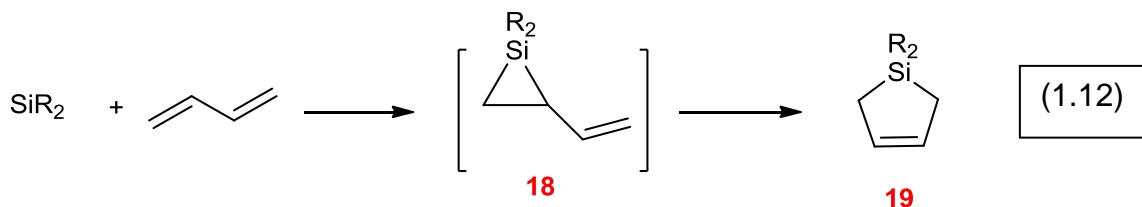
Kinetic studies of the reaction of acetic acid with diarylgermylenes ( $\text{GePh}_2$  and  $\text{GeMe}_2$ )<sup>38</sup> and methylphenylgermylene ( $\text{GeMePh}$ )<sup>42</sup> showed that these reactions can be classified as irreversible reactions with no detectable intermediate. The same reaction with dimethylgermylene ( $\text{GeMe}_2$ )<sup>2</sup> was reported to be clean and significantly faster than that with  $\text{GePh}_2$ . The reported absolute rate constants for the reaction of acetic acid in hexane solution with  $\text{GeMe}_2$  and  $\text{GePh}_2$  are  $7.5 \times 10^9 \text{ M}^{-1} \text{ s}^{-1}$  and  $3.9 \times 10^9 \text{ M}^{-1} \text{ s}^{-1}$  respectively.<sup>2</sup>

### 1.5.2. (1+4) Cycloaddition Reactions

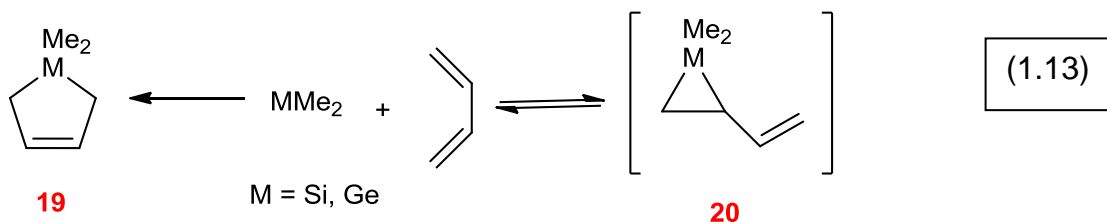
The cycloaddition reactions of carbenes with double and triple bonds are well established in the literature. Early studies of the reaction of singlet carbenes with 1,3-dienes showed that the major product of the reaction is that of (1+2) addition,<sup>43</sup> however a small amount of (1+4) addition product was also detected in a limited number of cases.<sup>44</sup> The (1+4) to (1+2)-product ratio was independent of the concentration of diene, and increased when the diene was forced into the z-conformation in sterically

congested compounds.<sup>44,45,46</sup> The reason behind this preference was investigated in a theoretical study of the reaction of singlet methylene with butadiene. This study concluded that while both additions are symmetry allowed, the (1+2) addition is much more efficiently stabilized by charge transfer interaction.<sup>47</sup> Another theoretical study suggested that the interaction between the HOMO of the carbene (the lone pair) and the LUMO of the diene ( $\pi^*_3$ ), the frontier orbitals that are thought to take part in (1+4) cycloaddition, is weakened due to repulsion between the HOMO of the carbene and the  $\pi_1$  orbital of the diene.<sup>48</sup>

The major product of the reaction of dimethylsilylene ( $\text{SiMe}_2$ ) with 1,3-butadiene was reported to be the (1+4) cycloaddition product.<sup>49,50</sup> The mechanism of this reaction has been studied by several researchers, and it was proposed that the direct concerted (1+4) addition is not the major pathway of the reaction. Instead, the formation of vinylsilirane resulting from (1+2) addition (**18**) followed by isomerization to give the (1+4) cycloadduct (**19**) was suggested to be the dominant mechanism of the reaction (eq 1.12). This mechanism is consistent with the lack of stereospecificity that has been observed for this reaction.<sup>49,50,51</sup> However in the case of germynes, the observed stereospecificity of the reaction of  $\text{GeMe}_2$  with different dienes argues in favour of a concerted mechanism for the (1+4) cycloaddition process.<sup>52,53,54</sup>

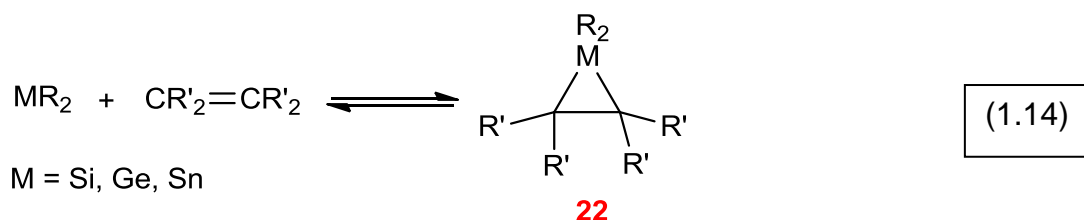


A detailed theoretical study of the reaction of the dimethylmetallylenes ( $\text{MMe}_2$ ,  $\text{M} = \text{Si}, \text{Ge}, \text{Sn}$ ) with 1,3-butadiene showed that the formation of 1-metallacyclopent-3-enes (**19**) via concerted (1+4) cycloaddition is much faster than an alternative pathway involving rearrangement of vinylmetalliranes (**20**).<sup>55</sup> Huck et al. reached a similar conclusion based on their kinetic study of the reaction of  $\text{GePh}_2$  and various derivatives with two aliphatic dienes (Isoprene and 2,3-dimethyl-1,3-butadiene). Their fast kinetics studies indicated that the formation of the thermodynamic product of the reaction, **19**, proceeds by a (1+4) mechanism, which is slower than reversible (1+2) cycloaddition to form **20**, the kinetic product of the reaction (eq 1.13).<sup>56</sup>



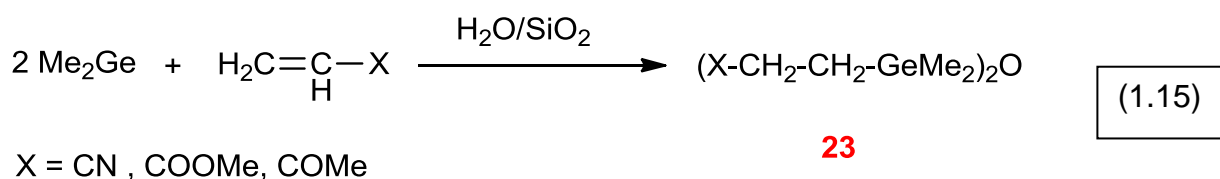
### 1.5.3. (1+2) Cycloaddition

The reactions of metallylenes (e.g. silylenes<sup>57,58</sup> and germlyenes<sup>1</sup>) with non-conjugated olefins yield the corresponding metallacyclopropanes (**22**), also known as metalliranes (eq 1.14). The corresponding three membered ring **22** becomes less stable as one proceeds down Group 14 due to the increase in DSSE and ring strain, in addition to a progressive reduction in M-C bond strength.<sup>59</sup>



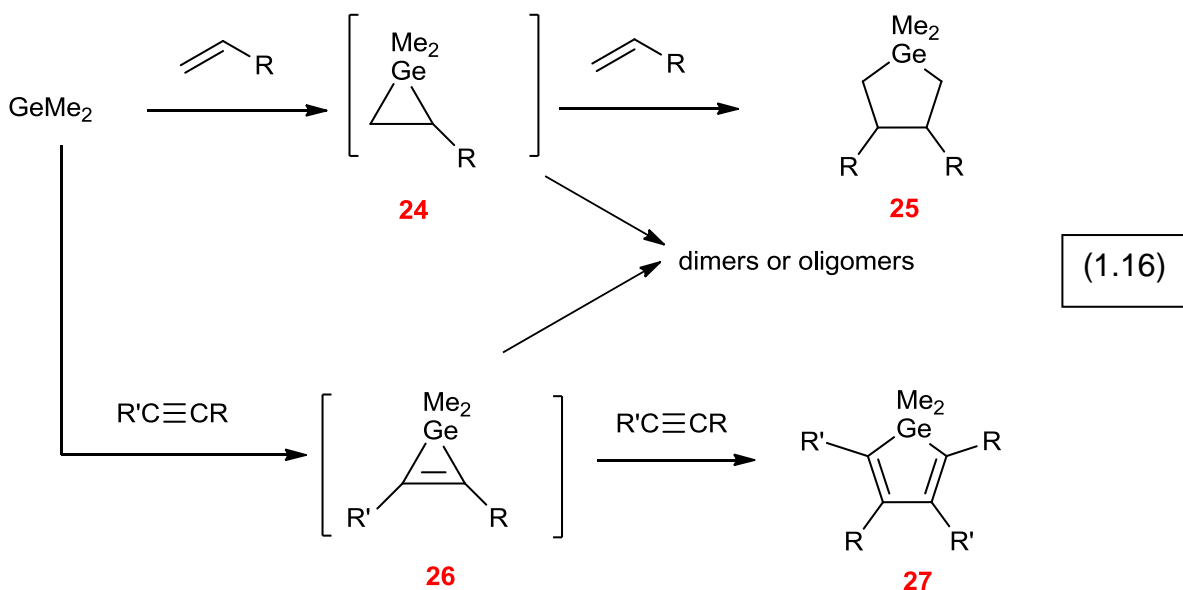
Gas phase kinetic studies of the parent silylene<sup>60,61</sup> and germylene<sup>62,63,64,65</sup> are consistent with a rapid and reversible addition to alkenes which occurs faster than their polymerization. It was shown that the addition in both cases has a negative activation energy and is more exergonic for siliranes. Becerra et al. studied the kinetic isotope effect of the addition reaction of GeH<sub>2</sub> with C<sub>2</sub>D<sub>4</sub>. They concluded that the formation of ethylgermylene is more favoured in the ring opening reaction of germiranes which does not proceed via a diradical intermediate.<sup>65</sup>

The reaction of GeMe<sub>2</sub> with simple alkenes such as 1-octene and cyclohexene does not lead to an isolable product,<sup>1</sup> but with styrene a 1:2 addition product (**23**) is formed.<sup>66</sup> In the presence of water, GeMe<sub>2</sub> also reacts with electron deficient alkenes such as acrylonitrile to form product **23** (eq 1.15).<sup>67</sup> The latter was proposed to proceed via the initial formation of the corresponding germirane, resulting from (1+2) cycloaddition.<sup>67</sup> Similarly, the formation of 1:2 cycloadducts with styrene was suggested to arise via reaction of the 1:1 adduct with the second molecule of alkene.<sup>68</sup>



Detailed studies of the reaction of GeMe<sub>2</sub> with alkenes and alkynes by Neumann et al. suggested that the primary products of the reaction resulting from (1+2) cycloaddition (**24** and **26**) are prone to react with a second molecule of substrate to form the 5 membered ring (**25** & **27**) or dimerize (eq 1.16).<sup>1,2,69</sup> Similarly, kinetic studies of the reaction of GeMePh<sup>42</sup> and GePh<sub>2</sub><sup>70</sup> with isoprene, DMP (4,4-dimethyl-1-pentene) and

TBE (3,3-dimethyl-1-butyne) have provided spectroscopic evidence for the transient three-membered-ring, however the reaction of  $\text{GePh}_2$  with the alkyne (TBE) is suggested to be irreversible ( $K_{\text{eq}} > 25000 \text{ M}^{-1}$ ) in contrast to its reaction with alkenes (DMP and isoprene) which are reversible under the same conditions.<sup>70</sup>

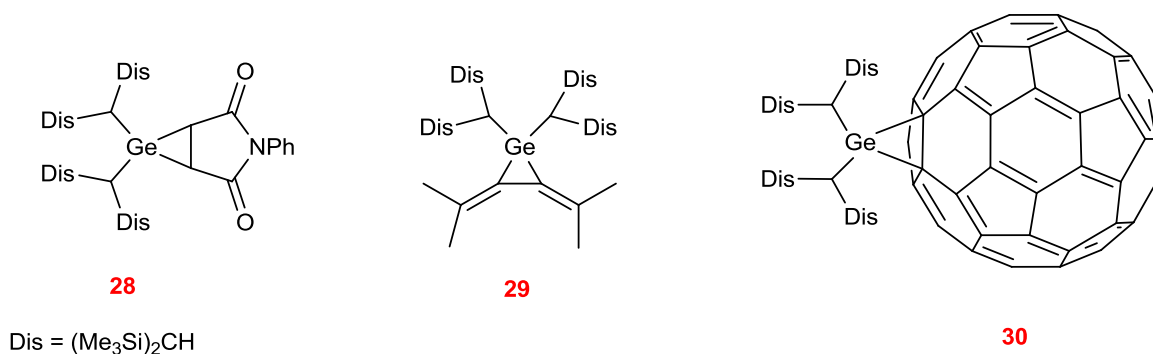


Computational investigations of the reactions of metallylenes with ethylene provided supporting evidence for the existence of a metallylene-alkene  $\pi$ -complex as an intermediate to the (1+2) addition product.<sup>64,71,72</sup> Su et al. emphasized the key role of the formation of the initial  $\pi$ -complex in the reaction of germylenes with ethylene in their computational study.<sup>72</sup> Becerra et al. used a higher level of calculation (G2) to explore the mechanism of the reaction of  $\text{GeH}_2$  with ethylene. They proposed two distinct stages for this reaction: the initial nucleophilic attack of  $\pi$  electrons of the unsaturated bond into germanium empty p orbital, followed by subsequent electrophilic donation of the Ge lone pair into the  $\pi^*$  molecular orbital of the C-C double bond.<sup>64</sup> In another computational study of the reaction of  $\text{GeH}_2$  and  $\text{GeMe}_2$  with ethylene and buta-1,2,3-

triene, the authors concluded that the addition occurs either as a barrierless single step or involves the initial formation of a  $\pi$ -complex, depending on the substituents on germanium and the alkene.<sup>73</sup>

### 1.6. Stability of Metalliranes, Steric vs. Electronic Effects

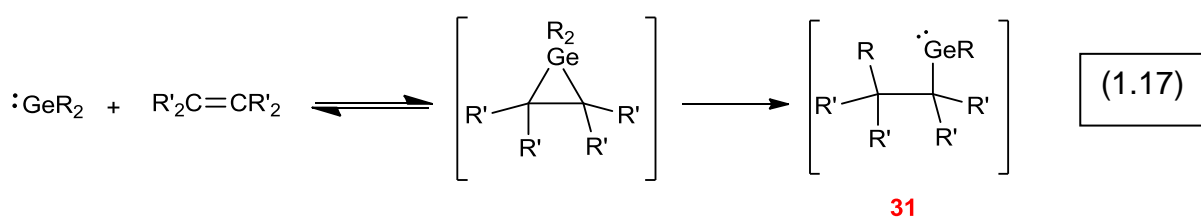
There are several examples of siliranes that are stable at room temperature in the absence of moisture and oxygen.<sup>74,75,76</sup> On the contrary, only three stable germiranes have been reported so far (compounds **28-30**).<sup>77,78</sup> As discussed in section 1.5.3, it is expected to see a decrease in the stability of metalliranes as one proceeds down Group 14.



Su et al. evaluated different germylenes to quantify the effect of germanium substitution on the (1+2) cycloaddition with ethylene. Their calculations showed that electropositive and/or bulky substituents on germanium make the addition feasible in contrast to the presence of electron-withdrawing substituents which prevent it.<sup>72</sup> Birukov et al. reported that the cycloaddition of GeMe<sub>2</sub> with ethylene is calculated to be less favourable (less exergonic) than that of GeH<sub>2</sub>,<sup>73</sup> which is consistent with the higher DSSE of GeMe<sub>2</sub> compared to GeH<sub>2</sub>.<sup>79</sup> They rationalized that the stability of germiranes



should be attributed to the stability against both the cycloreversion to starting materials and the 1,2-migration of a substituent to form another germylene (**31**) (eq 1.17). These calculations suggest alkyl groups on germanium inhibit migration but simultaneously increasing the tendency towards cycloreversion back to the free germylene. Consequently, the formation of germiranes from  $\text{GeMe}_2$  is less favorable compared to that of the parent germylene.<sup>73</sup>



The effect of alkene substituents on the stability of the corresponding germiranes was investigated in a theoretical study of the addition of  $\text{GeH}_2$  and  $\text{GeMe}_2$  to ethylene and tetramethylethylene (TME).<sup>73</sup> The Gibbs free energy of the reaction of  $\text{GeH}_2$  with ethylene is calculated to be lower than the reaction with TME. A similar trend was obtained for the reaction of  $\text{GeMe}_2$  with ethylene and TME.<sup>73</sup> This suggests that alkene substitution leads to the formation of less stable germiranes with respect to the cycloreversion towards starting materials.

### 1.7. Previous Studies of the Reaction of $\text{GePh}_2$ with alkenes in Dr. Leigh's group

After investigation of the reaction of diphenylgermylene ( $\text{GePh}_2$ ) and its various aryl-substituted derivatives with dienes (isoprene and DMB)<sup>56</sup> in Dr. Leigh's group, it was desirable to look at the reaction of diphenylgermylene with alkenes and make sense out of its chemistry. Therefore, a summer student (S.S. Chitnis) started to look at

the reaction of  $\text{GePh}_2$  with several alkenes. His results, which are summarized in Table 1.3, established a promising relationship between the Gibbs free energy of the reaction and the ionization potential<sup>80</sup> of the involved alkene (Figure 1.2). A similar correlation was found by Dr. Leigh's calculations. This promising agreement of theoretical and experimental data became the initiative for my thesis research.

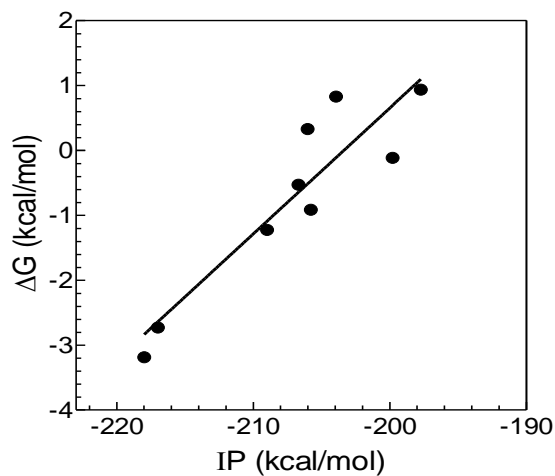


Figure 1.2. Gibbs free energies of reactions of  $\text{GePh}_2$  with alkenes vs the alkene ionization potential. (Table 1.3, S.S.Chitnis, unpublished). All IP values are taken from the National Institute of Standards and Technology of the United States (NIST).<sup>80</sup>

Table 1.3. Experimental equilibrium constants and Gibbs free energies of the reactions of  $\text{GePh}_2$  with alkenes in deoxygenated hexane solution at 25 °C.<sup>a</sup>

Alkene	$K_{\text{eq}} (\text{M}^{-1})$	$\Delta G^\circ (\text{kcal/mol})^b$
1-hexene	$5400 \pm 1800$	$-3.21 \pm 0.2$
isoprene	$6.0 \pm 1.6$	$0.83 \pm 0.16$
cyclohexene	$14 \pm 2$	$0.33 \pm 0.08$
cis-2-hexene	$60 \pm 8$	$0.53 \pm 0.08$
trans-2-hexene	$115 \pm 16$	$-0.91 \pm 0.08$
2-ethyl-1-butene	$195 \pm 20$	$-1.23 \pm 0.06$
2-methyl-2-pentene	$5.0 \pm 1$	$0.94 \pm 0.12$
methylcyclohexene	$30 \pm 6$	$-0.11 \pm 0.14$
4,4-dimethyl-1-pentene	$2500 \pm 600^c$	$-2.73 \pm 0.38$

(a) The equilibrium constants were measured by S.S.Chitnis (unpublished), unless otherwise stated. Errors are listed as  $\pm 2\sigma$ . (b)  $\Delta G^\circ$  is the gas phase Gibbs free energy (at 25 °C, 1 atm) and is calculated as follows: first, measured solution phase equilibrium constant ( $K_c$ ) is converted to the gas phase equilibrium constant ( $K_p$ ) using equation  $K_p = (K_c / RT)$  where  $R = 0.082 \text{ L}\cdot\text{atm}\cdot\text{K}^{-1}\cdot\text{mol}^{-1}$  and  $T = 298.15 \text{ K}$ . Then,  $K_p$  is placed in the equation  $\Delta G^\circ = -RT \ln K_p$ , where  $R = 0.00198 \text{ kcal}\cdot\text{K}^{-1}\cdot\text{mol}^{-1}$  and  $T = 298.15 \text{ K}$ . (c) Reference<sup>70</sup>.

## 1.8. Applications of Metallylene Chemistry

Chemical vapour deposition (CVD) is a chemical process used to produce high-purity, high-performance solid materials for low-cost solar cells, optical coatings, X-ray monochromators and microelectronics.<sup>81</sup> It has been shown that metallylenes, mainly the parent silylene and germylene, are key intermediates in the mechanism of this process.<sup>81,82</sup> In addition, metallylenes are very important in the modification of surfaces of crystalline silicon, germanium, and carbon (diamond) which are the starting point for integrated circuit manufacturing in the semiconductor industry.<sup>83</sup>

Metallylenes have been used for the synthesis of different silicon<sup>84,85</sup> and germanium<sup>69,77</sup> compounds. In synthesis, they have found useful applications for the preparation of binuclear Pd(0) complexes in the Suzuki reaction,<sup>86</sup> C-H bond activation of ethers and alkenes,<sup>87</sup> metal-catalyzed di-tert-butylsilylene transfer,<sup>88,89,90</sup> regio- and stereoselective formation of enolates,<sup>91</sup> stereoselective formation of 1,2,4-triols<sup>92</sup> as well as the synthesis of other organic compounds.<sup>93,94,95</sup> It is worth noting that some organosilicon compounds have been reported to show biological activity,<sup>96</sup> which further necessitates the development of novel techniques towards their synthesis.

### 1.9. Goals of This Work

This thesis is centered around the evaluation of alkene substitution effects on the thermodynamic stability of germiranes. Attempts were made to answer the following questions:

(1) What are the rate constants for the reaction of GePh<sub>2</sub> with mono, di, tri substituted alkenes?

(2) How does substitution of the alkene affect the stability of the resulting germiranes? What thermodynamic property can be a predictor for the effect of alkene substitution?

(3) What computational method is the best for modeling the reaction of germylenes with alkenes? Which one gives the closest results to the experimental values? What method is sufficient for performing calculations on larger, more complex molecules (GePh<sub>2</sub>) and simpler analogues (GeMe<sub>2</sub>, GeH<sub>2</sub>)?

## 1.10. References

- (1) Neumann, W. P. *Chem. Rev.* **1991**, *91*, 311.
- (2) Leigh, W. J.; Lollmahomed, F.; Harrington, C. R. *Organometallics* **2006**, *25*, 2055.
- (3) Mizuhata, Y.; Sasamori, T.; Tokitoh, N. *Chem. Rev.* **2009**, *109*, 3479.
- (4) P. Power, P. J. *Chem. Soc., Dalton Trans.* **1998**, 2939.
- (5) Takagi, N.; Tonner, R.; Frenking, G. *Chem. Eur. J.* **2012**, *18*, 1772.
- (6) Jutzi, P.; Schubert, U. *Silicon Chemistry: From the Atom to Extended Systems*; John Wiley & Sons, **2003**.
- (7) Huck, L. A. PhD Thesis, McMaster University, **2010**.
- (8) Tomioka, H. *Acc. Chem. Res.* **1997**, *30*, 315.
- (9) Wang, Y.; Hadad, C. M.; Toscano, J. P. *J. Am. Chem. Soc.* **2002**, *124*, 1761.
- (10) Jiang, P.; Gaspar, P. P. *J. Am. Chem. Soc.* **2001**, *123*, 8622.
- (11) Sekiguchi, A.; Tanaka, T.; Ichinohe, M.; Akiyama, K.; Tero-Kubota, S. *J. Am. Chem. Soc.* **2003**, *125*, 4962.
- (12) Sekiguchi, A.; Tanaka, T.; Ichinohe, M.; Akiyama, K.; Gaspar, P. P. *J. Am. Chem. Soc.* **2008**, *130*, 426.
- (13) Apeloig, Y.; Pauncz, R.; Karni, M.; West, R.; Steiner, W.; Chapman, D. *Organometallics* **2003**, *22*, 3250.
- (14) Walsh, R. *Acc. Chem. Res.* **1981**, *14*.
- (15) Grev, R. S. In *Advances in Organometallic Chemistry*; Stone, F. G. A., Robert, W., Eds.; Academic Press: **1991**; Volume 33, p 125
- (16) Becerra, R.; Walsh, R. *Phys. Chem. Chem. Phys.* **2007**, *9*, 2817.
- (17) Szabados, Á.; Hargittai, M. *J. Phys. Chem. A* **2003**, *107*, 4314.
- (18) Pople, J. A.; Head-Gordon, M.; Fox, D. J.; Raghavachari, K.; Curtiss, L. A. *J. Chem. Phys.* **1989**, *90*, 5622.
- (19) Walsh, R.; Patai, S. In *The chemistry of organic silicon compounds* Rappoport, Z., Ed.; John Wiley & Sons Ltd.: , **1989**, p 371.
- (20) Becerra, R.; Boganov, S. E.; Egorov, M. P.; Faustov, V. I.; Nefedov, O. M.; Walsh, R. *J. Am. Chem. Soc.* **1998**, *120*, 12657.
- (21) Allendorf, M. D.; Melius, C. F. *J. Phys. Chem. A* **2005**, *109*, 4939.
- (22) Harrington, C. R.; Leigh, W. J.; Chan, B. K.; Gaspar, P. P.; Zhou, D. *Can. J. Chem.* **2005**, *83*, 1324.
- (23) Baines, K. M.; Cooke, J. A.; Dixon, C. E.; Liu, H. W.; Netherton, M. R. *Organometallics* **1994**, *13*, 631.
- (24) Tsumuraya, T.; Kabe, Y.; Ando, W. *J. Organomet. Chem.* **1994**, *482*, 131.
- (25) Ando, W.; Tsumuraya, T.; Sekiguchi, A. *Chem. Lett.* **1987**, 317.
- (26) Ando, W.; Ito, H.; Tsumuraya, T.; Yoshida, H. *Organometallics* **1988**, *7*, 1880.
- (27) Ando, W.; Itoh, H.; Tsumuraya, T. *Organometallics* **1989**, *8*, 2759.
- (28) Tötl, N. P.; Leigh, W. J.; Kollegger, G. M.; Stibbs, W. G.; Baines, K. M. *Organometallics* **1996**, *15*, 3732.
- (29) Lollmahomed, F.; Leigh, W. J. *Organometallics* **2009**, *28*, 3239.

- (30) Barrau, J.; Bean, D. L.; Welsh, K. M.; West, R.; Michl, J. *Organometallics* **1989**, *8*, 2606.
- (31) Baceiredo, A.; Bertrand, G.; Mazerolles, P. *Tetrahedron Lett.* **1981**, *22*, 2553.
- (32) Tsumuraya, T.; Ando, W. *Chem. Lett.* **1989**, *18*, 1043.
- (33) Leigh, W. J.; Harrington, C. R.; Vargas-Baca, I. *J. Am. Chem. Soc.* **2004**, *126*, 16105.
- (34) Collins, S.; Murakami, S.; Snow, J. T.; Masamune, S. *Tetrahedron Lett.* **1985**, *26*, 1281.
- (35) Fjeldberg, T.; Haaland, A.; Schilling, B. E. R.; Lappert, M. F.; Thorne, A. J. *J. Chem. Soc., Dalton Trans.* **1986**, 1551.
- (36) Herrmann, W. A.; Denk, M.; Behm, J.; Scherer, W.; Klingan, F.-R.; Bock, H.; Solouki, B.; Wagner, M. *Angew. Chem. Int. Ed.* **1992**, *31*, 1485.
- (37) Bender, J. E.; Banaszak Holl, M. M.; Kampf, J. W. *Organometallics* **1997**, *16*, 2743.
- (38) Leigh, W. J.; Harrington, C. R.; Vargas-Baca, I. *J. Am. Chem. Soc.* **2004**, *126*, 16105.
- (39) Lawrence A. Huck; Leigh, W. J. *Organometallics* **2007**, *26*, 1339.
- (40) Leigh, W. J.; Lollmahomed, F.; Harrington, C. R.; M., M. J. *Organometallics* **2006**, *25*, 5424.
- (41) Klein, B.; Neumann, W. P.; Weisbeck, M. P.; Wienken, S. *J. Organomet. Chem.* **1993**, *446*, 149.
- (42) Leigh, W. J.; Dumbrava, I. G.; Lollmahomed, F. *Can. J. Chem.* **2006**, *84*, 934.
- (43) Mayr, H.; Heigl, U. W. *Angew. Chem. Int. Ed.* **1985**, *24*, 579.
- (44) Jenneskens, L. W.; de Wolf, W. H.; Bickelhaupt, F. *Angew. Chem. Int. Ed.* **1985**, *24*, 585.
- (45) Nguyet Anh, L.; Jones, M.; Bickelhaupt, F.; De Wolf, W. H. *J. Am. Chem. Soc.* **1989**, *111*, 8491.
- (46) Lambert, J. B.; Ziemnicka-Merchant, B. T. *J. Org. Chem.* **1990**, *55*, 3460.
- (47) Fujimoto, H.; Hoffmann, R. *J. Phys. Chem.* **1974**, *78*.
- (48) Schoeller, W. W.; Yurtsever, E. *J. Am. Chem. Soc.* **1978**, *100*, 7548.
- (49) Lei, D.; Hwang, R.-J.; Caspar, P. P. *J. Organomet. Chem.* **1984**, *271*, 1.
- (50) Clarke, M. P.; Davidson, I. M. T. *J. Chem. Soc., Chem. Commun.* **1988**, 241.
- (51) Lei, D.; Gaspar, P. *Res. Chem. Intermed.* **1989**, *12*, 103.
- (52) Schriewer, M.; Neumann, W. P. *Angew. Chem. Int. Ed.* **1981**, *20*, 1019.
- (53) Ching-Lin Ma, E.; Kobayashi, K.; Barzilai, M. W.; Gaspar, P. P. *J. Organomet. Chem.* **1982**, *224*, C13.
- (54) Koecher, J.; Neumann, W. P. *J. Am. Chem. Soc.* **1984**, *106*, 3861.
- (55) Nag, M.; Gaspar, P. P. *Organometallics* **2009**, *28*, 5612.
- (56) Huck, L. A.; Leigh, W. J. *Organometallics* **2009**, *28*, 6777.
- (57) Lambert, R. L.; Seyferth, D. *J. Am. Chem. Soc.* **1972**, *94*, 9246.
- (58) Ishikawa, M.; Kumada, M. *J. Organomet. Chem.* **1974**, *81*, C3.
- (59) Horner, D. A.; Grev, R. S.; Schaefer, H. F. *J. Am. Chem. Soc.* **1992**, *114*, 2093.

- (60) Al-Rubaiey, N.; Walsh, R. *J. Phys. Chem.* **1994**, *98*, 5303.
- (61) Al-Rubaiey, N.; Carpenter, I. W.; Walsh, R.; Becerra, R.; Gordon, M. S. *J. Phys. Chem. A* **1998**, *102*, 8564.
- (62) Becerra, R.; Boganov, S. E.; Egorov, M. P.; Nefedov, O. M.; Walsh, R. *Chem. Phys. Lett.* **1996**, *260*, 433.
- (63) Becerra, R.; Walsh, R. *J. Organomet. Chem.* **2001**, *636*, 49.
- (64) Becerra, R.; Boganov, S. E.; Egorov, M. P.; Faustov, V. I.; Promyslov, V. M.; Nefedov, O. M.; Walsh, R. *Phys. Chem. Chem. Phys.* **2002**, *4*, 5079.
- (65) Becerra, R.; Walsh, R. *Phys. Chem. Chem. Phys.* **2002**, *4*, 6001.
- (66) Koecher, J.; Neumann, W. P. *Organometallics* **1985**, *4*, 400.
- (67) Neumann, W. P.; Sakurai, H.; Billeb, G.; Brauer, H.; Köcher, J.; Viebahn, S. *Angew. Chem. Int. Ed.* **1989**, *28*, 1028.
- (68) Shusterman, A. J.; Landrum, B. E.; Miller, R. L. *Organometallics* **1989**, *8*, 1851.
- (69) Neumann, W. P.; Weisbeck, M. P.; Wienken, S. *Main Group Met. Chem.* **1994**, *17*.
- (70) Leigh, W. J.; Harrington, C. R. *J. Am. Chem. Soc.* **2005**, *127*, 5084
- (71) Sakai, S. *Int. J. Quantum Chem.* **1998**, *70*, 291.
- (72) Su, M.-D.; Chu, S.-Y. *J. Am. Chem. Soc.* **1999**, *121*, 11478.
- (73) Birukov, A.; Faustov, V.; Egorov, M.; Nefedov, O. *Russ. Chem. Bull.* **2005**, *54*, 2003.
- (74) Seyferth, D.; Annarelli, D. C. *J. Am. Chem. Soc.* **1975**, *97*, 2273.
- (75) Zhang, S.; Conlin, R. T. *J. Am. Chem. Soc.* **1991**, *113*, 4272.
- (76) Kroke, E.; Willms, S.; Weidenbruch, M.; Saak, W.; Pohl, S.; Marsmann, H. *Tetrahedron Lett.* **1996**, *37*, 3675.
- (77) Ando, W.; Ohgaki, H.; Kabe, Y. *Angew. Chem. Int. Ed.* **1994**, *33*, 659.
- (78) Kabe, Y.; Ohgaki, H.; Yamagaki, T.; Nakanishi, H.; Ando, W. *J. Organomet. Chem.* **2001**, *636*, 82.
- (79) Boganov, S.; Egorov, M.; Faustov, V.; Krylov, I.; Nefedov, O.; Becerra, R.; Walsh, R. *Russ. Chem. Bull.* **2005**, *54*, 483.
- (80) National Institute of Standards and Technology of the United States (NIST) chemwebook, June 8, **2011**, <http://webbook.nist.gov/chemistry>
- (81) Vepřek, S.; Prokop, J.; Glatz, F.; Merica, R.; Klingan, F. R.; Herrmann, W. *A. Chem. Mater.* **1996**, *8*, 825.
- (82) Isobe, C.; Cho, H.-C.; Crowell, J. E. *Surf. Sci.* **1993**, *295*, 117.
- (83) Hamers, R. J.; Coulter, S. K.; Ellison, M. D.; Hovis, J. S.; Padowitz, D. F.; Schwartz, M. P.; Greenlief, C. M.; Russell, J. N. *Acc. Chem. Res.* **2000**, *33*, 617.
- (84) Ćiraković, J.; Driver, T. G.; Woerpel, K. A. *J. Am. Chem. Soc.* **2002**, *124*, 9370.
- (85) Driver, T. G.; Franz, A. K.; Woerpel, K. A. *J. Am. Chem. Soc.* **2002**, *124*, 6524.
- (86) Furstner, A.; Krause, H.; Lehmann, C. W. *Chem. Commun.* **2001**, 2372.
- (87) Miller, K. A.; Bartolin, J. M.; O'Neill, R. M.; Sweeder, R. D.; Owens, T. M.; Kampf, J. W.; Holl, M. M. B.; Wells, N. J. *J. Am. Chem. Soc.* **2003**, *125*, 8986.
- (88) Driver, T. G.; Woerpel, K. A. *J. Am. Chem. Soc.* **2003**, *125*, 10659.
- (89) Ćiraković, J.; Driver, T. G.; Woerpel, K. A. *J. Org. Chem.* **2004**, *69*, 4007.

- (90) Driver, T. G.; Woerpel, K. A. *J. Am. Chem. Soc.* **2004**, *126*, 9993.
- (91) Calad, S. A.; Woerpel, K. A. *J. Am. Chem. Soc.* **2005**, *127*, 2046.
- (92) Clark, T. B.; Woerpel, K. A. *Organic Letters* **2006**, *8*, 4109.
- (93) Calad, S. A.; Ćiraković, J.; Woerpel, K. A. *J. Org. Chem.* **2006**, *72*, 1027.
- (94) Buchner, K. M.; Clark, T. B.; Loy, J. M. N.; Nguyen, T. X.; Woerpel, K. A. *Org. Lett.* **2009**, *11*, 2173.
- (95) Clark, T. B.; Woerpel, K. A. *J. Am. Chem. Soc.* **2004**, *126*, 9522.
- (96) Gately, S.; West, R. *Drug Dev. Res.* **2007**, *68*, 156.



## Chapter 2 – Reaction of Diphenylgermylene with Alkenes

### 2.1 Overview

As mentioned in the first Chapter, experimental and theoretical studies of the reaction of germylenes with alkenes are consistent with a fast and reversible (1+2) cycloaddition reaction. With just three exceptions,<sup>1,2</sup> the resulting product of the reaction, the corresponding germirane derivative, is not stable enough to be isolated. The normal fate of these compounds is either cycloreversion to the starting material followed by polymerization of germylene, or the addition of another molecule of substrate to form a five membered ring (eq 1.16).<sup>3</sup>

The reaction of diphenylgermylene ( $\text{GePh}_2$ ) with isoprene and 4,4-dimethyl-1-pentene (DMP) has been studied by steady-state and laser flash photolysis techniques.<sup>4</sup> For both reactions, the acquired germylene decay profiles are consistent with rapid and reversible reaction of  $\text{GePh}_2$  with the substrate, followed by a slower decay assigned to the formation of tetraphenyldigermene ( $\text{Ge}_2\text{Ph}_4$ ) via dimerization of free  $\text{GePh}_2$  in equilibrium with the  $\text{GePh}_2$ -alkene cycloadduct. The absolute rate and equilibrium constants for these reactions were reported to be  $(5.5 \pm 1.2) \times 10^9 \text{ M}^{-1} \text{ s}^{-1}$  and  $6000 \pm 2500 \text{ M}^{-1}$  respectively for isoprene, and  $(4.2 \pm 0.2) \times 10^9 \text{ M}^{-1} \text{ s}^{-1}$  and  $2500 \pm 600 \text{ M}^{-1}$  for DMP.<sup>4</sup>

## 2.2 Kinetic Measurements by Laser Flash Photolysis

### 2.2.1 Photochemistry of Precursor

3,4-Dimethyl-1,1-diphenylgermacyclopent-3-ene (**32**) was employed as the precursor for all the laser flash photolysis studies carried out in this thesis. A full description of the synthesis and characterization of this compound is given in the experimental chapter (chapter 5). The selection of this compound over other available precursors for the generation of  $\text{GePh}_2$  (chapter 1) was based on the following qualifications. (1) it undergoes clean cheletropic photocycloreversion to yield transient diphenylgermylene ( $\text{GePh}_2$ ) (**34**) and 2,3-dimethyl-1,3-butadiene (DMB) (**33**) (eq 2.1) in high quantum yield ( $\Phi = 0.55$ ) and high chemical yield (>95%);<sup>5</sup> (2) the absorption spectrum of DMB is centered at  $\lambda_{\text{max}} \approx 224 \text{ nm}$ <sup>6</sup> which does not interfere in the region of our interest (260 nm – 700 nm), and the diene does not undergo any side reactions with added alkenes in the laser experiments; (3) **32** can be prepared by a fairly easy four step synthesis in high yield.<sup>5</sup>

### 2.2.2. Transient UV-Vis Absorption Spectra of the Precursor

The UV-Visible absorption spectra of the transient products of laser photolysis of **32** in dry deoxygenated hexanes can be obtained by laser flash photolysis. The laser pulse leads to the formation of two transient species (eq 2.1). The first transient formed is  $\text{GePh}_2$  **34**, which exhibits absorption maxima at  $\lambda_{\text{max}} = 300$  and 500 nm and decays over  $\sim 4 \mu\text{s}$  to form tetraphenyldigermene ( $\text{Ge}_2\text{Ph}_4$ ) (**35**), which is much longer-lived and exhibits an absorption maximum at  $\lambda_{\text{max}} = 440 \text{ nm}$  (Figure 2.1).<sup>5</sup> The molar extinction

coefficients of  $\text{GePh}_2$  and  $\text{Ge}_2\text{Ph}_4$  are reported to be  $\epsilon_{\text{GePh}_2(500\text{nm})} = 1850 \pm 400 \text{ dm}^3\text{mol}^{-1}\text{cm}^{-1}$  and  $\epsilon_{\text{Ge}_2\text{Ph}_4(440\text{nm})} > 12000 \text{ dm}^3\text{mol}^{-1}\text{cm}^{-1}$ , respectively.<sup>3,5</sup>

The spectra of the two species overlap considerably, so in order to get accurate kinetic information for the germylene, the contribution to the signal at 500nm from the digermene needs to be subtracted out. This is done by subtraction of the decay at 440 nm, after scaling to account for the difference in the extinction coefficients of the digemene spectrum at 440 and 500 nm ( $\epsilon_{500}/\epsilon_{440} \approx 0.15$ ), from the decay profile at 500 nm.<sup>5</sup>

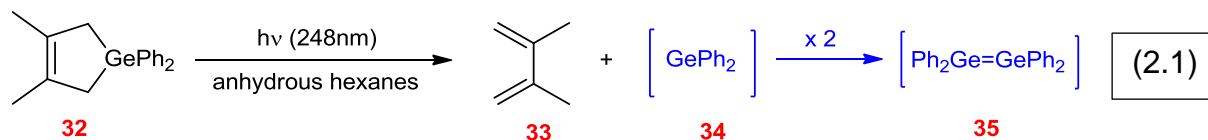
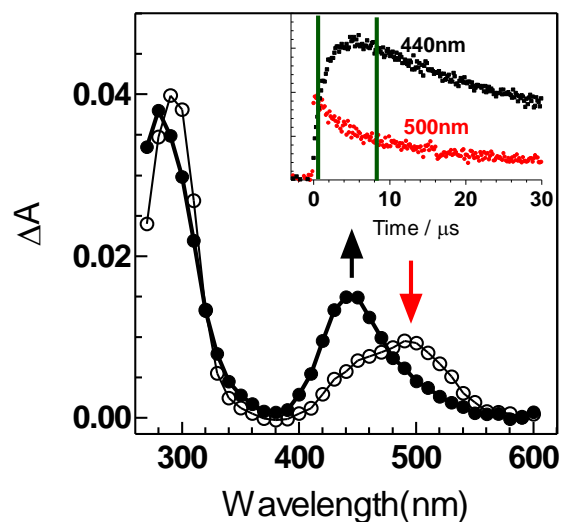


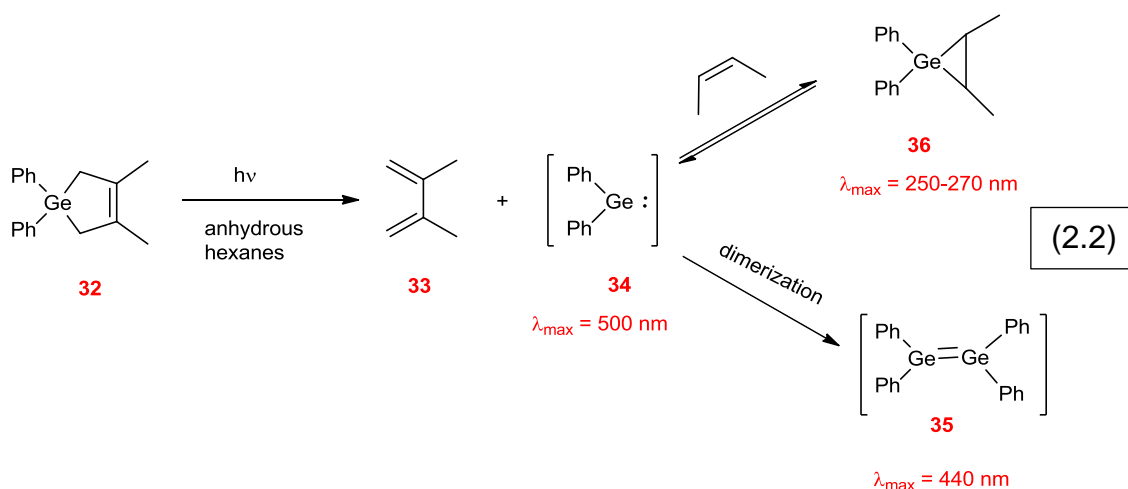
Figure 2.1. Transient absorption spectra recorded 480-1120 ns ( $\circ$ ) and 8.32-9.28  $\mu\text{s}$  ( $\bullet$ ) after the laser pulse, by laser flash photolysis of a solution of **32** in deoxygenated, anhydrous hexanes; the inset shows transient growth/decay profiles recorded at 440 and 500 nm, with the time windows represented by the two spectra indicated by solid bars.



### 2.2.3. Data Analysis

A detailed description of the procedure employed in the laser flash photolysis experiments is given in chapter 5. Briefly, a solution of the precursor **32** in dry deoxygenated hexanes was prepared in a reservoir connected to the laser flash photolysis set up (see section 5.2.2, Figure 5.3). The alkene of interest was then added to the reservoir as aliquots of a standard solution, and transient absorbance-time profiles at 500 nm and 440 nm were acquired as a function of alkene concentration. A general scheme of the reaction of  $\text{GePh}_2$  with alkenes is shown in eq 2.2.

In each experiment, addition of the alkene results in quenching of the germylene and digermene signals in a manner that is consistent with a reversible reaction of the germylene with the added substrate. Since the reactions are set up in a way that the concentration of alkene is much higher than germylene, each decay profile is expected to consist of two components: a very fast first-order component due to the approach to equilibrium with the primary reaction product (**36**), and a slower second-order component due to dimerization of free germylene remaining at equilibrium.



Equations 2.3-2.5 are used to analyze the data obtained in the experiments, where  $k_{\text{decay}}$  is the pseudo-first-order decay rate coefficient of the germylene,  $k_Q$  and  $k_{-Q}$  are the forward and reverse rate constants for the reactions with quencher (alkene),  $K_{\text{eq}}$  is the equilibrium constant ( $= k_Q/k_{-Q}$ ),  $\Delta A_0$  is the transient absorbance immediately after the laser pulse in the absence of alkene,  $\Delta A_t$  is the transient absorbance at time  $t$  after the laser pulse, and  $\Delta A_{\text{res}}$  is the transient absorbance due to the free germylene at the end of the initial rapid decay.<sup>7</sup>

- $\Delta A_t = \Delta A_{\text{res}} + (\Delta A_0 - \Delta A_{\text{res}}) \exp(-k_{\text{decay}}t)$  (2.3)

- $k_{\text{decay}} = k_{-Q} + k_Q[Q]$  (2.4)

- $\Delta A_0/\Delta A_{\text{res}} = 1 + K_{\text{eq}}[Q]$  (2.5)

In practice, the response of the germylene signal to added alkene takes on one of three forms depending on the magnitude of the equilibrium constant of the reaction<sup>7</sup>:

(1) Large- $K_{\text{eq}}$  regime: when the equilibrium constant is larger than ca.  $25000 \text{ M}^{-1}$ , the concentration of remaining free germylene at equilibrium is too small to be detected. Thus, only the forward rate constant for the reaction ( $k_Q$ ) is measurable.<sup>7</sup>

(2) Intermediate- $K_{\text{eq}}$  regime ( $1000 < K_{\text{eq}} < 25000 \text{ M}^{-1}$ ): in this case, both the equilibrium and rate constants of the reaction are measurable.<sup>7</sup>

(3) Small- $K_{\text{eq}}$  regime ( $K_{\text{eq}} < 1000 \text{ M}^{-1}$ ): in this case only  $K_{\text{eq}}$  is measurable because at high enough concentrations of alkene to cause a detectable reduction in the amount of remaining free germylene at equilibrium, the initial pseudo-first-order decay is too fast to be resolved.<sup>7</sup>

#### 2.2.4. Alkenes for Study

Ten different alkenes were chosen for study, as presented in Table 2.1. Their UV-Vis spectra were each obtained in hexanes at high concentrations in order to confirm that they contained no impurities that absorb at the laser wavelength of 248nm. Purification was required for several of them in order to remove absorbing impurities. For detailed information on the purification procedures, see chapter 5 (section 5.2.1).

#### 2.2.5. Results

Equilibrium constants for the reactions of  $\text{GePh}_2$  with the ten alkenes were measured in dried deoxygenated hexanes solution at 25 °C. The measured equilibrium constants fall into two ranges:

(1) Medium- $K_{\text{eq}}$  regime: The equilibrium constant for the reaction of  $\text{GePh}_2$  with 1-hexene was determined to be  $9400 \pm 1200 \text{ M}^{-1}$ . The  $k_{\text{decay}}$  value at each concentration was acquired by nonlinear least-squares analysis of the absorbance-time profile (using the Prism 3.0 software package), and was plotted against the concentration of 1-hexene to give the forward rate constant of the reaction (eq 2.4 , Figure 2.2.a). The value obtained was  $(7 \pm 2) \times 10^9 \text{ M}^{-1}\text{s}^{-1}$  and it is higher than previous measurement ( $k_{\text{Q}} = (4.5 \pm 0.6) \times 10^9 \text{ M}^{-1}\text{s}^{-1}$ ; S.S.Chitnis, unpublished). Moreover, the ratio of the transient absorbance immediately after the laser pulse in the absence of 1-hexene to the absorbance at equilibrium (absorbance of plateau) at each concentration was plotted against the concentration of 1-hexene in solution to give equilibrium constant of the reaction (eq 2.5, Figure 2.2.b).The acquired value was  $(9400 \pm 1200) \text{ M}^{-1}$  which is higher than that measured previously ( $K_{\text{eq}} = (6600 \pm 1200) \text{ M}^{-1}$ , S.S.Chitnis, unpublished).

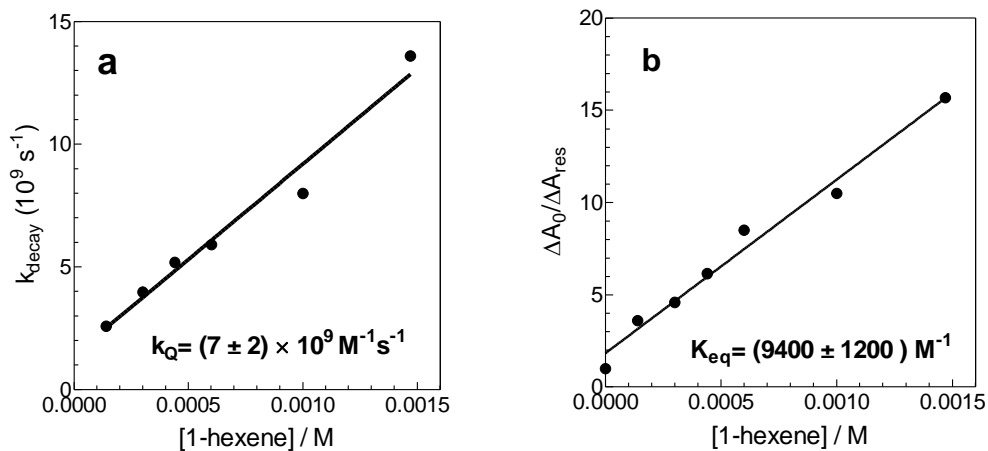
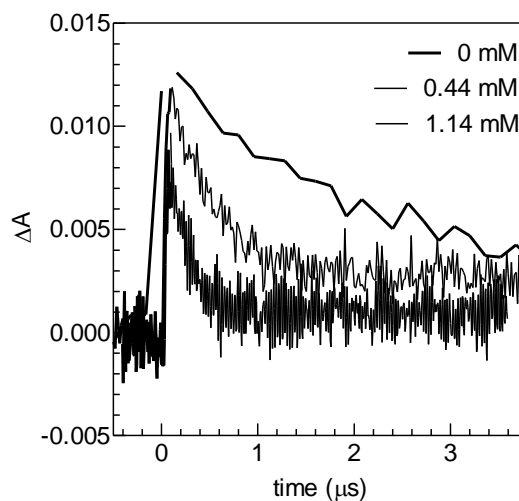


Figure 2.2. (a) Plot of  $k_{\text{decay}}$  vs concentration of 1-hexene from laser flash photolysis of a deoxygenated solution of compound **32** in the presence of 1-hexene (b) plot of  $\Delta A_0 / \Delta A_{\text{res}}$  vs concentration of 1-hexene from the same experiment.

Figure 2.3. Corrected transient decay traces recorded at 500 nm by laser flash photolysis of a deoxygenated hexanes solution of compound **32** in the presence of various concentrations of 1-hexene at 25 °C.



2- Small- $K_{\text{eq}}$  regime: The equilibrium constants measured for the reaction of  $\text{GePh}_2$  with the other nine alkenes (cyclic and acyclic) in dried deoxygenated hexanes solution at 25 °C were in the range of 2 to 400  $\text{M}^{-1}$ . In these cases, the addition of alkenes to the deoxygenated solutions of precursor **32** led to a significant drop in the apparent top OD (maximum signal intensity). That is, the pseudo-first order part of the decay was too fast to be resolved from the laser pulse at any concentration of alkene added. Plotting the ratio of top OD immediately after the laser pulse in the absence of alkene over top OD at each concentration versus the concentration of the alkenes gave the equilibrium constant (eq 2.5). Representative transient decay profiles and the equilibrium constant plots of these experiments are shown in Figures 2.4 - 2.12. The results obtained for all ten of the alkenes that were studied are collected in Tables 2.1 and 2.2. (pp. 36-37)

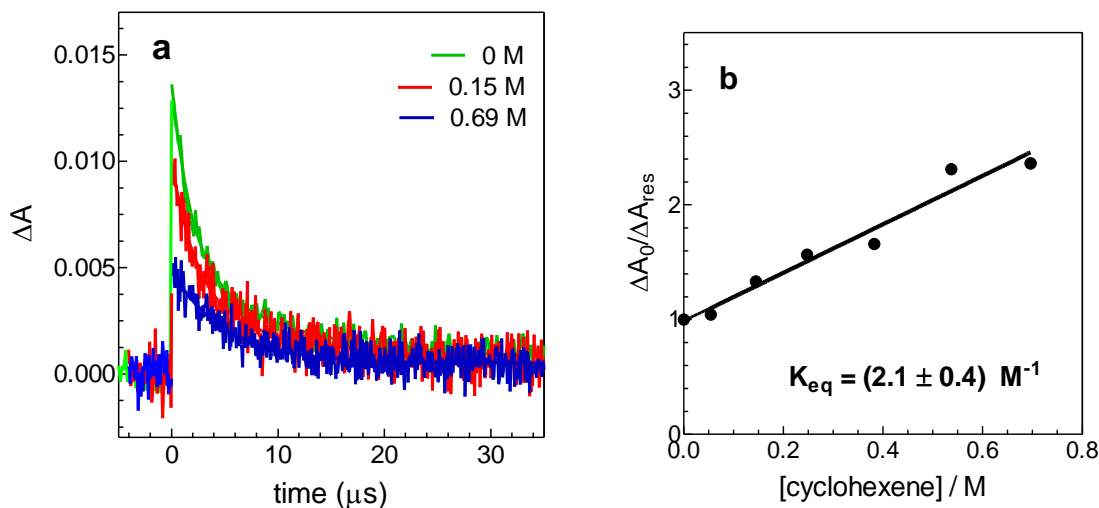


Figure 2.4. (a) Corrected transient decay traces recorded at 500 nm by laser flash photolysis of a deoxygenated hexanes solution of compound **32** in the presence of various concentrations of cyclohexene at 25 °C; (b) plot of  $\Delta A_0/\Delta A_{\text{res}}$  vs concentration of cyclohexene from the same experiment. Error is reported as  $\pm 2\sigma$ .



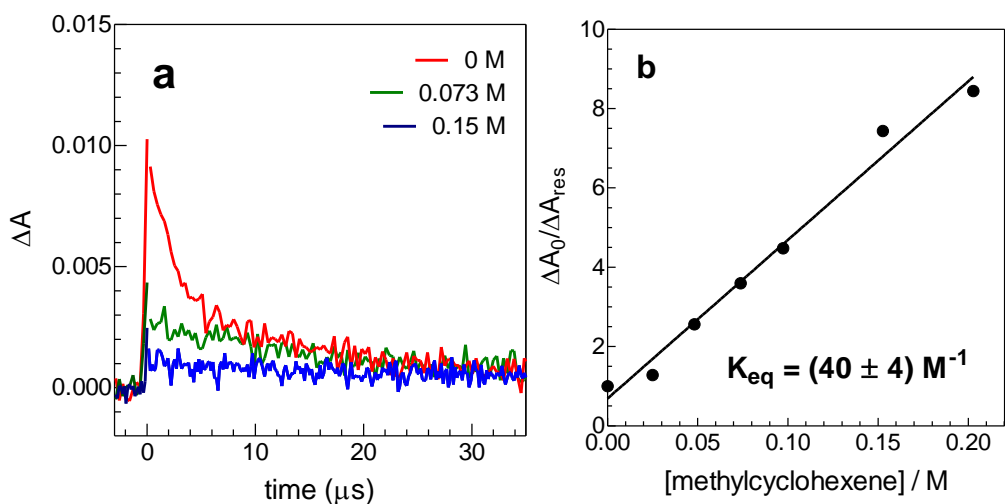


Figure 2.5. Corrected transient decay traces recorded at 500 nm by laser flash photolysis of a deoxygenated hexanes solution of compound **32** in the presence of various concentrations of methylcyclohexene at 25 °C; (b) plot of  $\Delta A_0/\Delta A_{\text{res}}$  vs concentration of methylcyclohexene from the same experiment. Error is reported as  $\pm 2\sigma$ .

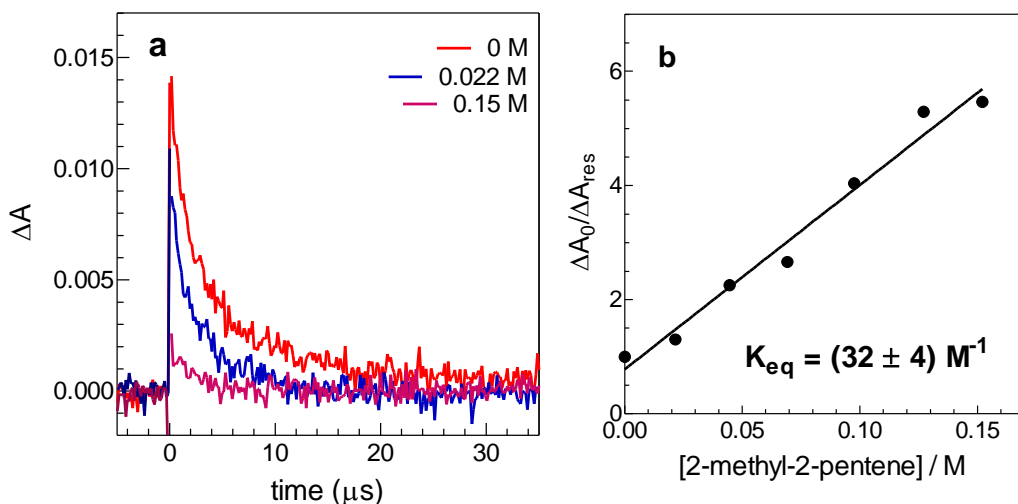


Figure 2.6. (a) Corrected transient decay traces recorded at 500 nm by laser flash photolysis of a deoxygenated hexanes solution of compound **32** in the presence of various concentrations of 2-methyl-2-pentene at 25 °C; (b) plot of  $\Delta A_0/\Delta A_{\text{res}}$  vs concentration of 2-methyl-2-pentene from the same experiment. Error is reported as  $\pm 2\sigma$ .

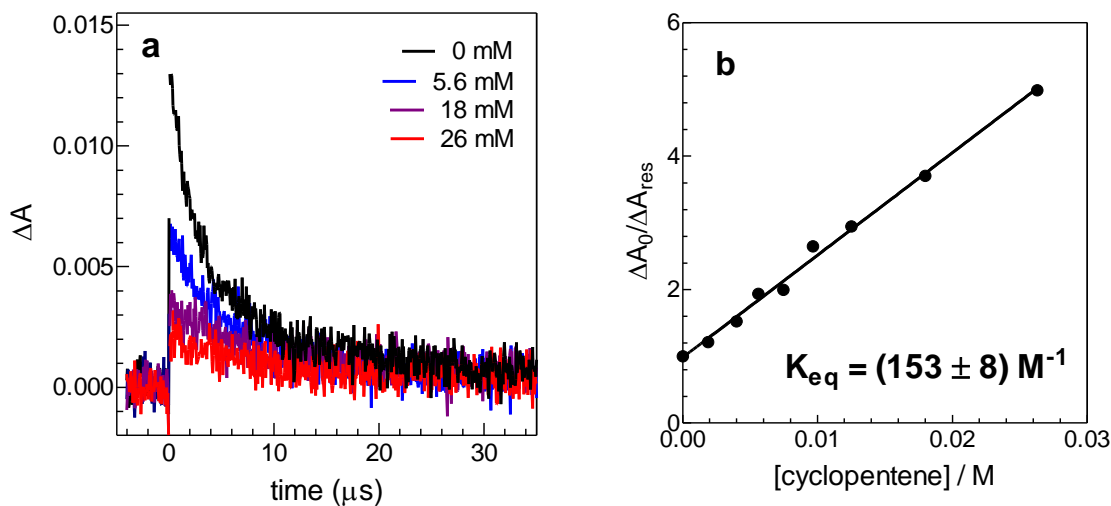


Figure 2.7. (a) Corrected transient decay traces recorded at 500 nm by laser flash photolysis of a deoxygenated hexanes solution of compound **32** in the presence of various concentrations of cyclopentene at 25 °C; (b) plot of  $\Delta A_0/\Delta A_{\text{res}}$  vs concentration of cyclopentene from the same experiment. Error is reported as  $\pm 2\sigma$ .

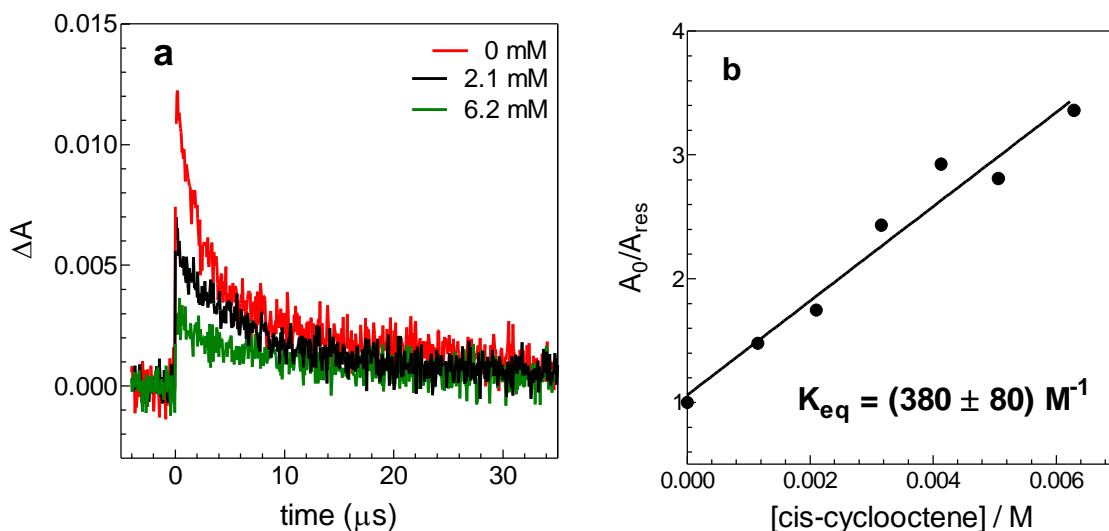


Figure 2.8. (a) Corrected transient decay traces recorded at 500 nm by laser flash photolysis of a deoxygenated hexanes solution of compound **32** in the presence of various concentrations of cis-cyclooctene at 25 °C; (b) plot of  $\Delta A_0/\Delta A_{\text{res}}$  vs concentration of cis-cyclooctene from the same experiment. Error is reported as  $\pm 2\sigma$ .

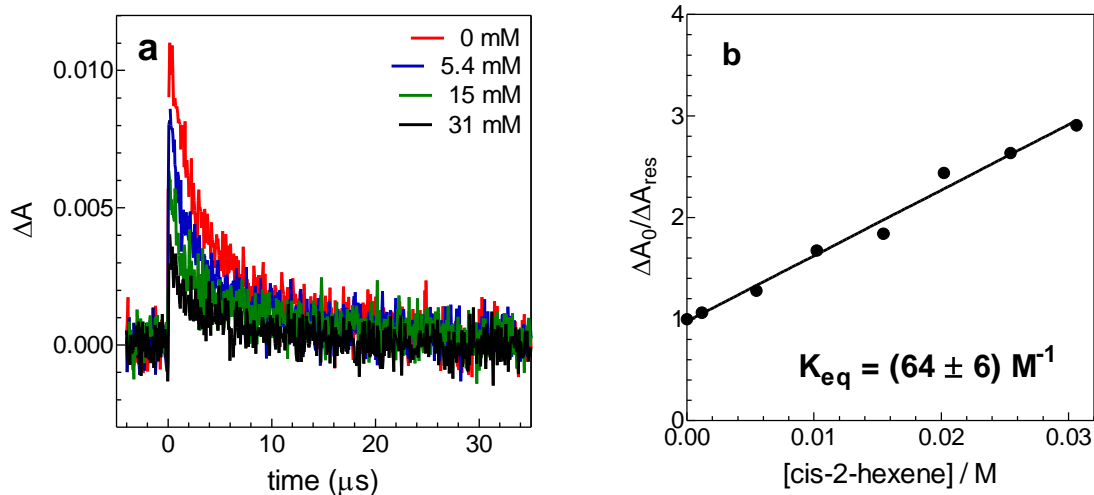


Figure 2.9. (a) Corrected transient decay traces recorded at 500 nm by laser flash photolysis of a deoxygenated hexanes solution of compound **32** in the presence of various concentrations of cis-2-hexene at 25 °C; (b) plot of  $\Delta A_0/\Delta A_{\text{res}}$  vs concentration of cis-2-hexene from the same experiment. Error is reported as  $\pm 2\sigma$ .

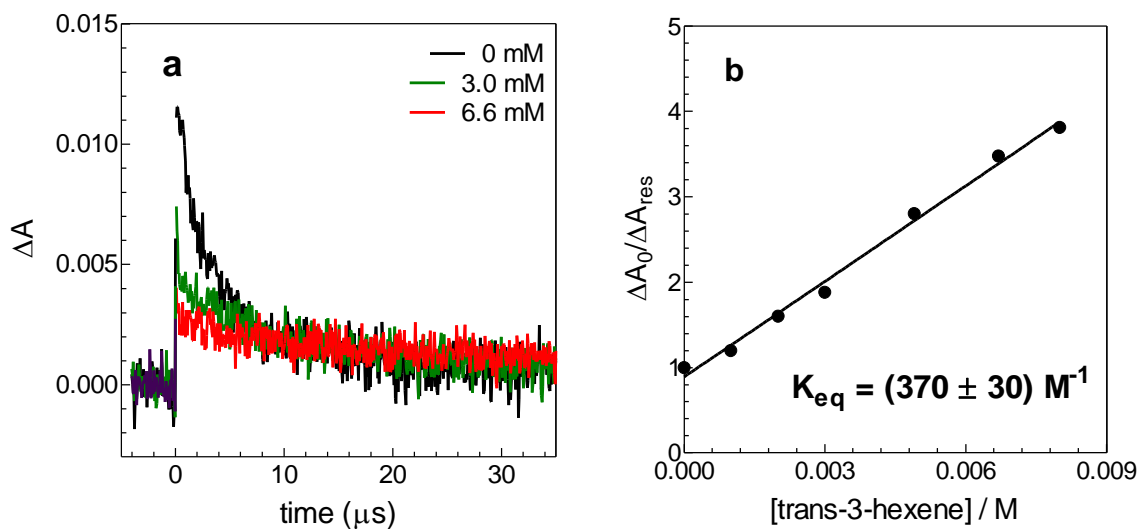


Figure 2.10. (a) Corrected transient decay traces recorded at 500 nm by laser flash photolysis of a deoxygenated hexanes solution of compound **32** in the presence of various concentrations of trans-3-hexene at 25 °C; (b) plot of  $\Delta A_0/\Delta A_{\text{res}}$  vs concentration of trans-3-hexene from the same experiment. Error is reported as  $\pm 2\sigma$ .

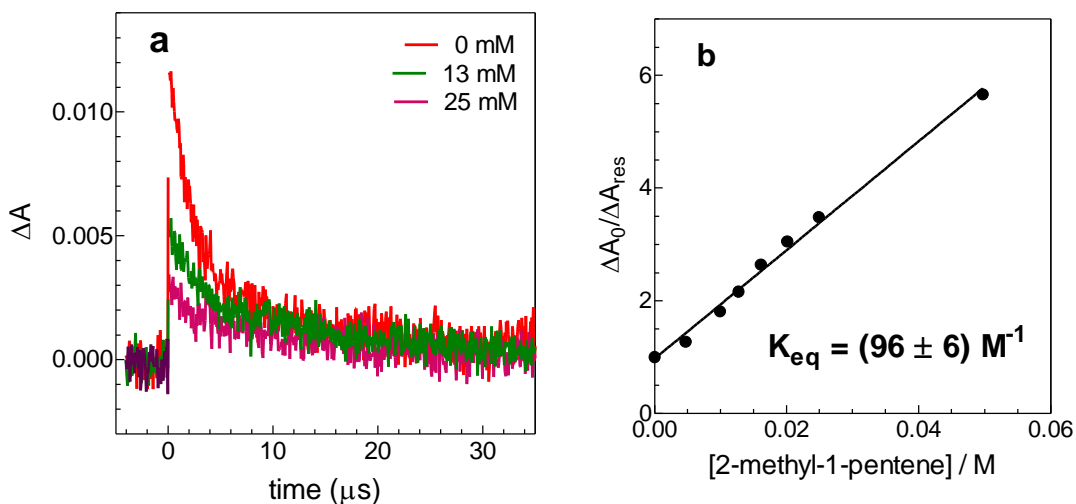


Figure 2.11. (a) Corrected transient decay traces recorded at 500nm by laser flash photolysis of a deoxygenated hexanes solution of compound **32** in the presence of various concentrations of 2-methyl-1-pentene at 25 °C; (b) plot of  $\Delta A_0/\Delta A_{\text{res}}$  vs concentration of 2-methyl-1-pentene from the same experiment. Error is reported as  $\pm 2\sigma$ .

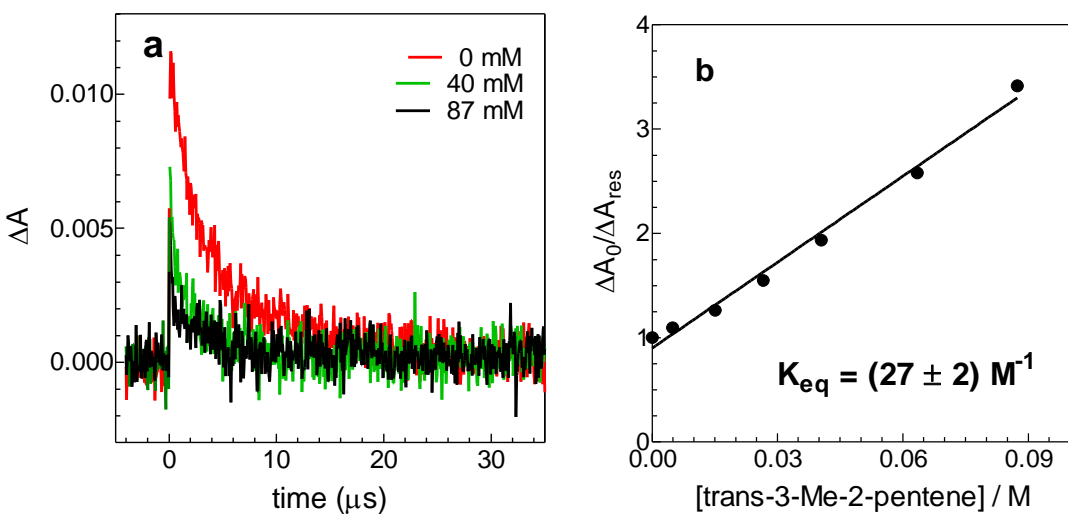


Figure 2.12. (a) Corrected transient decay traces recorded at 500 nm by laser flash photolysis of a deoxygenated hexanes solution of compound **32** in the presence of various concentrations of trans-3-methyl-2-pentene at 25 °C; (b) plot of  $\Delta A_0/\Delta A_{\text{res}}$  vs concentration of trans-3-methyl-2-pentene from the same experiment. Error is reported as  $\pm 2\sigma$ .

Table 2.1. Parameters from the laser experiment studies of the reaction of  $\text{GePh}_2$  with alkenes **a-j**, including the concentration range of the alkenes used in the experiments and the absorbance of the alkene solution at 248 nm. Slope, Y-intercept and  $r^2$  values are obtained from the linear regression analysis of the plots of  $\Delta A_0/\Delta A_{\text{res}}$  versus concentration of alkene in each experiment.<sup>a</sup>

alkene	Concentration range(M)	Slope $r^2$	Y-intercept	Absorbance at 248 nm <sup>b</sup>
(a) 2-methyl-2-pentene	0 - 0.152	$32 \pm 4$ 0.9781	$0.78 \pm 0.19$	0.27 (0.2M)
(b) 2-methyl-1-pentene	0 - 0.049	$96 \pm 6$ 0.9938	$0.96 \pm 0.07$	0.21 (0.17M)
(c) methylcyclohexene	0 - 0.022	$40 \pm 4$ 0.9838	$0.69 \pm 0.25$	0.24 (0.12M)
(d) cyclohexene	0 - 0.69	$2.1 \pm 0.4$ 0.9606	$0.99 \pm 0.07$	0.20 (0.2M)
(e) trans-3-hexene	0 - 0.008	$370 \pm 30$ 0.9928	$0.89 \pm 0.06$	0.21 (0.19M)
(f) cis-cyclooctene	0 - 0.0062	$380 \pm 80$ 0.9614	$1.06 \pm 0.13$	0.24 (0.16M)
(g) cyclopentene	0 - 0.026	$153 \pm 8$ 0.9946	$0.98 \pm 0.05$	0.25 (0.23M)
(h) 1-hexene	0 - 0.0015	$(k_D) 7800 \pm 1400$ $(K_{\text{eq}}) 9400 \pm 1200$	$(k_D) 1.42 \pm 0.53$ $(K_{\text{eq}}) 1.83 \pm 0.42$	Not available
(i) cis-2-hexene	0 - 0.030	$64 \pm 6$ 0.9867	$0.98 \pm 0.05$	0.22 (0.14M)
(j) trans-3-methyl-2-pentene	0 - 0.087	$27 \pm 2$ 0.9901	$0.89 \pm 0.05$	0.34 (2.2M)

(a) Errors are listed as  $\pm 2\sigma$  (b) The number in parenthesis shows the concentration of the alkene solution prepared for the static UV measurements prior to the laser experiment. All the stock solutions of alkenes were prepared in dry hexanes. Path length for the UV measurements was 7mm in all experiments.

Table 2.2. Experimental equilibrium constants and Gibbs free energies for the reactions of GePh<sub>2</sub> with alkenes in deoxygenated hexane solution at 25 °C along with the ionization potential of the involved alkene. All IP values are taken from the National Institute of Standards and Technology of the United States (NIST).<sup>6</sup>

Compound name	$K_{eq} (M^{-1})^a$	$\Delta G^\circ(kcal/mol)^b$	IP(kcal/mol) <sup>6</sup>
(a) 2-methyl-2-pentene	32 ± 4	-0.19 ± 0.07	198 ± 3
(b) 2-methyl-1-pentene	96 ± 6	-0.81 ± 0.02	208.0 ± 0.2
(c) methylcyclohexene	40 ± 4	-0.31 ± 0.04	200.0 ± 0.9
(d) cyclohexene	2.1 ± 0.4	1.45 ± 0.06	206.0 ± 0.4
(e) trans-3-hexene	370 ± 30	-1.61 ± 0.02	207.0 ± 0.4
(f) cis-cyclooctene	380 ± 80 (416 ± 40)	-1.60 ± 0.08	208
(g) cyclopentene	153 ± 8 (129 ± 4)	-1.08 ± 0.02	210.0 ± 0.4
(h) 1-hexene	9400 ± 1200	-3.51 ± 0.04	218 ± 2
(i) cis-2-hexene	64 ± 6	-0.57 ± 0.03	207.0 ± 0.2
(j) trans-3-methyl-2-pentene	27 ± 2	-0.09 ± 0.04	198 <sup>c</sup>

(a) The number in parenthesis shows the result of a replicate experiment. Errors are listed as  $\pm 2\sigma$  (b)  $\Delta G^\circ$  is the gas phase Gibbs free energy (at 25 °C, 1 atm) and is calculated as follows: first, measured solution phase equilibrium constant ( $K_c$ ) is converted to the gas phase equilibrium constant ( $K_p$ ) using equation  $K_p = (K_c / RT)$  where  $R = 0.082 \text{ L.atm.K}^{-1}.\text{mol}^{-1}$  and  $T = 298.15 \text{ K}$ . Then,  $K_p$  is placed in the equation  $\Delta G^\circ = -RT \ln K_p$ , where  $R = 0.00198 \text{ kcal.K}^{-1}.\text{mol}^{-1}$  and  $T = 298.15 \text{ K}$ . (c) Reference 8.

## 2.2.6. Discussion

The reactions of diphenylgermylene with 10 different alkenes (half of them are measured for the first time) were investigated in this project in continuation of previous works of our group devoted to the reaction of diphenylgermylene with dienes (published)<sup>9</sup> and alkenes (unpublished) to evaluate the effect of alkene substitution on the thermodynamic stabilities of germiranes.

The experimental results, which are summarized in Table 2.2, show that the reaction of diphenylgermylene with alkenes suits in the small- $K_{eq}$  regimes (except for 1-hexene) so only equilibrium constants for these reactions were measurable experimentally.

The measured equilibrium constants are in good general agreement with the previous results of S.S. Chitnis (chapter1, Table 1.3) except for cyclohexene and 1-hexene, for which significant differences were observed. In regard to cyclohexene, the equilibrium constant was measured to be  $2.1 \pm 0.4 \text{ M}^{-1}$  which is seven times higher than the Chitnis's number ( $14 \pm 2 \text{ M}^{-1}$ ). This difference is most likely due to the absorbance of impurities in the alkene sample which was previously unaccounted for.

The results presented in Table 2.2 establish a rough correlation between the Gibbs free energy of the reaction and the experimental gas-phase ionization potential of the involved alkene (Figure 2.13). The difficulty is cyclohexene which is somewhat off this line. The expected Gibbs free energy is about  $-0.69 \text{ kcal/mol}$  based on the correlation line, but it is found to be  $1.45 \pm 0.12 \text{ kcal/mol}$  ( $K_{eq} = 2.1 \text{ M}^{-1}$ ). This difference could be assigned to the effect of ring strain on the stability of the resulting germiranes which has a boat-like conformation. This could be supported by studies of the cyclohexene conformation in the literature. Statistical mechanics calculations by Pitzer et al. showed  $2.7 \text{ kcal/mol}$  difference in stability between the boat and half chair conformations of cyclohexene.<sup>10</sup> Later, empirical force field studies suggested that there are two half chair conformations of cyclohexene interconverting to each other via a boat conformation which is  $6\text{-}7 \text{ kcal/mol}$  higher in energy.<sup>11</sup> This analysis was enforced by

Anet et al, who calculated a 5.5-6 kcal/mol energy difference between the two conformers using MP2, MP4SDQ, QCISD and QCISD(T) methods.<sup>12</sup>

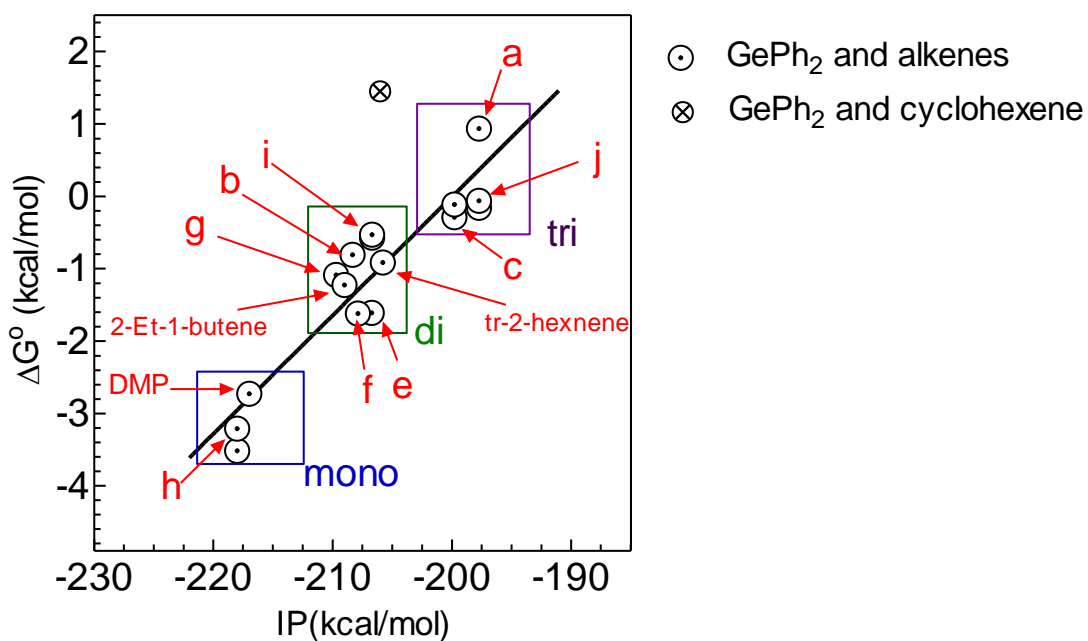
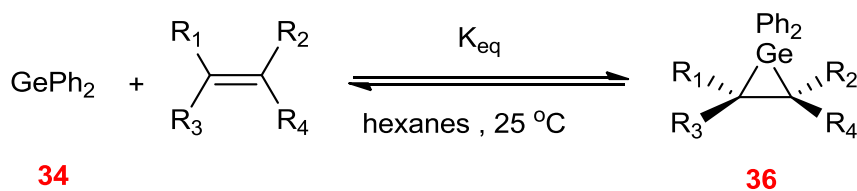


Figure 2.13. Gibbs free energy of reaction vs ionization potential of alkenes from the photolysis of **32** in the presence of different alkenes (Table 2.1 in addition to unpublished results of S.S. Chitnis). All IP values are taken from the National Institute of Standards and Technology of the United States (NIST).<sup>6</sup>



## 2.3. Steady-State Photolysis Studies of the Reactions of GePh<sub>2</sub> with Acrylonitrile and 4,4-Dimethyl-1-Pentene (DMP)

### 2.3.1. Overview

One conclusion from the results presented in Figure 2.13 is that the alkenes having higher ionization potential lead to more stable germiranes. Since the electron poor alkenes have higher ionization potential, this suggests that more stable germiranes should result from reaction with nitro-, cyano- and carbonyl- functionalized alkenes. This prediction was tested with an investigation of the reaction of GePh<sub>2</sub> with acrylonitrile, which is expected to proceed irreversibly based on the experimental correlation line in Figure 2.13 (predicted  $K_{\text{eq}} > 25000 \text{ M}^{-1}$ , IP of acrylonitrile<sup>6</sup> is -251 kcal/mol).

Transient decay traces of **32** in the presence of acrylonitrile (Figure 2.14a) showed that decays of germylene proceeded completely to the pre-pulse level at all concentrations of alkene studied. This indicates that the equilibrium constant for the reaction responsible for consumption of the germylene is higher than  $25000 \text{ M}^{-1}$ . The forward rate constant for the reaction was measured to be  $k_{\text{Q}} = (1.3 \pm 0.2) \times 10^9 \text{ M}^{-1}\text{s}^{-1}$ , from a plot of  $k_{\text{decay}}$  versus acrylonitrile concentration (eq 2.4) (Figure 2.14b)

Transient absorption spectra recorded with a solution of **32** in hexanes containing 3 mM acrylonitrile (Figure 2.15a) showed a new transient species, exhibiting an absorption band in the 360-450nm region of the spectrum and centered at  $\lambda_{\text{max}} = 340 \text{ nm}$ . This led to some difficulties for the interpretation of the results and raised the possibility of another competing reaction leading to the consumption of germylene.

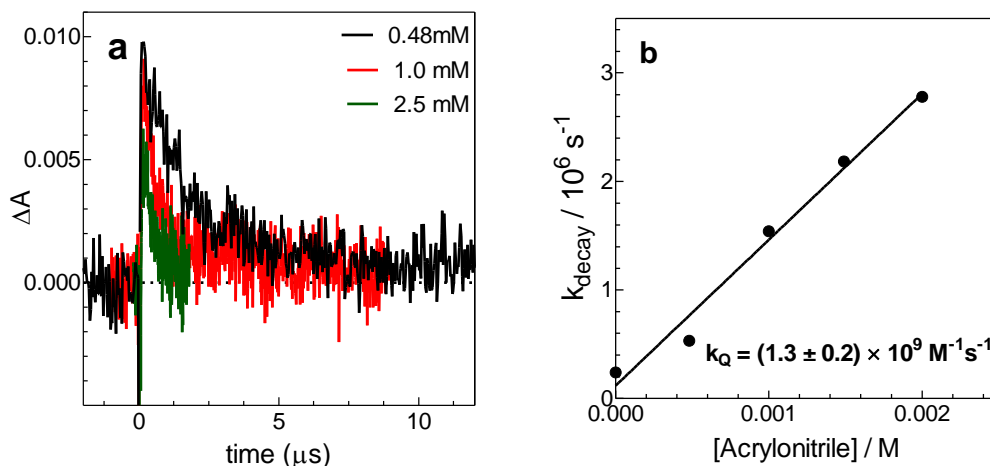


Figure 2.14. (a) Transient decay traces recorded at 500 nm by laser flash photolysis of a deoxygenated hexanes solution of compound **32** in the presence of various concentrations of acrylonitrile at 25 °C (b) Plot of  $k_{\text{decay}}$  vs concentration of acrylonitrile from the same experiment. Error is reported as  $\pm 2\sigma$ .

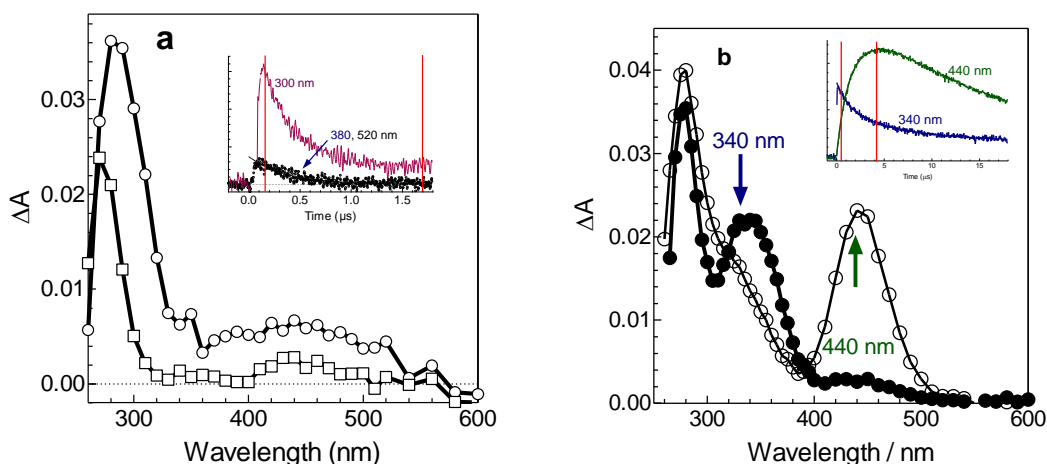
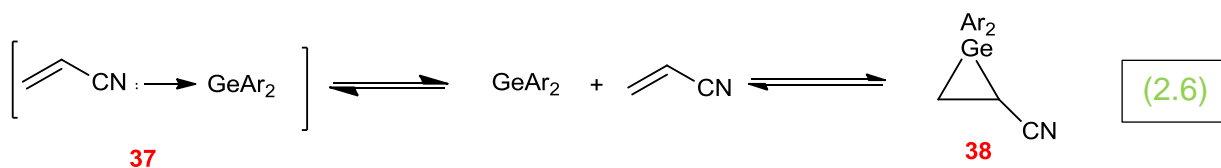
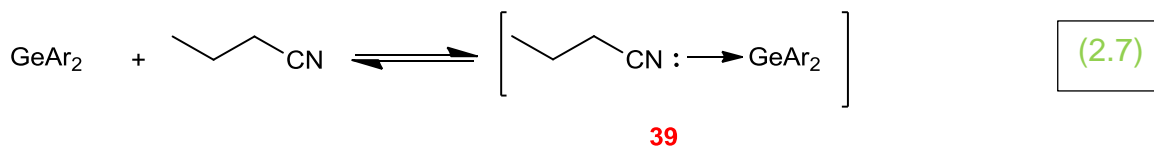


Figure 2.15. (a) Transient UV-vis absorption spectra recorded with a ca. 0.003 M solution of **32** in deoxygenated hexanes containing 3.0 mM acrylonitrile, 170-176 ns ( $\circ$ ), 1.71-1.73  $\mu\text{s}$  ( $\square$ ) after the laser pulse; the inset shows absorbance-time profiles recorded at 300, 380, and 520 nm. (S. S. Chitnis; unpublished) (b) Transient absorption spectra recorded 130-200 ns ( $\circ$ ) and 3.38-4.38  $\mu\text{s}$  ( $\bullet$ ) after the laser pulse, by laser flash photolysis of **32** in deoxygenated, anhydrous hexanes containing 40 mM butyronitrile; the inset shows transient growth/decay profiles recorded at 340 and 440 nm (S. S. Chitnis; unpublished).

The complexity results from the fact that there are now two possible reactions which can compete with germylene dimerization: (1+2)-cycloaddition of germylene to the C=C double bond, leading to the formation of germirane (**38**), and the coordination of acrylonitrile by the lone pair on nitrogen to form a Lewis acid-base complex (**37**) (eq 2.6). Therefore it is reasonable to assume that the new absorption band centered at  $\lambda_{\max} = 340$  nm is due to the Lewis acid-base complex **37**.



The validity of this assignment was tested by examining the reaction of the germylene with n-butyronitrile, without possibility of a (1+2)-cycloaddition reaction (eq 2.7). The transient spectra recorded after addition of n-butyronitrile to a 3 mM solution of **32** in hexanes showed a new transient absorption centered at  $\lambda_{\max} = 340$  nm along with the absorption at  $\lambda_{\max} = 500$  nm (germylene) and 440 nm (digermene) (Figure 2.15b). This transient decays on a similar time scale to that of the germylene absorptions, and it is the only species observable in the presence of 52 mM butyronitrile.



Since the complexation process can be assumed to be sensitive to the Lewis acidity of the germylene, it is reasonable to expect that installation of electron donors on germanium should disfavour the complexation step. Therefore in the hope of suppressing the complexation step, transient spectra of bis(4-methylphenyl)germylene in dry deoxygenated solution of hexanes in the presence of 5.5 mM of acrylonitrile was recorded (Figure 2.16b). The spectra showed the same characteristics as the  $\text{GePh}_2$  spectra and a transient absorption band centered at  $\lambda_{\text{max}} = 370 \text{ nm}$  was indicative of the complexation process. The spectrum of the complex appeared to be red-shifted from that of  $\text{GePh}_2$  due to the difference in the Lewis acidity between the two germylenes.

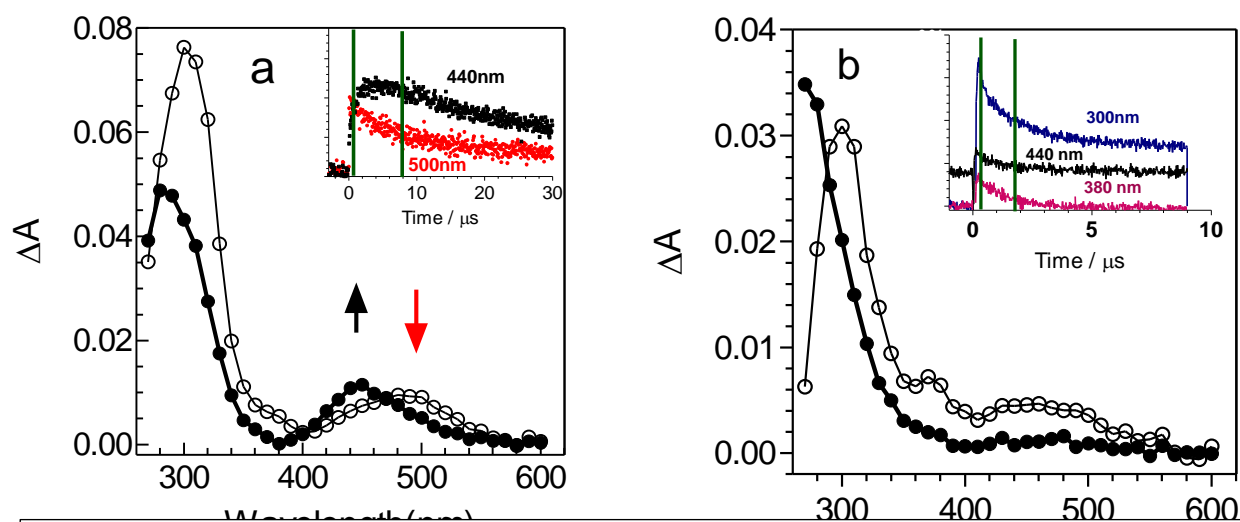


Figure 2.16. (a) Transient absorption spectra recorded 320-576 ns( $\circ$ ) and 8.77-9.15  $\mu\text{s}$ ( $\bullet$ ) after the laser pulse, by laser flash photolysis of a deoxygenated hexanes solution of 1,1-bis-(4-methylphenyl)-3,4-dimethyl-1-germacyclopent-3-ene; the inset shows transient growth/decay profiles recorded at 440 and 500 nm. (b) Transient absorption spectra recorded 208-272 ns( $\circ$ ) and 1.87-1.97  $\mu\text{s}$ ( $\bullet$ ) after the laser pulse, by laser flash photolysis of a deoxygenated hexanes solution of 1,1-bis-(4-methylphenyl)-3,4-dimethyl-1-germacyclopent-3-ene containing 5.5 mM of acrylonitrile; the inset shows transient growth/decay profiles recorded at 300, 380 and 440 nm (offset).

Considering the presented data for the reaction of  $\text{GePh}_2$  with acrylonitrile, it should be determined whether the corresponding germirane was formed in the reaction mixture or not. Germiranes are short lived reactive species and only spectroscopic evidences were provided in this thesis in support of their existence. Since the spectroscopic data for the reaction of  $\text{GePh}_2$  with acrylonitrile was hard to interpret, more information was needed to prove the formation of the germirane. For this purpose, there was no better option than finding a way to trap the transient germirane. There were several reports about using methanol as trapping reagent for germynes<sup>3,5,7</sup> and Neumann et al proposed a mechanism for a germirane being trapped by water.<sup>13</sup> Therefore, a series of product studies were performed to investigate further the reaction of  $\text{GePh}_2$  with acrylonitrile, in the hope of trapping the resulting germirane with methanol.

### 2.3.2. Steady-State Photolysis Study of the Reaction of $\text{GePh}_2$ with Acrylonitrile

A 0.055 M solution of **32** in cyclohexane- $\text{d}_{12}$  in the presence of 0.087 M acrylonitrile was irradiated using 4 lamps (254 nm). The total irradiation time was 16 minutes, with  $^1\text{H}$  NMR spectra being recorded in 1 minute intervals up to the sixth minute and then in 2 minute intervals up to the end of the experiment. The consumption of **32** after 16 minutes irradiation was 23%.

Figure 2.17 shows the  $^1\text{H}$  NMR spectra of the reaction mixture before irradiation and after 16 minutes irradiation. In the first spectrum (A), the peaks due to **32**, acrylonitrile, internal standard ( $\text{Si}_2\text{Me}_6$ ) and solvent (cyclohexane- $\text{d}_{12}$ ) are distinguishable. Upon irradiation,  $\text{GePh}_2$  extrudes and DMB forms after a photochemical

reaction of the precursor; the formed germylene reacts with acrylonitrile in a competition with germylene dimerization reaction (eq 2.8).

The lifetime of all possible products (Lewis acid-base complex, germirane and digermene) are at most milliseconds so they will not show up in  $^1\text{H}$  NMR spectra. That's why the most obvious changes in the  $^1\text{H}$  NMR taken after irradiation (Figure 2.17.B) are the peaks that belong to DMB. In addition, broadening of the aliphatic ( $\delta$  1.0-2.5) and aromatic ( $\delta$  6.8-7.7) regions were observed in the spectrum. This broadening became more noticeable as the reaction progressed which was an indication that the fate of formed germylene in the solution was polymerization.<sup>4</sup>

As irradiation proceeded, more precursor was consumed and additional amounts of DMB were formed. Thus, the integration of precursor decreases and the integration of DMB peaks increases during experiment. Since the initial concentration of all materials was known, the changes in integration can be converted to changes of concentrations. Plotting this concentration changes (Figure 2.18) gave the rates of precursor consumption and DMB formation.

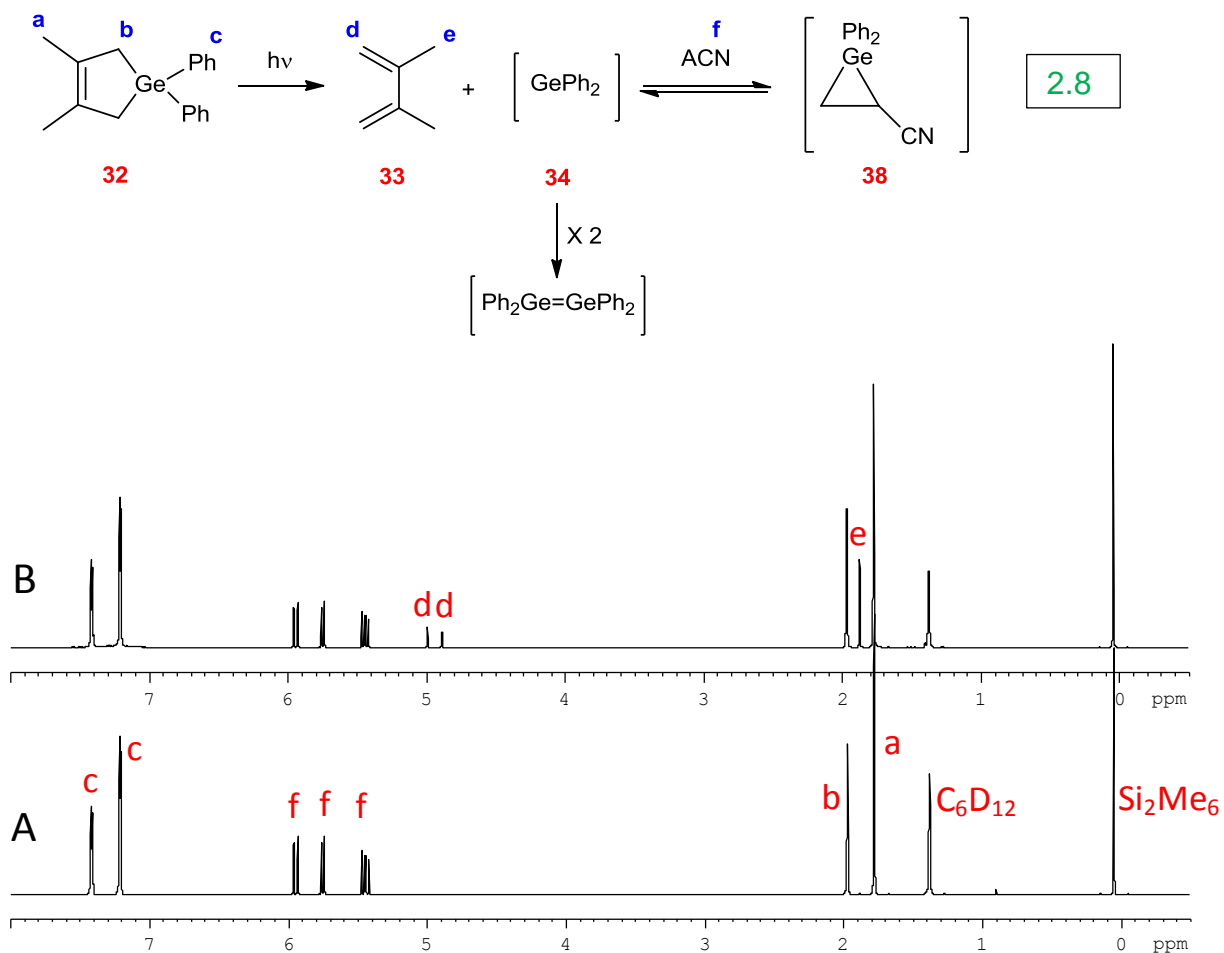


Figure 2.17. Photolysis of argon-saturated cyclohexane- $\text{d}_{12}$  solution of **32** (0.055 M) with four low-pressure mercury lamps (254 nm) in the presence of acrylonitrile (0.087 M) (A) before irradiation (B) after irradiation for 16 minutes.

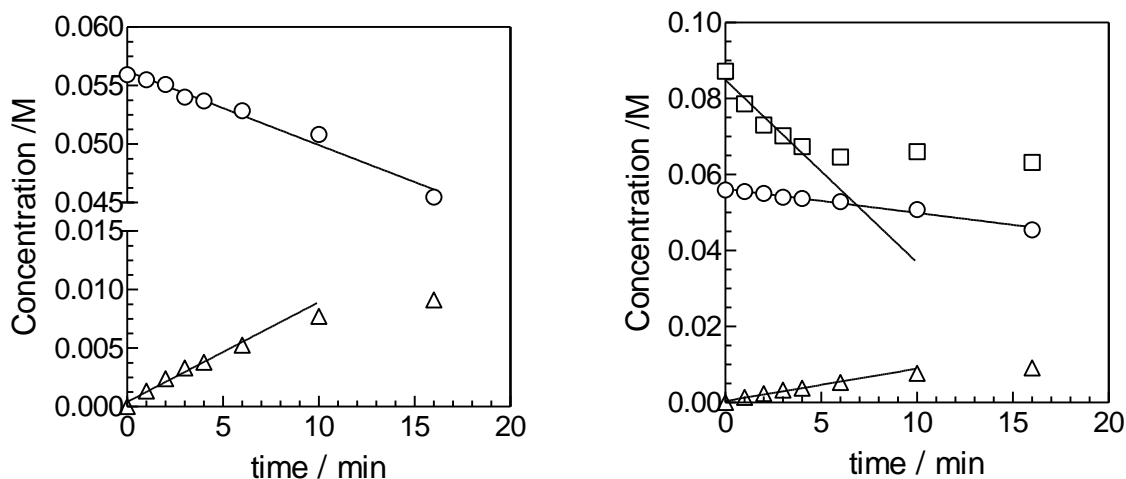
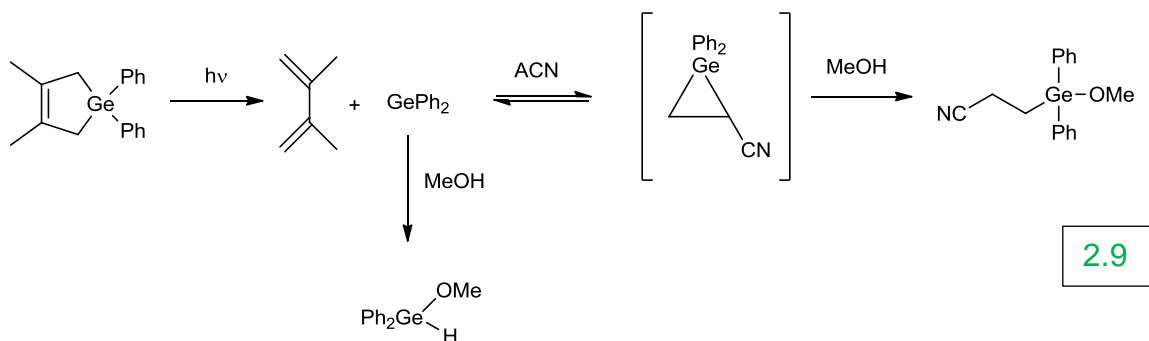


Figure 2.18. Concentration vs. time plot from irradiation of an argon-saturated cyclohexane-d<sub>12</sub> solution of the **32** (0.055 M) with four low-pressure mercury lamps in the presence of acrylonitrile (0.087 M). Precursor **32** (○), slope:  $-0.00063 \pm 0.00004$ ; DMB (Δ), slope:  $+0.00072 \pm 0.00007$ ; Acrylonitrile (□), slope:  $-0.0048 \pm 0.0007$ .

#### 2.3.4. Steady-State Photolysis Studies of the Reaction of GePh<sub>2</sub> with Acrylonitrile in the Presence of Methanol

In another product study, methanol was added to the solution to trap the resulting germirane. Methanol however can also directly react with germylene to give the insertion product (eq 2.9). The rate and equilibrium constants for the reaction of methanol with GePh<sub>2</sub> were reported to be  $(6.1 \pm 1.1) \times 10^9 \text{ M}^{-1}\text{s}^{-1}$  and  $(3300 \pm 800) \text{ M}^{-1}$  respectively in hexanes at 25 °C.<sup>7</sup>





A 0.050 M solution of **32** in cyclohexane- $d_{12}$  containing 0.071 M of acrylonitrile and 0.022 M of methanol was irradiated with four lamps (254 nm) for a total of 14 minutes. The irradiation was done in 2 minute intervals and the reaction was monitored by  $^1\text{H}$  NMR spectroscopy.

The  $^1\text{H}$  NMR spectrum of the sample before irradiation showed peaks due to the precursor, acrylonitrile and methanol (Figure 2.19A). After irradiation, new peaks appeared in the spectrum (Figure 2.19B). The peaks of DMB were easy to assign, but the challenge was the correct assignment for the insertion product **41** and the new alkyl-alkoxy germane resulting from trapping of germirane by methanol, the trapped product, (**40**) (Figure 2.19).

In a previous study of the reaction of  $\text{GePh}_2$  with methanol<sup>5,14</sup> the NMR spectrum of **41** was reported as follows:  $^1\text{H}$  NMR ( $\text{C}_6\text{D}_{12}$ )<sup>14</sup>,  $\delta = 3.54$  (s, 3H), 6.12 (s, 1H), 7.2-7.32 (m, 6H), 7.59-7.63 (m, 4H). Thus, the peak appearing at 6.09 ppm would be assigned to the Ge-H proton in the insertion product **41** (Figure 2.19B, proton *m*), and its methoxy group should be the peak found at 3.53 ppm (Figure 2.19B, protons *h*).

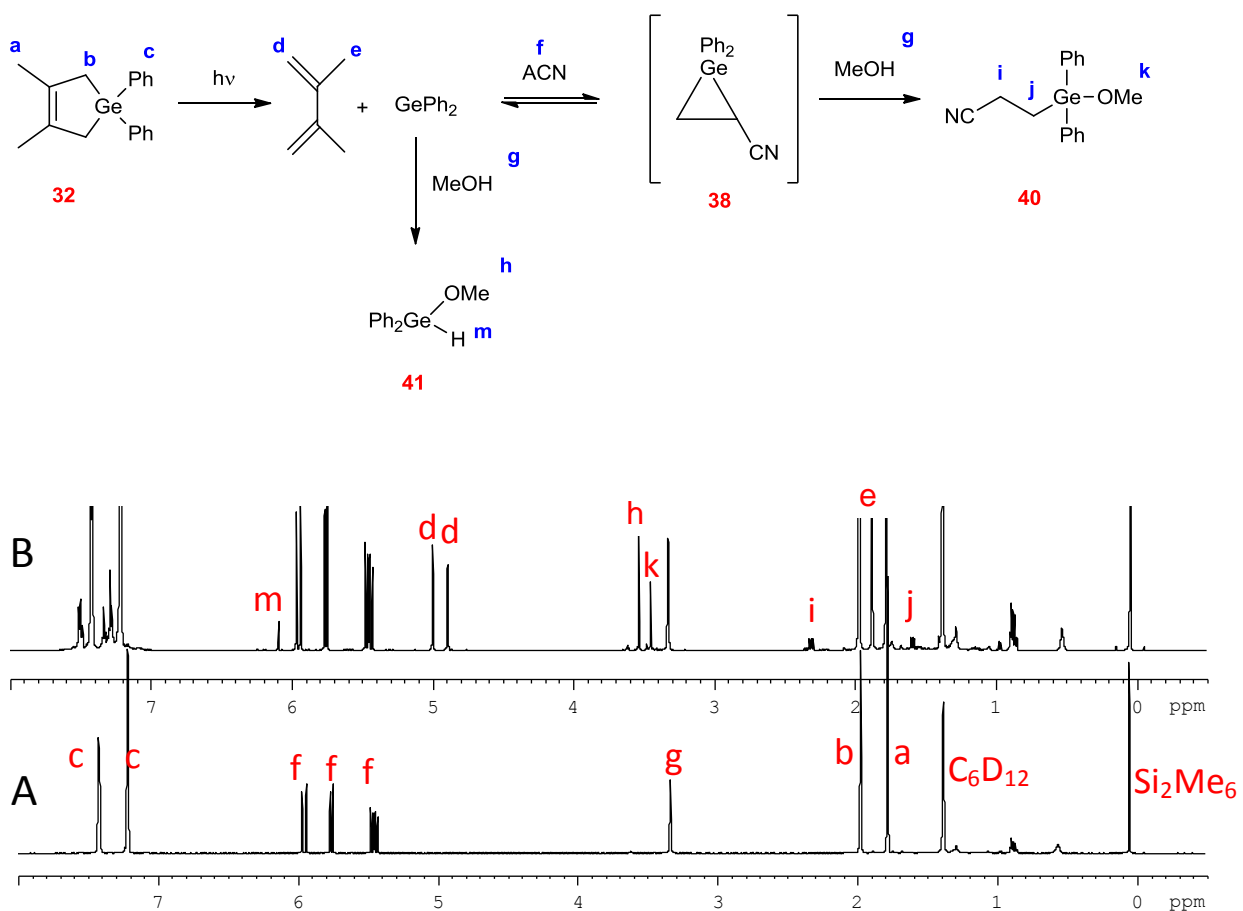


Figure 2.19. Photolysis of an argon-saturated cyclohexane- $\text{d}_{12}$  solution of **32** (0.050 M) with four low-pressure mercury lamps (254 nm) in the presence of acrylonitrile (0.071 M) and MeOH (0.022 M) a- before irradiation b-after 14 min irradiation.

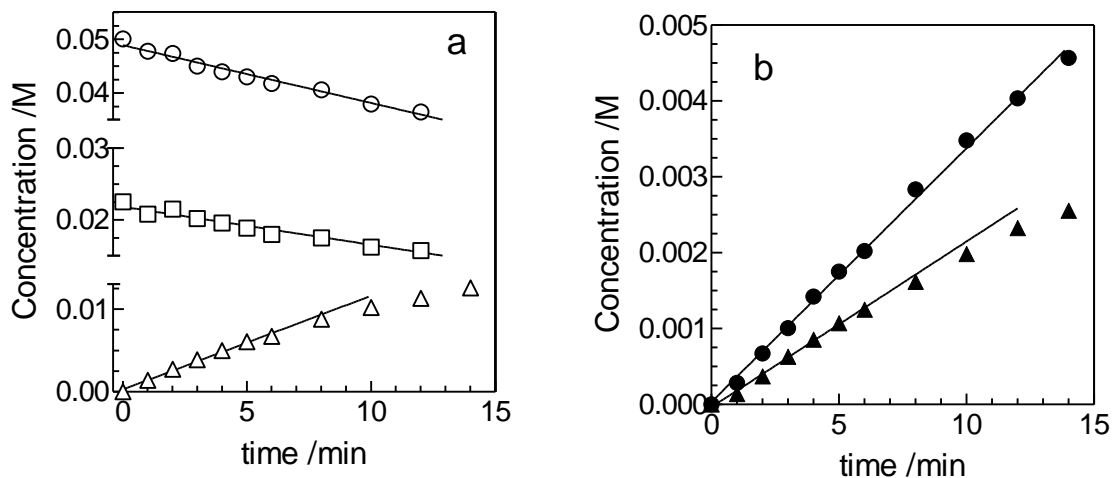
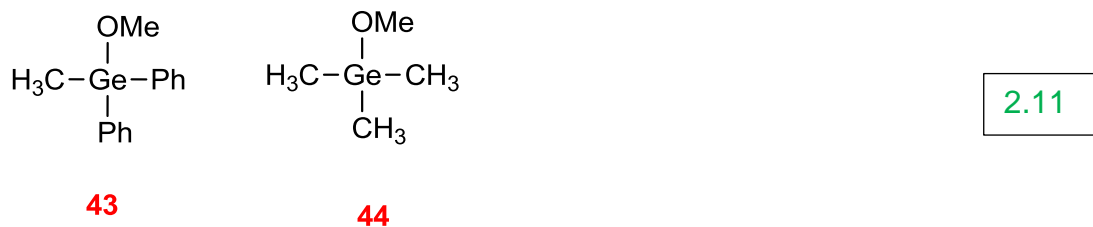
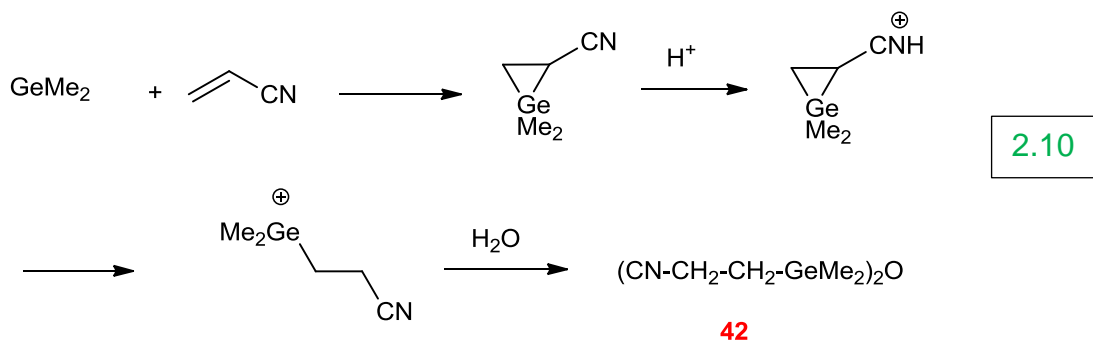


Figure 2.20. Concentration vs. time plots from irradiation of an argon-saturated cyclohexane- $d_{12}$  solution of **32** (0.050 M) with four low-pressure mercury lamps in the presence of acrylonitrile (0.071 M) and MeOH (0.022 M) a- precursor **32** ( $\circ$ ), slope:  $-0.00107 \pm 0.00004$ ; DMB ( $\Delta$ ), slope:  $+0.00113 \pm 0.00005$ ; methanol ( $\square$ ), slope:  $-0.00053 \pm 0.00003$ ; b- trapped product **40** ( $\blacktriangle$ ), slope:  $+0.000218 \pm 0.000006$ ; insertion product **41** ( $\bullet$ ), slope:  $-0.000335 \pm 0.000006$

The only compound similar to **40** was reported by Neumann et.al. in a study of the reaction of  $\text{GeMe}_2$  with acrylonitrile in the presence of water on silica gel (eq 2.10).<sup>13</sup> They concluded that after formation of the corresponding germirane (from (1+2)-cycloaddition of  $\text{GeMe}_2$  into the double bond of acrylonitrile), it reacts with water to form the formal hydrogermylation product of the reaction. The reported  $^1\text{H}$  NMR spectrum of the trapped product (**42**) is:  $^1\text{H}$  NMR( $\text{CDCl}_3$ )  $\delta=0.44$  (s, 12H,  $\text{GeMe}_2$ ), 1.18 (t,  $J = 7.8$  Hz, 4H,  $\text{CH}_2$ ), 2.51 (t,  $J = 7.8$  Hz, 4H,  $\text{CH}_2$ ).

The reported  $^1\text{H}$  NMR spectra of two other methoxygermane derivatives are helpful in making assignments for **40**. First is compound **43** whose  $^1\text{H}$  NMR spectra was reported as follows<sup>15</sup>:  $^1\text{H}$  NMR( $\text{CDCl}_3$ )  $\delta = 0.71$  (s, 3H), 3.44 (s, 3H), 7.10–7.35 (m, 6H), 7.42–7.61 (m, 4H). The other one is compound **44** whose spectra was reported<sup>16</sup> as  $\delta =$

0.32 (s, 9H), 3.35 (s, 3H) (eq 2.11). The assignment of the peak at  $\delta$  3.45 ppm to the methoxy protons in **40** is consistent with the chemical shift of the methoxy protons in **43**.



Considering the reported  $^1\text{H}$  NMR spectra of **42**, it is reasonable to expect that protons *i* and *j* appear as two triplets. Protons *j* are similar to protons of the  $\text{CH}_2$  group attached to germanium on compound **42** which was reported to appear at 1.18 ppm. Since the methyl group on compound **43** has appeared 0.5 ppm higher than their counterpart on compound **44**, protons *j* are expected to appear 0.5 ppm higher than 1.18 ppm, somewhere around 1.6 ppm. Protons *i* are further from germanium and their chemical shift are expected to get affected less than protons *j*, from compound **42** to **40**. Therefore, two sets of peaks at 2.30 and 1.58 ppm which were growing during photolysis (Figure 2.19B) were assigned to protons *i* and *j* respectively. The integration

of the *i* and *j* peaks are 2.3 and 3.3 relative to an integral of three for the methoxy group of **41** (protons *k*). As shown in the expansion of the spectrum (Fig 2.22 C), the splitting of *i* and *j* is like a distorted triplet, probably due to the effect of other unassigned peaks that were appeared close to them.

The ratio of protons *h* over *k* in the  $^1\text{H}$  NMR spectra decreased during the first 3 minutes of the experiment and then it remained roughly constant, suggesting that the yield of the insertion product (**41**) relative to that of **40** was higher in the initial stages of the photolysis (Figure 2.20).

In a similar experiment, the NMR tube was placed in the dark after 30 min irradiation (room temperature; 22 - 24 °C) to check for any possible dark reaction. A  $^1\text{H}$  NMR spectrum taken after 48 hours showed that the peaks of insertion product **41** (protons *m* and *h*) had decreased to half of their original values, in contrast to a small reduction in the intensity of the signal assigned to the trapped product **40** (protons *k*) (Figure 2.21).

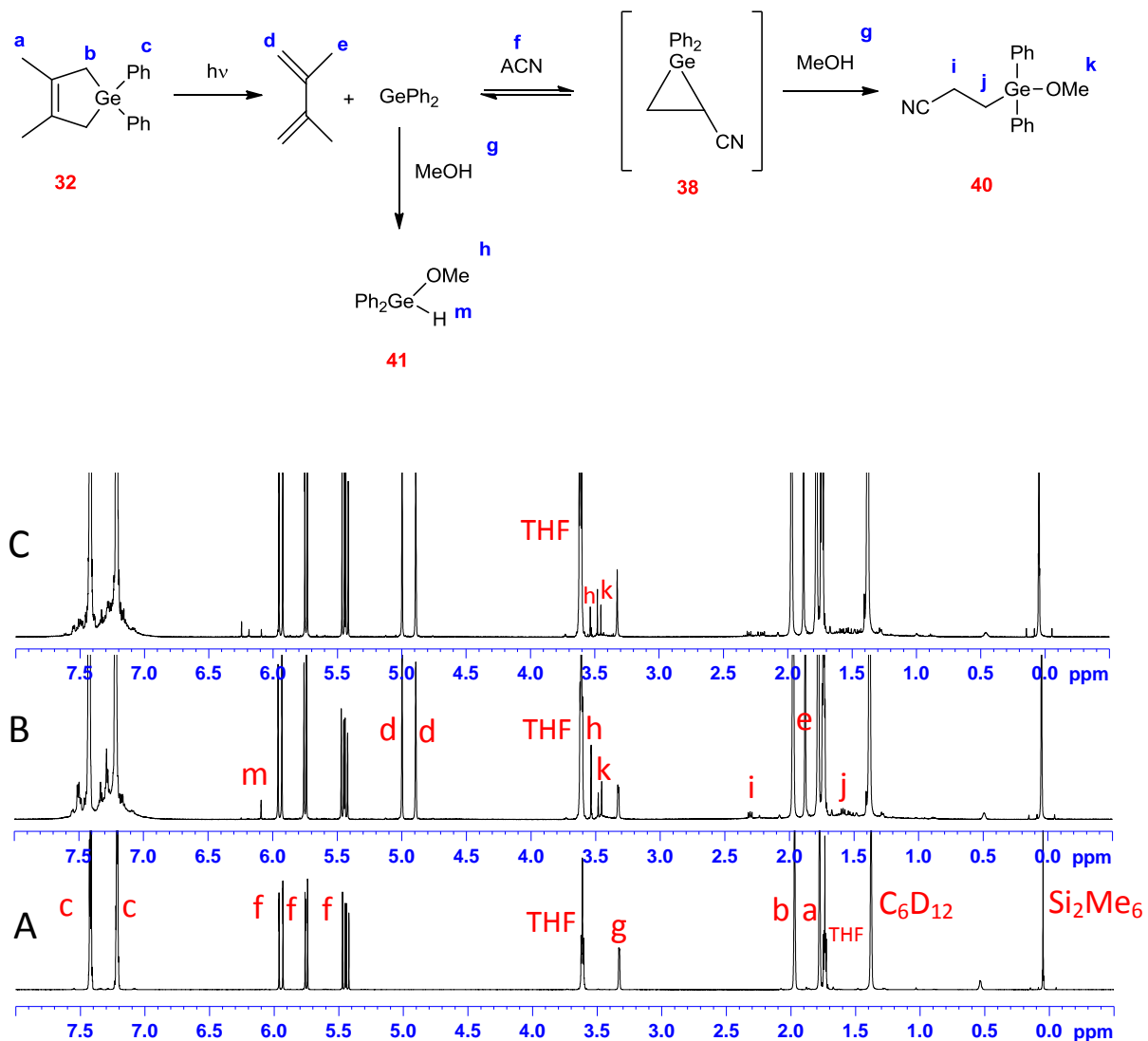


Figure 2.21. Photolysis of an argon-saturated cyclohexane- $\text{d}_{12}$  solution of **32** (0.05 M) with four low-pressure mercury lamps (254 nm) in the presence of acrylonitrile (0.06 M) and MeOH (0.04 M). a- before irradiation; b-after 30 min irradiation; c- after leaving the sample for 48 hours in dark.

In the hope of providing more evidence of the existence of the trapped product it was decided to increase the irradiation time to build more concentration of **40**. Therefore, a 0.055 M solution of **32** in cyclohexane-d<sub>12</sub> containing 0.082 M of acrylonitrile and 0.030 M of methanol was irradiated for 30 minutes which yielded 49% and 55% consumption of the precursor and methanol respectively. After removal of the volatile components by rotary evaporator, the residue was dissolved in C<sub>6</sub>D<sub>12</sub> and the existence of the products was checked. It appeared that the insertion product **41** (protons *h* and *m*) were gone but the peaks assigned to the trapped product **40** (protons *i*, *j* and *k*) were still in the sample (Figure 2.22C).

Since methoxygermanes are reported not to survive column chromatography without substantial decomposition,<sup>17</sup> no attempts were made to isolate **40** by column chromatography. Normal-phase HPLC showed that the products **40** and **41** have high retention times and are not isolable. GC-MS analysis also was not successful to show indication of **40**, probably due to low concentration or strange fragmentation patterns.

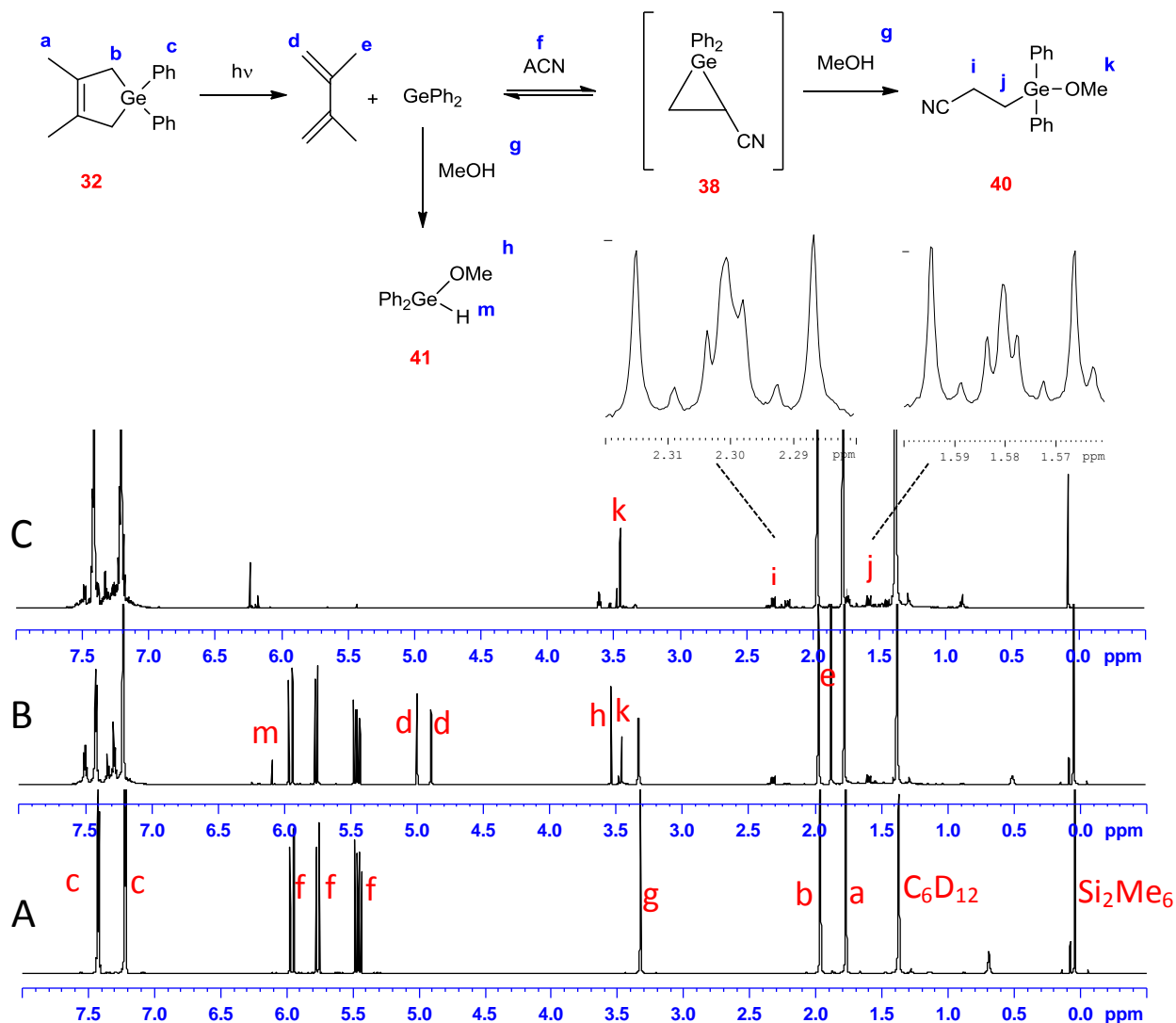


Figure 2.22. Photolysis of an argon-saturated cyclohexane- $d_{12}$  solution of **32** (0.055 M) with four low-pressure mercury lamps (254 nm) in the presence of acrylonitrile (0.082 M) and MeOH (0.03 M). a- before irradiation; b-after 30 min irradiation; c- after removing volatile components.

### 2.3.5. Steady-State Photolysis Studies of the Reaction of $\text{GePh}_2$ with 4,4-Dimethyl-1-Pentene (DMP) in the Presence of Methanol (MeOH)

Acrylonitrile is a very reactive compound mainly because of the activation of its double bond due to conjugation with the nitrile group. It polymerizes spontaneously



(which accelerates in the presence of radiation)<sup>18</sup> and undergoes different reactions such as hydrogenation, hydroformylation and Diels-Alder cycloaddition.<sup>18</sup> The nitrile group of acrylonitrile is also reactive, and its hydrolysis and alcoholysis are well known.<sup>18</sup> This level of reactivity and the possibility of side reactions limit the applicable concentration of acrylonitrile in the trapping experiment and make the interpretation of the steady state photolysis more complicated. This is especially problematic in our analysis because we made assignments for a new compound that is not reported in the literature. Therefore, another alkene was chosen to perform the trapping experiment. DMP was a very good candidate because it is not as reactive as acrylonitrile, it has a relatively high ionization potential<sup>6</sup> ( $-221.3 \text{ kcal mol}^{-1}$ ) and its reaction with  $\text{GePh}_2$  was investigated before (rate constant =  $(4.2 \pm 0.2) \times 10^9 \text{ M}^{-1}\text{s}^{-1}$ , equilibrium constant =  $2500 \pm 600 \text{ M}^{-1}$ ).<sup>4</sup> A series of steady state photolysis experiments have been carried out to investigate reactivity of the germirane resulting from the reaction of  $\text{GePh}_2$  with DMP toward methanol.

In the first experiment, a 0.058 M solution of **32** in cyclohexane- $\text{d}_{12}$  in the presence of DMP (0.49 M) and methanol (0.024M) was irradiated using 2 lamps (254 nm). The total irradiation time was 24 minutes which resulted in 30% consumption of the precursor and  $84 \pm 10\%$  conversion of methanol.

The  $^1\text{H}$  NMR spectra of the reaction mixture before and after irradiation are shown in Figure 2.23. The peaks due to the precursor **32**, DMP, methanol, internal standard ( $\text{Si}_2\text{Me}_6$ ) and solvent (cyclohexane- $\text{d}_{12}$ ) are obvious in the spectrum acquired just before irradiation (Figure 2.23 A). After irradiation and subsequent extrusion of free  $\text{GePh}_2$ , two possible reaction paths can occur. The first is the direct insertion of the

germylene into the OH bond of methanol to give the insertion product **41**, and the second is the (1+2) cycloaddition to yield the corresponding germirane. The latter is not stable and may react with methanol to give the trapped product (**45**) or dissociate back to germylene (eq 2.12).

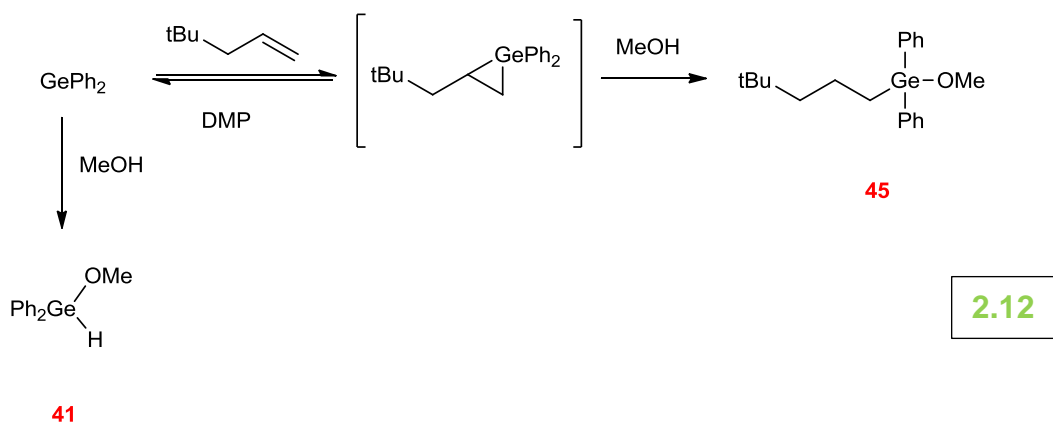
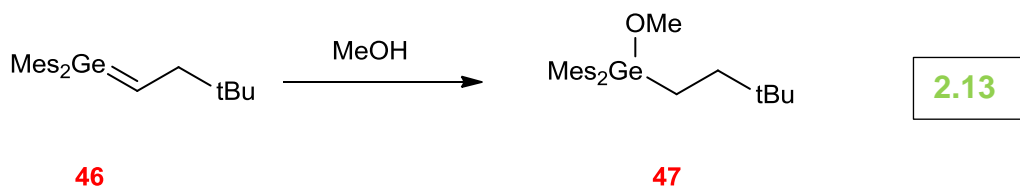


Figure 2.23 B shows the  $^1\text{H}$  NMR spectrum of the sample mixture after 24 minutes irradiation. DMB and the insertion product are easily detectable as major photolysis products. The trapped product **45** is not reported in the literature, but a similar compound (**47**), was reported by Couret et al in a study of the reactivity of dimesitylneopentylgermene **46** (eq 2.13).<sup>19</sup> The  $^1\text{H}$  NMR spectrum of **47** was reported in  $\text{CDCl}_3$  as follows: 0.84 (s, 9H, tBu), 1.52 (br s, 4H,  $\text{CH}_2\text{CH}_2$ ), 2.23 (s, 6H, p-Me), 2.30 (s, 12H, o-Me), 3.31 (s, 3H, OMe), 6.77 (s, 4H, m-H, Mes).



Knowing that, the most reasonable assignment for the peak at 3.48 ppm in Figure 2.23 B is the methoxy group on the trapped product **45** (protons *u*). However, the expected peaks for protons *r*, *s* and *t* were not observed around 1.5 ppm (in the range of 1 ppm - 2 ppm). They might be buried under other peaks in the aliphatic region. According to the concentration-time plots (Figure 2.24) conversions of the insertion **41** and trapped **45** products were  $67 \pm 9\%$  and  $4 \pm 5\%$  respectively.

A comparison of the results of this experiment (Figure 2.23) and the experiment with acrylonitrile (Figure 2.19) allows the conclusion that the germirane resulting from reaction of  $\text{GePh}_2$  with DMP is less reactive toward methanol than the corresponding one derived from acrylonitrile.

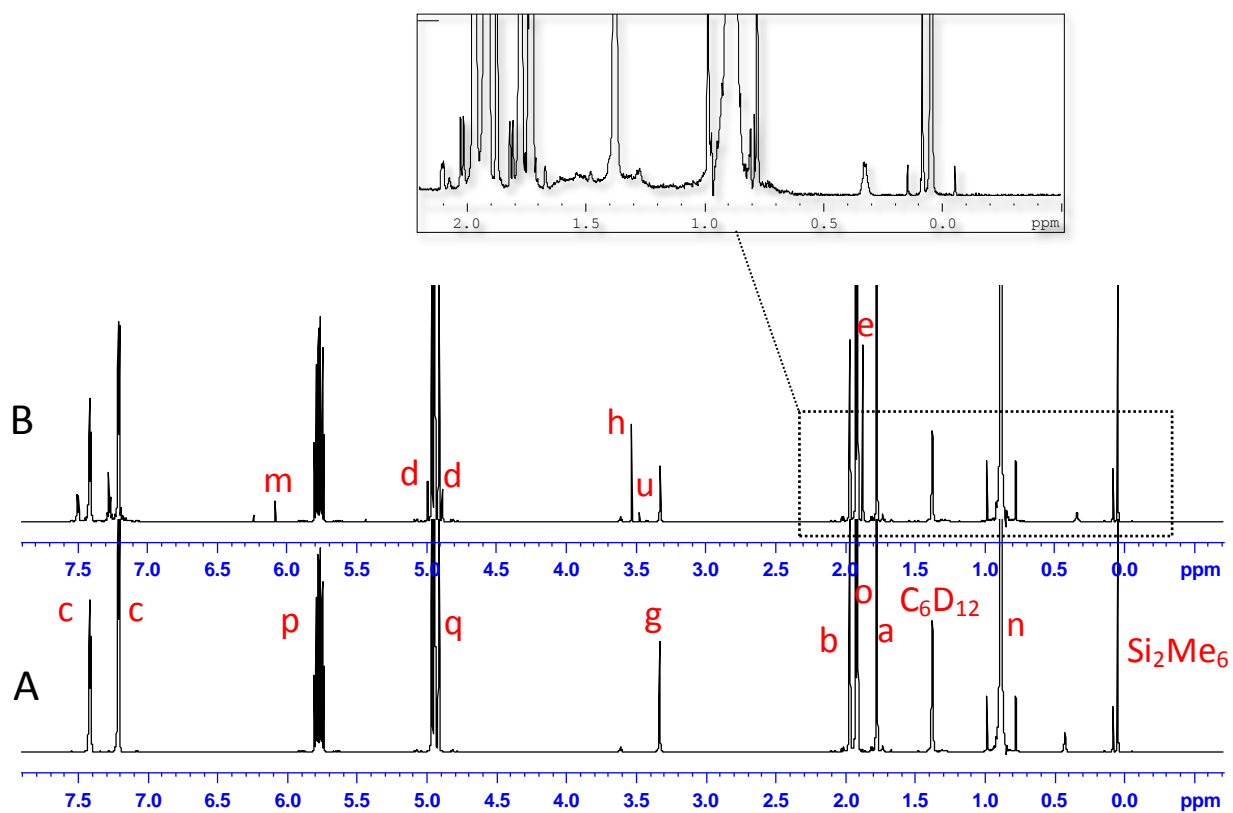
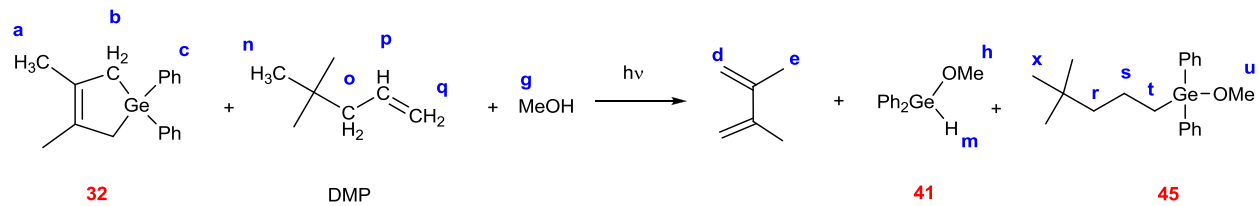


Figure 2.23. Photolysis of an argon-saturated cyclohexane- $\text{d}_{12}$  solution of **32** (0.058 M) with two low-pressure mercury lamps (254 nm) in the presence of DMP (0.49 M) and MeOH (0.024 M). a- before irradiation; b- after 24 min irradiation.

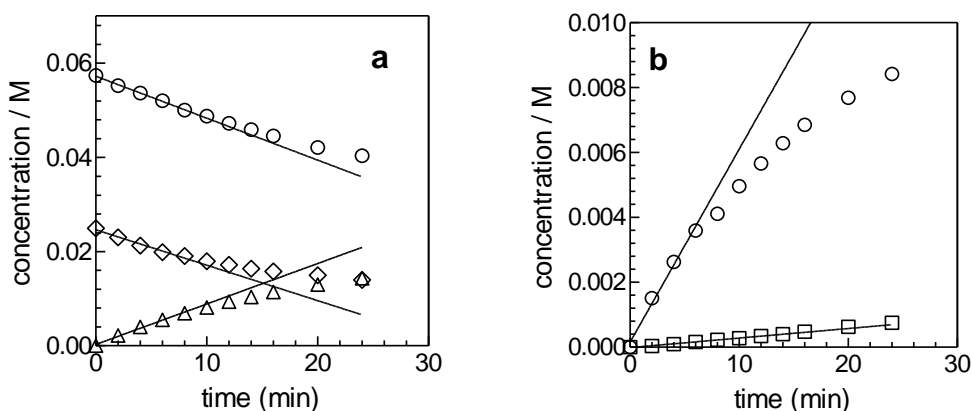


Figure 2.24..Concentration vs. time plots from irradiation of an argon-saturated cyclohexane-d<sub>12</sub> solution of **32** (0.058 M) with two low-pressure mercury lamps in the presence of DMP (0.49 M) and MeOH (0.024M). a- precursor **32** (○), slope:  $-0.00089 \pm 0.00004$ ; DMB (△), slope:  $+0.00086 \pm 0.00004$ ; MeOH (□), slope:  $-0.00075 \pm 0.00006$ ; b- Insertion product **41** (○), slope:  $+0.00059 \pm 0.00004$ ; assigned trapped product **45** (□), slope:  $+0.0000297 \pm 0.0000007$ .

The irradiated sample was left in the dark at room temperature (22 - 24 °C) for two days and the acquired <sup>1</sup>H NMR spectra revealed a sharp decrease in protons *h* and *m* (to the half of its original value), in contrast to protons *u* which showed a slight reduction. This is similar to the changes observed for the assigned peaks of the trapped and insertion products in the acrylonitrile experiment upon placing in the dark.

In the second experiment, the reaction of GePh<sub>2</sub> with DMP was investigated in the presence of a smaller amount of methanol in the hope of minimizing the insertion reaction. For this purpose, A 0.047 M solution of **32** in cyclohexane-d<sub>12</sub> in the presence of DMP (0.46 M) and methanol (0.0078M) was irradiated using 2 lamps (254 nm) (Figure 2.24). After 24 minutes irradiation there was 23% consumption of the precursor and  $66 \pm 25\%$  conversion of methanol. The <sup>1</sup>H NMR spectra acquired during the experiment (Figure 2.25) showed similar changes to those observed in the first experiment except for the relative yields of **45** and **41** ( $10 \pm 23\%$  and  $48 \pm 21\%$

respectively). Since the ratio of product **41** over **45** at the end of this experiment (1.86) was lower than the same ratio in the last experiment (11.11), it can be concluded that the germirane is more effectively trapped in the presence of very low concentrations of methanol than at higher concentrations.

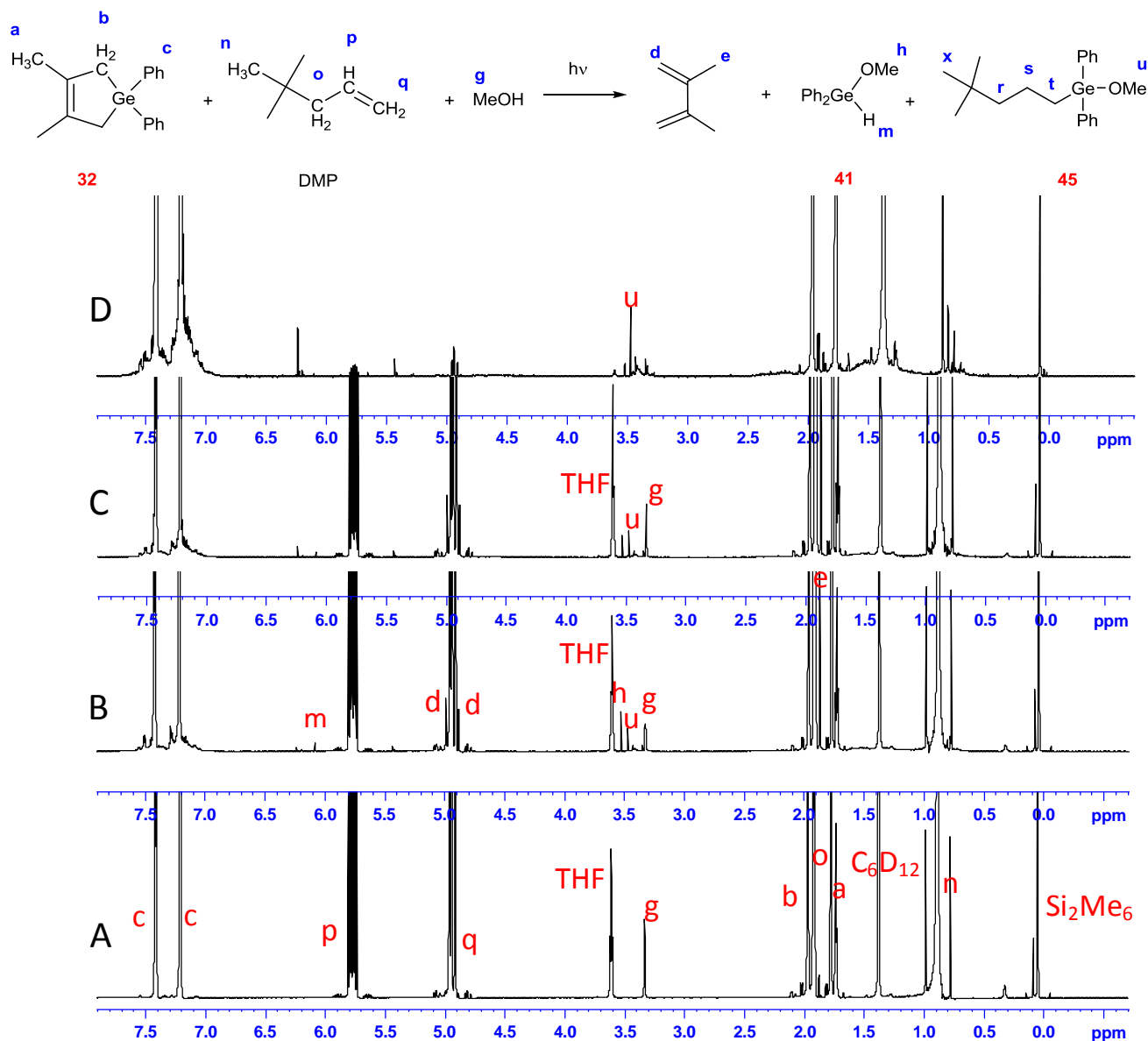


Figure 2.25. Photolysis of an argon-saturated cyclohexane- $\text{d}_{12}$  solution of **32** (0.047 M) with two low-pressure mercury lamps (254 nm) in the presence of DMP (0.46 M) and MeOH (0.0078 M). a- before irradiation; b- after 24 min irradiation; c- after leaving the sample for 48 hours in dark; d- after removing volatile components.

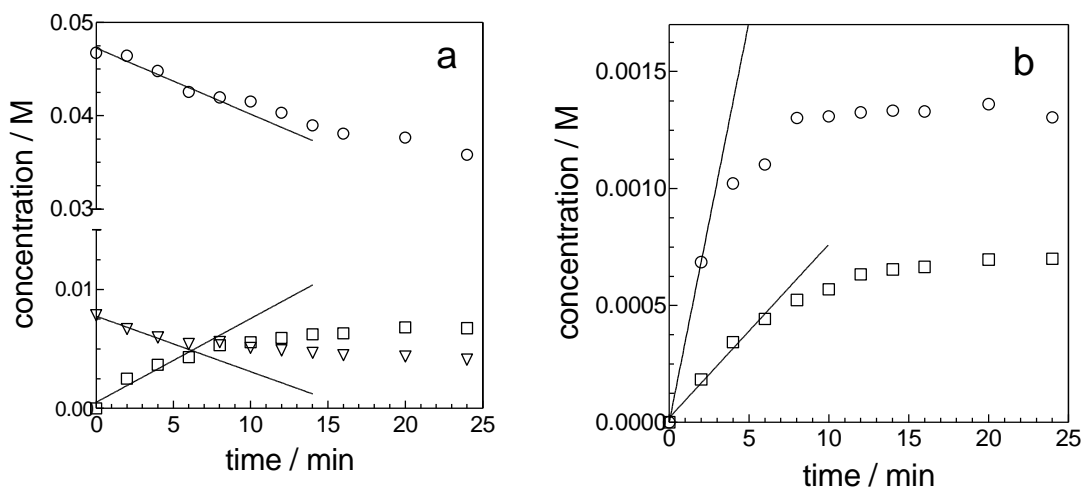


Figure 2.26..Concentration vs. time plots from irradiation of an argon-saturated cyclohexane-d<sub>12</sub> solution of **32** (0.047 M) with two low-pressure mercury lamps in the presence of DMP (0.46 M) and MeOH (0.0078M), a- precursor **32** (○), slope:  $-0.0007 \pm 0.0001$ ; MeOH (Δ), slope:  $+0.00047 \pm 0.00006$ ; DMB (□), slope:  $-0.00062 \pm 0.00009$ ; b- Insertion product **41** (○), slope:  $+0.00034 \pm 0.00005$ ; assigned trapped product **45** (□), slope:  $+0.000074 \pm 0.000007$ .

After removal of the volatile components of the irradiated sample, the <sup>1</sup>H NMR spectrum of the residue in C<sub>6</sub>D<sub>12</sub> showed that the peaks due to the insertion product (protons *m* and *h*) had disappeared, but the peak assigned to **45** (protons *u*) was still present. Additionally, a peak at 0.85 ppm which was previously buried under the DMP peak (protons *n*) appeared as a singlet with integration of nine hydrogen atoms relative to three hydrogen atoms for the methoxy peak (protons *u*). This could be assigned to the tert-butyl group on the trapped product (protons *x*).

### 2.3.6. Conclusion

Attempts were made to trap the product of the (1+2) cycloaddition of diphenylgermylene with acrylonitrile. Methanol as the trapping reagent also reacts directly with the germylene to give the insertion product **41**. Steady state photolysis

showed that two peaks are produced in the range of 3.3 - 3.6 ppm in the  $^1\text{H}$  NMR spectrum. Based on the reported  $^1\text{H}$  NMR spectrum of **41**, the peak at 3.53 ppm can be positively assigned to the methoxy group of **41**. The most reasonable assignment for the other one (3.45 ppm) is the methoxy group of the trapped product **40**. Similarly, steady state photolysis of the reaction of  $\text{GePh}_2$  with DMP in the presence of methanol showed a growing peak in the  $^1\text{H}$  NMR spectrum at 3.48ppm, which was assigned later to **45**. These two peaks for compounds **40** and **45** have shown same behavior: they were grown during the photolysis and their formation became faster as the formation of the insertion product slowed down, they were formed in a higher amount at the presence of higher ratio of alkene to methanol in the sample, and they remained stable after photolysis. This resemblance suggests that both of them are similar compounds and the most sensible assignment for a similar reaction in both experiments is the formation of the trapped product.

### 2.3.7. References

- (1) Ando, W.; Ohgaki, H.; Kabe, Y. *Angew. Chem. Int. Ed.* **1994**, 33, 659.
- (2) Kabe, Y.; Ohgaki, H.; Yamagaki, T.; Nakanishi, H.; Ando, W. *J. Organomet. Chem.* **2001**, 636, 82.
- (3) Leigh, W. J.; Lollmahomed, F.; Harrington, C. R. *Organometallics* **2006**, 25, 2055.
- (4) Leigh, W. J.; Harrington, C. R. *J. Am. Chem. Soc.* **2005**, 127, 5084
- (5) Leigh, W. J.; Harrington, C. R.; Vargas-Baca, I. *J. Am. Chem. Soc.* **2004**, 126, 16105.
- (6) National Institute of Standards and Technology of the United States (NIST) chemwebook, June8, **2011**, <http://webbook.nist.gov/chemistry>



- (7) Leigh, W. J.; Lollmahomed, F.; Harrington, C. R.; M., M. J. *Organometallics* **2006**, *25*, 5424.
- (8) Padmaja, S.; Neta, P.; Huie, R. E. *J. Phys. Chem.* **1992**, *96*, 3354.
- (9) Huck, L. A.; Leigh, W. J. *Organometallics* **2009**, *28*, 6777.
- (10) Beckett, C. W.; Freeman, N. K.; Pitzer, K. S. *J. Am. Chem. Soc.* **1948**, *70*, 4227.
- (11) Rabideau, P. W. *The conformational analysis of cyclohexenes, cyclohexadienes, and related hydroaromatic compounds*; VCH publishers, Inc., **1989**.
- (12) Anet, F. A. L.; Freedberg, D. I.; Storer, J. W.; Houk, K. N. *J. Am. Chem. Soc.* **1992**, *114*, 10969.
- (13) Neumann, W. P.; Sakurai, H.; Billeb, G.; Brauer, H.; Köcher, J.; Viebahn, S. *Angew. Chem. Int. Ed.* **1989**, *28*, 1028.
- (14) Harrington, C. R.; Leigh, W. J.; Chan, B. K.; Gaspar, P. P.; Zhou, D. *Can. J. Chem.* **2005**, *83*, 1324.
- (15) Nicholas P. Tolti; Leigh, W. J. *J. Am. Chem. Soc.* **1998**, *120*.
- (16) Riviere, P.; Satge, J.; Boy, A. *J. Organomet. Chem.* **1975**, *96*, 25.
- (17) Lawrence A. Huck; Leigh, W. J. *Organometallics* **2007**, *26*, 1339.
- (18) Langvardt, P. W. In *Ullmann's Encyclopedia of Industrial Chemistry*; Wiley-VCH Verlag GmbH & Co. KGaA: 2000.
- (19) Couret, C.; Escudie, J.; Delphon-Lacaze, G.; Stage, J. *Organometallics* **1992**, *11*, 3176.
- (20) Takagi, N.; Tonner, R.; Frenking, G. *Chem. Eur. J.* **2012**, *18*, 1772.

## Chapter 3 – Computational Studies of the Reaction of Germylenes with Alkenes

### 3.1 Introduction

A review of several computational studies on the structures, transition states and reaction mechanisms of the (1+2) and (1+4) cycloaddition of germylenes with alkenes or dienes were given in chapter 1. Not surprisingly, methods employing density functional theory (DFT), most notably with the B3LYP method, have been utilized with greater frequency as these methods are less computationally demanding than higher levels of calculations (coupled cluster methods, Møller-Plesset perturbation methods and etc) and it can be completed within a reasonable timeframe while the results are found to be accurate compared to the calculation time and cost.

Establishment of a reliable computational method for the prediction of germirane stability would be helpful in the design and interpretation of our kinetic experiments. For this purpose, it is necessary to evaluate the validity of different computational methods in relation to experimental values. The experimentally measured equilibrium constants for the (1+2) cycloaddition reaction of  $\text{GePh}_2$  with alkenes (Chapter 2) created the opportunity to benchmark computational results. Additional calculations of the reactions of simpler germylenes ( $\text{GeH}_2$  and  $\text{GeMe}_2$ ) with three alkenes were performed to broaden the scope of the investigation. Calculations were then extended to the reaction of  $\text{GePh}_2$  with a series of mono, di, tri and tetra substituted alkenes (Figure 3.1). Several DFT methods were chosen for calculation, some that have been used in earlier studies

in organogermanium chemistry by other groups, and some whose use for systems of the type we are interested in has not been previously reported.

### 3.2 General Method

Gaussian<sup>®</sup> software (Version 09, Gaussian Inc.) was employed to perform the calculations for this project using the Canadian computing network named SHARCNET (Shared Hierarchical Academic Research Computing Network). Structures of molecules were drawn either with GaussView 5.0.8<sup>®</sup> (Gaussian Inc.) or Chem3D (11.0.1 CambridgeSoft) software.

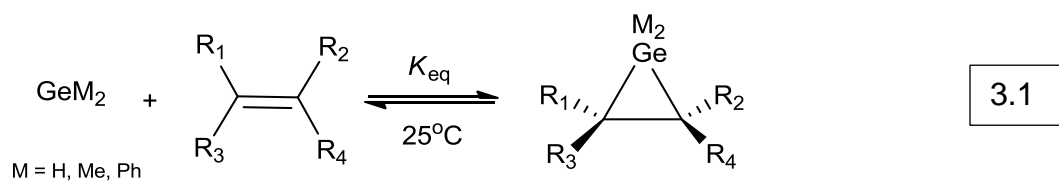
### 3.3. Geometry Optimization and Thermochemistry

The geometries of three germynes ( $\text{GeH}_2$ ,  $\text{GeMe}_2$  and  $\text{GePh}_2$ ), six alkenes (Figure 3.1) and the corresponding germiranes resulting from (1+2) cycloaddition (Figure 3.2) were optimized. A few examples of the optimized structures are shown in Figure 3.3 and selected structural properties (bond lengths and angles) of all optimized structures are given in the following tables. Tables 3.1 and 3.2 summarize the most important geometric aspects of these optimized structures. Table 3.3 presents a comparison of calculated structural parameters of the three germiranes using four different DFT methods. The structures selected for this comparison are all asymmetrically substituted germiranes in order to show the effect of substitution of the alkene on the bond distances of the three-membered ring.

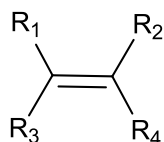
The obtained bond lengths and angles for the optimized germynes ( $\text{GeH}_2$ : 1.609 Å, 90.04° /  $\text{GeMe}_2$ : 2.015 Å, 95.47° /  $\text{GePh}_2$ : 2.003 Å, 100.47°) are in good

agreement with literature<sup>1</sup> (GeH<sub>2</sub>: 1.606 Å, 89.90° / GeMe<sub>2</sub>: 2.015 Å, 97.10° / GePh<sub>2</sub>: 1.993 Å, 98.70°) (Table 3.2). With respect to germiranes, the bond distances resulting from (1+2) cycloaddition of GeH<sub>2</sub> with ethylene were reported<sup>2</sup> to be 1.53 Å for C-C and 1.97 Å for C-Ge bond, which matches acquired data for **48a** (C-C:1.53 Å, C-Ge:1.96 Å) (Table 3.1). These authors also investigated the reaction of GeMe<sub>2</sub> with ethylene, where the C-C and C-Ge bonds of the resulting germirane were calculated to be 1.55 and 1.96 Å respectively. These numbers are equal to the parameters obtained for **49a** (C-C:1.55 Å, C-Ge:1.96 Å) (Table 3.1).

The reaction total energies ( $\Delta E_r$ ), enthalpies ( $\Delta H_r^\circ$ ) and Gibbs free energies ( $\Delta G_r^\circ$ ) of the (1+2) cycloaddition reaction of germynes with alkenes (eq 3.1) were calculated using eq 3.2, and the results are summarized in Tables 3.4 – 3.10. The reported  $\Delta G_r^\circ$  for the reactions of GeH<sub>2</sub> and GeMe<sub>2</sub> with ethylene using PBE/TZ2P<sup>2</sup> (-12.7 and -8.4 kcalmol<sup>-1</sup> respectively) are a little different from the obtained  $\Delta G^\circ$  values using the PBE/PBE/6-311+G(d,p) method (-13.7 and -8.2 kcalmol<sup>-1</sup> for GeH<sub>2</sub> and GeMe<sub>2</sub> respectively) (Table 3.10), most likely due to the difference in basis sets.

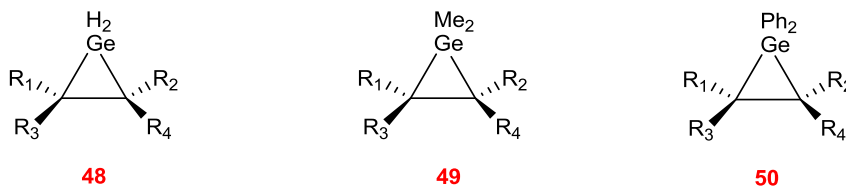


$$\Delta E_{\text{reaction}} = \Delta E_{\text{germirane}} - (\Delta E_{\text{germylene}} + \Delta E_{\text{alkene}}) \quad E = G \text{ or } H \quad \boxed{3.2}$$



- a** ethylene ( $R_1=R_2=R_3=R_4=H$ )
- b** propene ( $R_1=R_2=R_3=H, R_4=Me$ )
- c** 2-methyl propene ( $R_1=R_3=H, R_2=R_4=Me$ )
- d** cis-2-butene ( $R_1=R_2=H, R_3=R_4=Me$ )
- e** trans-2-butene ( $R_1=R_4=H, R_2=R_3=Me$ )
- f** 2-methyl-2-butene ( $R_1=H, R_2=R_3=R_4=Me$ )
- g** 2,3-dimethyl-2-butene ( $R_1=R_2=R_3=R_4=Me$ )

Figure 3.1. Alkenes selected for the computational studies in this thesis.



- a**  $R_1=R_2=R_3=R_4=H$
- b**  $R_1=R_2=R_3=H, R_4=Me$
- c**  $R_1=R_3=H, R_2=R_4=Me$
- d**  $R_1=R_2=H, R_3=R_4=Me$
- e**  $R_1=R_4=H, R_2=R_3=Me$
- f**  $R_1=H, R_2=R_3=R_4=Me$
- g**  $R_1=R_2=R_3=R_4=Me$

Figure 3.2. Germiranes studied computationally in this thesis.

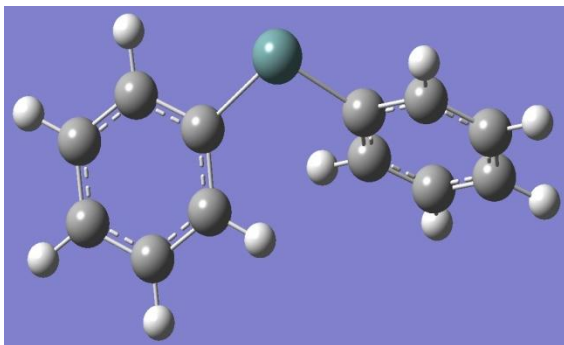
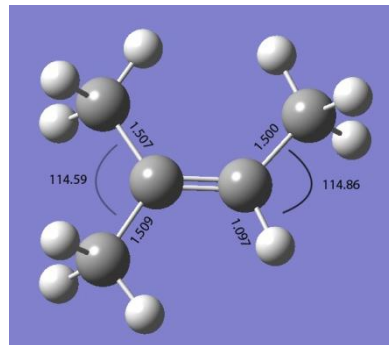
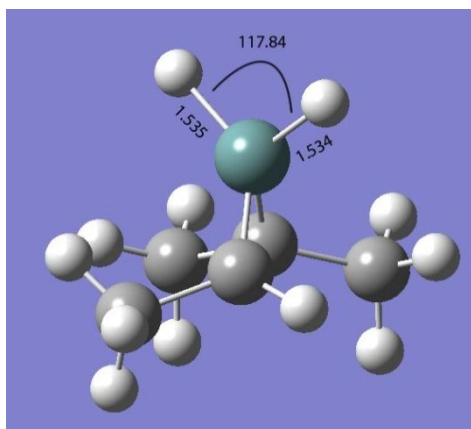
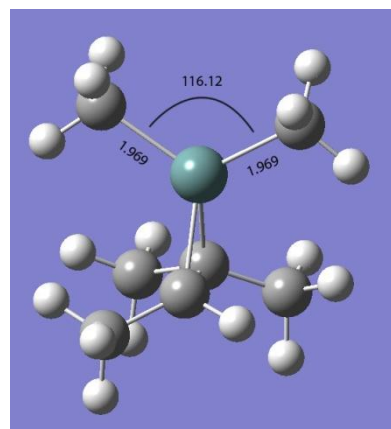
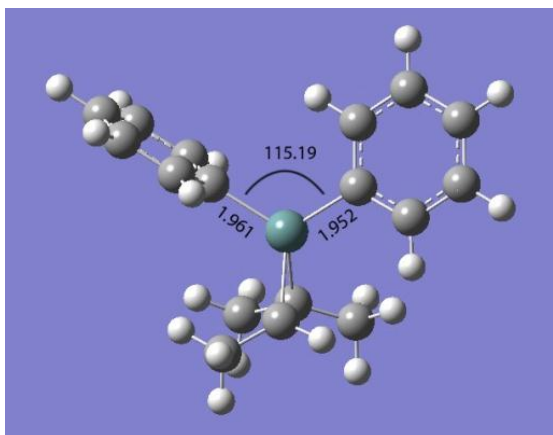
**GePh<sub>2</sub>****2-methyl-2-butene (f)****48f****49f****50f**

Figure 3.3. Structures of diphenylgermylene, 2-methyl-2-butene (**f**) and three germyranes resulting from (1+2) cycloaddition of GeH<sub>2</sub>, GeMe<sub>2</sub> and GePh<sub>2</sub> with alkene **f**. All the structures were optimized at the PBE/PBE/6-311+G(d,p) level of theory.

Table 3.1. Summary of selected bond lengths (Å) and angles (°) from the geometry optimized structures of alkenes **a–h** and their corresponding germiranes at the PBEPBE/6-311+G(d,p) level of theory.

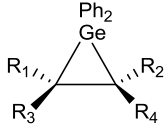
compound	C=C <sup>a</sup>	C-C <sup>b</sup>	Ge-C <sup>c</sup>	Ge-C <sup>d</sup>	C-Ge-C	R-Ge-R
<b>48a</b> (M=H) R <sub>1</sub> =R <sub>2</sub> =R <sub>3</sub> =R <sub>4</sub> =H	1.336	1.532	1.966	1.966	45.85	118.36
<b>48d</b> (M=H) R <sub>1</sub> =R <sub>2</sub> =H, R <sub>3</sub> =R <sub>4</sub> =Me	1.345	1.541	1.977	1.977	45.87	118.06
<b>48f</b> (M=H) R <sub>1</sub> =H, R <sub>2</sub> =R <sub>3</sub> =R <sub>4</sub> =Me	1.349	1.544	1.981	1.987	45.79	117.84
<b>49a</b> (M=Me) R <sub>1</sub> =R <sub>2</sub> =R <sub>3</sub> =R <sub>4</sub> =H	1.336	1.547	1.962	1.962	46.44	117.66
<b>49d</b> (M=Me) R <sub>1</sub> =R <sub>2</sub> =H, R <sub>3</sub> =R <sub>4</sub> =Me	1.345	1.557	1.974	1.974	46.46	116.88
<b>49f</b> (M=Me) R <sub>1</sub> =H, R <sub>2</sub> =R <sub>3</sub> =R <sub>4</sub> =Me	1.349	1.560	1.977	1.985	46.37	116.11
<b>50a</b> (M=Ph) R <sub>1</sub> =R <sub>2</sub> =R <sub>3</sub> =R <sub>4</sub> =H	1.336	1.538	1.967	1.967	46.03	116.64
<b>50b</b> (M=Ph) R <sub>1</sub> =R <sub>2</sub> =R <sub>3</sub> =H, R <sub>4</sub> =Me	1.339	1.538	1.970	1.980	45.83	117.13
<b>50c</b> (M=Ph) R <sub>1</sub> =R <sub>3</sub> =H, R <sub>2</sub> =R <sub>4</sub> =Me	1.343	1.542	1.969	1.995	45.78	116.28
<b>50d</b> (M=Ph) R <sub>1</sub> =R <sub>2</sub> =H, R <sub>3</sub> =R <sub>4</sub> =Me	1.345	1.548	1.979	1.979	46.05	116.32
<b>50e</b> (M=Ph) R <sub>1</sub> =R <sub>4</sub> =H, R <sub>2</sub> =R <sub>3</sub> =Me	1.341	1.539	1.982	1.981	45.69	116.10
<b>50f</b> (M=Ph) R <sub>1</sub> =H, R <sub>2</sub> =R <sub>3</sub> =R <sub>4</sub> =Me	1.349	1.552	1.978	1.995	45.98	115.18
<b>50g</b> (M=Ph) R <sub>1</sub> =R <sub>2</sub> =R <sub>3</sub> =R <sub>4</sub> =Me	1.356	1.568	1.997	1.996	46.26	112.91

a. C=C bond length of the alkene. b. ring C-C bond length in the corresponding germacyclopropane moiety. Ge-C bond lengths of the (c) less and (d) more substituted carbon.

Table 3.2. Summary of selected bond lengths (Å) and angles (°) from the geometry optimized structures of germylenes at the PBEPBE/6-311+G(d,p) level of theory. Numbers in parenthesis are from reference 2 (PW91/TZ2P/ZORA).

compound	Ge-R	R-Ge-R
<b>GeH<sub>2</sub></b>	1.609 (1.606)	90.04 (89.90)
<b>GeMe<sub>2</sub></b>	2.015 (2.015)	95.47 (97.10)
<b>GePh<sub>2</sub></b>	2.003 (1.993)	100.47 (98.70)

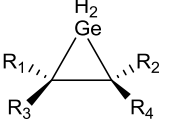
Table 3.3. Effect of DFT method on calculated structural parameters. Selected bond lengths (Å) and angles (°) from the geometry of three germiranes, optimized with different DFT methods using the 6-311+G(d,p) basis set.

compound	C=C <sup>a</sup>	C-C <sup>b</sup>	Ge-C <sup>c</sup>	Ge-C <sup>d</sup>	C-Ge-C	R-Ge-R
						
<b>50b</b> R <sub>1</sub> =R <sub>2</sub> =R <sub>3</sub> =H, R <sub>4</sub> =Me						
<b>PBEPBE</b>	1.339	1.538	1.970	1.980	45.83	117.13
<b>mPW1PW91</b>	1.328	1.534	1.947	1.954	46.30	116.31
<b>B3PW91</b>	1.330	1.535	1.952	1.959	46.22	116.35
<b>ωB97XD</b>	1.327	1.542	1.939	1.944	46.79	116.10
<b>50f</b> R <sub>1</sub> =H, R <sub>2</sub> =R <sub>3</sub> =R <sub>4</sub> =Me						
<b>PBEPBE</b>	1.349	1.552	1.978	1.995	45.98	115.18
<b>mPW1PW91</b>	1.336	1.545	1.954	1.969	46.40	114.70
<b>B3PW91</b>	1.338	1.548	1.959	1.975	46.33	114.65
<b>ωB97XD</b>	1.334	1.552	1.945	1.954	46.93	115.53
<b>50g</b> R <sub>1</sub> =R <sub>2</sub> =R <sub>3</sub> =R <sub>4</sub> =Me						
<b>PBEPBE</b>	1.356	1.568	1.997	1.996	46.26	112.91
<b>mPW1PW91</b>	1.343	1.560	1.970	1.970	46.64	112.55
<b>B3PW91</b>	1.345	1.562	1.976	1.976	46.58	112.55
<b>ωB97XD</b>	1.340	1.567	1.956	1.957	47.22	112.93

a. C=C bond length of the alkene. b. ring C-C bond length in the corresponding germacyclopropane moiety. Ge-C bond lengths of the (c) less and (d) more substituted carbon.



Table 3.4. Calculated reaction energies, zero-point corrected energies, enthalpies and Gibbs free energies of the (1+2) cycloaddition reaction of  $\text{GeH}_2$  with alkenes **a**, **d** and **f** (eq 3.2) using the 6-311G+(d,p) basis set. ( $\text{kcal mol}^{-1}$  at 298 K)

 <b>(48)</b>	$\Delta E_r$			$\Delta E_r^\circ$		
	<b>a</b> R <sub>1</sub> =R <sub>2</sub> = R <sub>3</sub> =R <sub>4</sub> =H	<b>d</b> R <sub>1</sub> =R <sub>2</sub> =H R <sub>3</sub> =R <sub>4</sub> =Me	<b>f</b> R <sub>1</sub> =H R <sub>2</sub> =R <sub>3</sub> =R <sub>4</sub> =Me	<b>a</b> R <sub>1</sub> =R <sub>2</sub> = R <sub>3</sub> =R <sub>4</sub> =H	<b>d</b> R <sub>1</sub> =R <sub>2</sub> =H R <sub>3</sub> =R <sub>4</sub> =Me	<b>f</b> R <sub>1</sub> =H R <sub>2</sub> =R <sub>3</sub> =R <sub>4</sub> =Me
<b>B3LYP</b>	-17.6	-11.6	-9.8	-13.8	-8.0	-6.4
<b>CAM-B3LYP</b>	-22.2	-16.3	-14.7	-18.3	-12.6	-11.1
<b>PBEPBE</b>	-27.3	-21.2	-19.7	-23.5	-17.7	-16.4

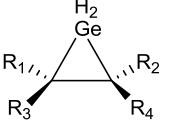
 <b>(48)</b>	$\Delta H_r^\circ$			$\Delta G_r^\circ$		
	<b>a</b> R <sub>1</sub> =R <sub>2</sub> = R <sub>3</sub> =R <sub>4</sub> =H	<b>d</b> R <sub>1</sub> =R <sub>2</sub> =H R <sub>3</sub> =R <sub>4</sub> =Me	<b>f</b> R <sub>1</sub> =H R <sub>2</sub> =R <sub>3</sub> =R <sub>4</sub> =Me	<b>a</b> R <sub>1</sub> =R <sub>2</sub> = R <sub>3</sub> =R <sub>4</sub> =H	<b>d</b> R <sub>1</sub> =R <sub>2</sub> =H R <sub>3</sub> =R <sub>4</sub> =Me	<b>f</b> R <sub>1</sub> =H R <sub>2</sub> =R <sub>3</sub> =R <sub>4</sub> =Me
<b>B3LYP</b>	-15.3	-9.2	-7.6	-4.0	3.2	5.1
<b>CAM-B3LYP</b>	-19.8	-13.9	-12.3	-8.4	-1.3	0.5
<b>PBEPBE</b>	-24.9	-18.8	-17.4	-13.7	-6.5	-5.0

Table 3.5. Calculated reaction energies and zero-point corrected energies of the (1+2) cycloaddition reaction of  $\text{GeMe}_2$  with alkenes **a**, **d** and **f** (eq 3.2) using the 6-311G+(d,p) basis set. ( $\text{kcal mol}^{-1}$  at 298 K)

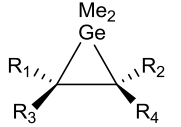
 <b>(49)</b>	$\Delta E_r$			$\Delta E_r^\circ$		
	<b>a</b> R <sub>1</sub> =R <sub>2</sub> = R <sub>3</sub> =R <sub>4</sub> =H	<b>d</b> R <sub>1</sub> =R <sub>2</sub> =H R <sub>3</sub> =R <sub>4</sub> =Me	<b>f</b> R <sub>1</sub> =H R <sub>2</sub> =R <sub>3</sub> =R <sub>4</sub> =Me	<b>a</b> R <sub>1</sub> =R <sub>2</sub> = R <sub>3</sub> =R <sub>4</sub> =H	<b>d</b> R <sub>1</sub> =R <sub>2</sub> =H R <sub>3</sub> =R <sub>4</sub> =Me	<b>f</b> R <sub>1</sub> =H R <sub>2</sub> =R <sub>3</sub> =R <sub>4</sub> =Me
<b>B3LYP</b>	-14.1	-7.1	-5.1	-10.9	-4.4	-2.4
<b>CAM-B3LYP</b>	-19.1	-12.4	-10.5	-15.9	-9.6	-7.8
<b>mPW1PW91</b>	-24.7	-17.7	-15.8	-21.5	-15.0	-13.0
<b>PBEPBE</b>	-22.8	-16.0	-14.2	-19.7	-13.4	-11.5
<b>B3PW91</b>	-22.3	-15.1	-12.9	-19.1	-12.3	-10.2

Table 3.6. Calculated reaction enthalpies and Gibbs free energies of the (1+2) cycloaddition reaction of  $\text{GeMe}_2$  with alkenes **a**, **d** and **f** (eq 3.2) using the 6-311G+(d,p) basis set. (kcal mol<sup>-1</sup> at 298 K)

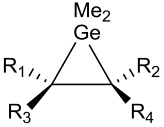
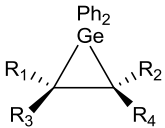
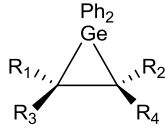
 <b>(49)</b>	$\Delta H_r^\circ$			$\Delta G_r^\circ$		
	<b>a</b> R <sub>1</sub> =R <sub>2</sub> = R <sub>3</sub> =R <sub>4</sub> =H	<b>d</b> R <sub>1</sub> =R <sub>2</sub> =H R <sub>3</sub> =R <sub>4</sub> =Me	<b>f</b> R <sub>1</sub> =H R <sub>2</sub> =R <sub>3</sub> =R <sub>4</sub> =Me	<b>a</b> R <sub>1</sub> =R <sub>2</sub> = R <sub>3</sub> =R <sub>4</sub> =H	<b>d</b> R <sub>1</sub> =R <sub>2</sub> =H R <sub>3</sub> =R <sub>4</sub> =Me	<b>f</b> R <sub>1</sub> =H R <sub>2</sub> =R <sub>3</sub> =R <sub>4</sub> =Me
<b>B3LYP</b>	-12.0	-5.0	-3.0	0.8	8.1	10.8
<b>CAM-B3LYP</b>	-17.0	-10.2	-8.4	-4.2	3.3	5.6
<b>mPW1PW91</b>	-22.6	-15.6	-13.6	-9.8	-2.7	0.2
<b>PBEPBE</b>	-20.7	-14.4	-12.1	-8.2	0.0	1.6
<b>B3PW91</b>	-20.1	-12.9	-10.8	-7.4	0.0	2.9

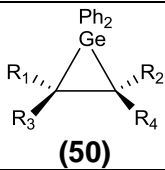
Table 3.7. Calculated reaction energies and zero-point corrected energies of the (1+2) cycloaddition reaction of  $\text{GePh}_2$  with alkenes **a-g** (eq 3.2) using the 6-311G+(d,p) basis set. (kcal mol<sup>-1</sup> at 298 K)

 <b>(50)</b>	$\Delta E_r$						
	<b>a</b> R <sub>1</sub> =R <sub>2</sub> = R <sub>3</sub> =R <sub>4</sub> =H	<b>b</b> R <sub>1</sub> =R <sub>2</sub> = R <sub>3</sub> =H, R <sub>4</sub> =Me	<b>c</b> R <sub>1</sub> =R <sub>3</sub> =H R <sub>2</sub> =R <sub>4</sub> =Me	<b>d</b> R <sub>1</sub> =R <sub>2</sub> =H R <sub>3</sub> =R <sub>4</sub> =Me	<b>e</b> R <sub>1</sub> =R <sub>4</sub> =H R <sub>2</sub> =R <sub>3</sub> =Me	<b>f</b> R <sub>1</sub> =H, R <sub>2</sub> = R <sub>3</sub> =R <sub>4</sub> =Me	<b>g</b> R <sub>1</sub> =R <sub>2</sub> = R <sub>3</sub> =R <sub>4</sub> =Me
<b>B3PW91</b>	-17.1	-13.8	-10.8	-10.4	-11.0	-8.0	-5.5
<b>mPW1MPW91</b>	-19.6	-16.5	-13.6	-13.2	-13.8	-11.0	-8.7
<b><math>\omega</math>B97XD)</b>	-20.9	-18.6	-16.9	-16.7	-17.4	-16.1	-15.3
<b>PBEPBE</b>	-18.2	-15.1	-12.4	-11.7	-12.6	-9.8	-7.6
<b>PBEPBE<sup>a</sup></b>	-17.9	-14.8		-11.3		-9.4	
<b>PBEPBE/split<sup>b</sup></b>	-20.3	-16.5		-12.4		-8.5	

 <b>(50)</b>	$\Delta E_r^\circ$						
	<b>a</b> R <sub>1</sub> =R <sub>2</sub> = R <sub>3</sub> =R <sub>4</sub> =H	<b>b</b> R <sub>1</sub> =R <sub>2</sub> = R <sub>3</sub> =H, R <sub>4</sub> =Me	<b>c</b> R <sub>1</sub> =R <sub>3</sub> =H R <sub>2</sub> =R <sub>4</sub> =Me	<b>d</b> R <sub>1</sub> =R <sub>2</sub> =H R <sub>3</sub> =R <sub>4</sub> =Me	<b>e</b> R <sub>1</sub> =R <sub>4</sub> =H R <sub>2</sub> =R <sub>3</sub> =Me	<b>f</b> R <sub>1</sub> =H, R <sub>2</sub> = R <sub>3</sub> =R <sub>4</sub> =Me	<b>g</b> R <sub>1</sub> =R <sub>2</sub> = R <sub>3</sub> =R <sub>4</sub> =Me
<b>B3PW91</b>	-15.3	-12.3	-9.4	-8.8	-9.6	-6.6	-3.8
<b>mPW1MPW91</b>	-17.8	-14.9	-12.2	-11.6	-12.4	-9.6	-7.0
<b><math>\omega</math>B97XD</b>	-18.8	-17.1	-15.6	-15.2	-15.6	-14.2	-13.8
<b>PBEPBE</b>	-16.4	-13.6	-11.2	-10.3	-11.2	-8.5	-6.1
<b>PBEPBE<sup>a</sup></b>	-16.1	-13.3		-9.9		-8.1	
<b>PBEPBE/split<sup>b</sup></b>	-18.4	-14.9		-10.9		-7.1	

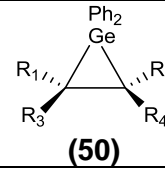
a. PBEPBE/6-311+G(d,p) scrf=(solvent=heptane). b. PBEPBE/6-311G(2df,p) for Ge / 6-31G(d) for others

Table 3.8. Calculated reaction enthalpies of the (1+2) cycloaddition reaction of GePh<sub>2</sub> with alkenes **a-g** (eq 3.2) using the 6-311G+(d,p) basis set. (kcal mol<sup>-1</sup> at 298 K)

 (50)	$\Delta H_r^\circ$						
	<b>a</b> R <sub>1</sub> =R <sub>2</sub> = R <sub>3</sub> =R <sub>4</sub> =H	<b>b</b> R <sub>1</sub> =R <sub>2</sub> = R <sub>3</sub> =H, R <sub>4</sub> =Me	<b>c</b> R <sub>1</sub> =R <sub>3</sub> =H R <sub>2</sub> =R <sub>4</sub> =Me	<b>d</b> R <sub>1</sub> =R <sub>2</sub> =H R <sub>3</sub> =R <sub>4</sub> =Me	<b>e</b> R <sub>1</sub> =R <sub>4</sub> =H R <sub>2</sub> =R <sub>3</sub> =Me	<b>f</b> R <sub>1</sub> =H, R <sub>2</sub> = R <sub>3</sub> =R <sub>4</sub> =Me	<b>g</b> R <sub>1</sub> =R <sub>2</sub> = R <sub>3</sub> =R <sub>4</sub> =Me
<b>B3PW91</b>	-16	-12.7	-9.7	-9.8	-9.9	-6.9	-4.3
<b>mPW1MPW91</b>	-18.5	-15.3	-12.6	-11.9	-12.6	-9.9	-7.5
<b>ωB97XD</b>	-19.3	-17.5	-15.9	-15.6	-16.1	-14.7	-14.2
<b>PBEPBE</b>	-17.1	-14.0	-11.4	-10.5	-11.5	-8.7	-6.6
<b>PBEPBE<sup>a</sup></b>	-16.8	-13.7		-10.2		-8.3	
<b>PBEPBE/split<sup>b</sup></b>	-19.2	-15.3		-11.2		-7.4	

a. PBEPBE/6-311+G(d,p) scrf=(solvent=heptane). b. PBEPBE/6-311G(2df,p) for Ge / 6-31G(d) for others

Table 3.9. Calculated reaction Gibbs free energies of the (1+2) cycloaddition reaction of GePh<sub>2</sub> with alkenes **a-g** (eq 3.2) using the 6-311G+(d,p) basis set. (kcal mol<sup>-1</sup> at 298 K)

 (50)	$\Delta G_r^\circ$						
	<b>a</b> R <sub>1</sub> =R <sub>2</sub> = R <sub>3</sub> =R <sub>4</sub> =H	<b>b</b> R <sub>1</sub> =R <sub>2</sub> = R <sub>3</sub> =H, R <sub>4</sub> =Me	<b>c</b> R <sub>1</sub> =R <sub>3</sub> =H R <sub>2</sub> =R <sub>4</sub> =Me	<b>d</b> R <sub>1</sub> =R <sub>2</sub> =H R <sub>3</sub> =R <sub>4</sub> =Me	<b>e</b> R <sub>1</sub> =R <sub>4</sub> =H R <sub>2</sub> =R <sub>3</sub> =Me	<b>f</b> R <sub>1</sub> =H, R <sub>2</sub> = R <sub>3</sub> =R <sub>4</sub> =Me	<b>g</b> R <sub>1</sub> =R <sub>2</sub> = R <sub>3</sub> =R <sub>4</sub> =Me
<b>B3PW91</b>	-4.5	-0.3	3.3	3.3	2.6	6.3	10.1
<b>mPW1MPW91</b>	-7.3	-2.9	0.5	0.6	-0.1	3.3	6.7
<b>ωB97XD</b>	-6.9	-5.0	-3.1	-3.9	-2.6	-0.7	0.0
<b>PBEPBE</b>	-5.4	-1.7	1.4	1.8	0.8	4.4	8.1
<b>PBEPBE<sup>a</sup></b>	-5.0	-1.3		2.1		4.8	
<b>PBEPBE/split<sup>b</sup></b>	-7.5	-3.2		1.1		5.5	

a. PBEPBE/6-311+g(d,p) scrf=(solvent=heptane). b. PBEPBE/6-311G(2df,p) for Ge / 6-31G(d) for others

### 3.4. Discussion

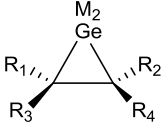
A comparison of the structural parameters of compounds **48a**, **49a** and **50a** (Table 3.1) reveal some trends in the bond distances as a function of substituents at germanium; the Ge-C and C-C bond lengths were found to increase in the order **49a** < **48a**  $\approx$  **50a** and **48a** < **50a** < **49a**, respectively. This trend can be rationalized as follows: because the methyl substituents are stronger electron donors than the phenyl groups, the increase of electron density around germanium strengthens the Ge-C bond.

The Ge-C bonds of the germiranes derived from asymmetric alkenes (Figure 3.1. **b**, **c** and **f**) are not equal, where the less substituted Ge-C bond is shorter than the other. This can be attributed to steric repulsion between the substituents on germanium and the substituents on carbon. As a result, a larger number of substituents on carbon are expected to increase the Ge-C bond length with the more substituted carbon; this is exactly the trend observed with **50b** and **50c** (1.980 and 1.995 Å respectively).

A comparison of the calculated thermochemical parameters for the reaction of GeH<sub>2</sub>, GeMe<sub>2</sub> and GePh<sub>2</sub> with alkenes **a**, **d** and **f** (Table 3.10) shows that the reaction generally becomes less exothermic and less exergonic in the order GeH<sub>2</sub> > GeMe<sub>2</sub> > GePh<sub>2</sub>. This trend is in agreement with both previous calculations<sup>2</sup> and experimental measurements<sup>4,5</sup> that have been reported in the literature. The more negative  $\Delta G^{\circ}_r$  values for the (1+2) cycloaddition reactions of GeH<sub>2</sub> compared to those of GeMe<sub>2</sub> are likely to be the result of the higher DSSE of GeMe<sub>2</sub> versus GeH<sub>2</sub>.<sup>6</sup> The same argument can be made to explain the difference in the  $\Delta G^{\circ}_r$  values between GeMe<sub>2</sub> and GePh<sub>2</sub>. The DSSE of GePh<sub>2</sub> is not reported, but a study by Walsh et al. have revealed a direct correlation between DSSE and the electronegativity of substituents in silylenes.<sup>7</sup>

Assuming a similar trend for germynes,  $\text{GeMe}_2$  is expected to have a lower DSSE than  $\text{GePh}_2$  due to the relative decrease in electronegativity of the methyl group compared to the phenyl group. (group electronegativity of  $\text{CH}_3 = 2.472$  and  $\text{C}_6\text{H}_5 = 2.717$ )<sup>3</sup>. It should be noted that a similar trend in reaction exergonicities was observed with all the DFT methods that were used.

Table 3.10. Calculated reaction enthalpies and Gibbs free energies of the (1+2) cycloaddition reactions of  $\text{GeH}_2$ ,  $\text{GeMe}_2$  and  $\text{GePh}_2$  with alkenes **a**, **d** and **f** (eq 3.2) at the PBE/PBE/6-311G+(d,p) level of theory. ( $\text{kcal mol}^{-1}$  at 298 K)

	$\Delta H_r^\circ$			$\Delta G_r^\circ$		
	<b>a</b> $R_1=R_2=$ $R_3=R_4=H$	<b>d</b> $R_1=R_2=H$ $R_3=R_4=Me$	<b>F</b> $R_1=H, R_2=$ $R_3=R_4=Me$	<b>a</b> $R_1=R_2=$ $R_3=R_4=H$	<b>d</b> $R_1=R_2=H$ $R_3=R_4=Me$	<b>F</b> $R_1=H, R_2=$ $R_3=R_4=Me$
<b><math>\text{GeH}_2</math></b> (M=H)	-24.9	-18.8	-17.4	-13.7	-6.5	-5.0
<b><math>\text{GeMe}_2</math></b> (M=Me)	-20.7	-14.4	-12.1	-8.2	0	1.6
<b><math>\text{GePh}_2</math></b> (M=Ph)	-17.1	-10.5	-8.7	-5.4	1.8	4.4

We examined further the experimental relationship between  $\Delta G_r^\circ$  and ionization potential of the respective alkene (Figure 2.13), by investigating the possibility that the experimental correlation is reproduced computationally. The calculated Gibbs free energies of the reaction of  $\text{GeH}_2$ ,  $\text{GeMe}_2$  and  $\text{GePh}_2$  were plotted against the experimental ionization potentials of the alkenes that were examined. It should be noted that all experimental ionization potential values were obtained from the National Institute of Standards and Technology of the United States (NIST)<sup>8</sup> (Figure 3.4–3.6).

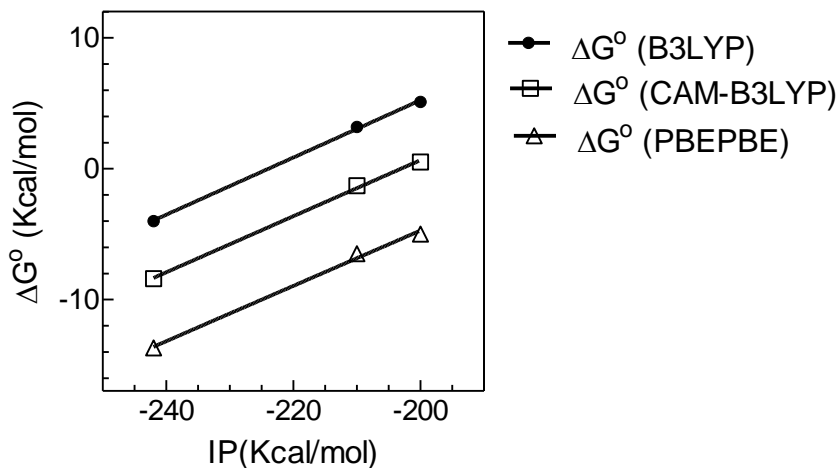


Figure 3.4. Calculated reaction Gibbs free energies employing three DFT methods versus the experimental ionization potential of the alkenes for the reaction of  $\text{GeH}_2$  with alkenes **a**, **d** and **f** (Table 3.4). The 6-311G+(d,p) basis set was employed in all cases. The experimental IP numbers were obtained from NIST (National Institute of Standards and Technology of the United States).<sup>8</sup>

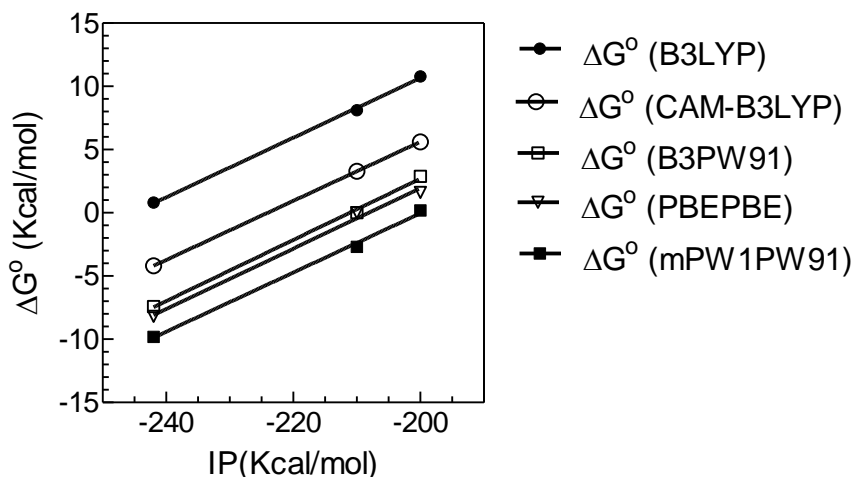


Figure 3.5. Calculated reaction Gibbs free energies employing several DFT methods versus the experimental ionization potential of the examined alkenes for the reaction of  $\text{GeMe}_2$  with alkenes **a**, **d** and **f** (Table 3.6). The 6-311G+(d,p) basis set was employed in all cases. The experimental IP numbers were obtained from NIST (National Institute of Standards and Technology of the United States).<sup>8</sup>

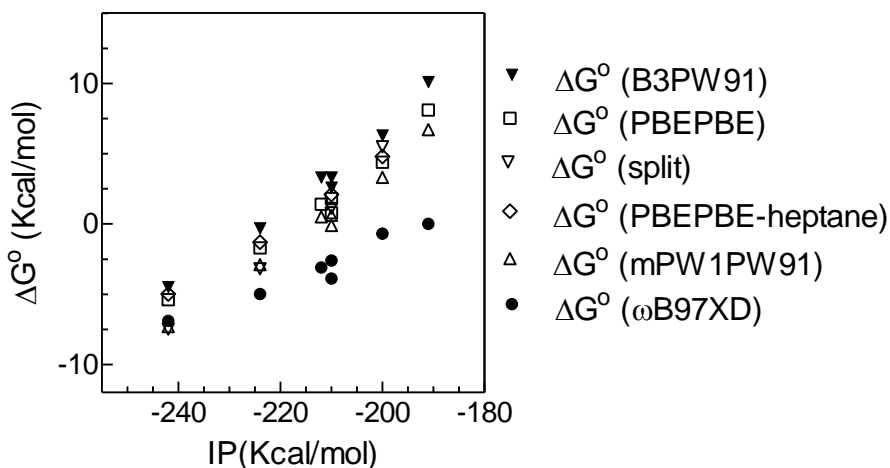


Figure 3.6. Calculated reaction Gibbs free energies employing several DFT methods versus the experimental ionization potential of the examined alkenes for the reaction of  $\text{GePh}_2$  with alkenes **a-g** (Table 3.9). The 6-31G+(d,p) basis set was employed in all cases. The experimental IP numbers were obtained from NIST (National Institute of Standards and Technology of the United States).<sup>8</sup>

The observed experimental correlation was successfully reproduced computationally in the case of  $\text{GePh}_2$ , and a similar trend was observed computationally with  $\text{GeH}_2$  and  $\text{GeMe}_2$  (Figure 3.4-3.6). Since the tried DFT methods yielded variable results, a benchmark is needed to evaluate the reliability of these computational results.

Experimental studies of the reaction of  $\text{GeMe}_2$  with alkenes have only yielded a lower limit for the equilibrium constant for the reaction with DMP ( $K_{\text{eq}} > 20000 \text{ M}^{-1}$ ).<sup>5</sup> As a result, a higher level of calculation (G4) was instead used as a computational benchmark to evaluate the various DFT methods employed for the  $\text{GeMe}_2$  calculations (Figure 3.7), where those yielding the closest results with that of G4 were deemed the most reliable. These computed values suggest that B3LYP consistently underestimates

the stability of the resulting germirane, in contrast to the other three methods which slightly overestimate it. The closest results to G4 were B3PW91 and PBEPBE and consequently were deemed the most reliable amongst the DFT methods that were studied.

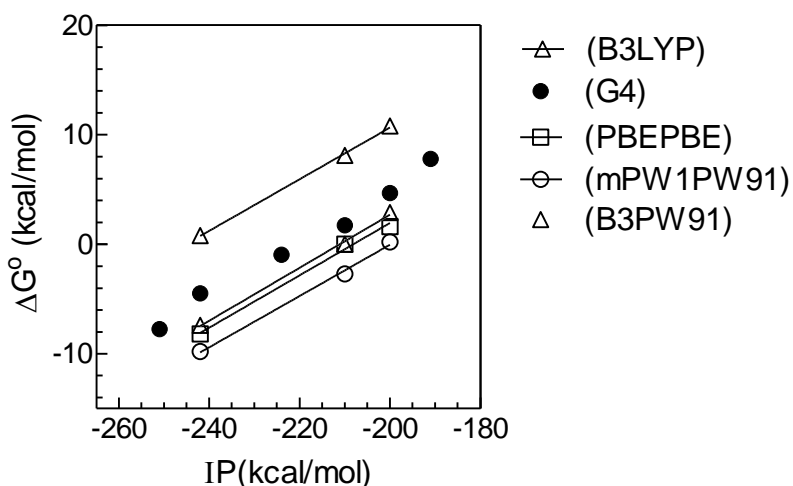


Figure 3.7. Calculated reaction Gibbs free energies using G4 and several DFT methods versus the experimental ionization potential of the examined alkenes for the reaction of  $\text{GeMe}_2$  with alkenes (eq 3.1). The 6-31G+(d,p) basis set was employed in all cases. The experimental IP numbers were obtained from NIST (National Institute of Standards and Technology of the United States).<sup>8</sup> The G4 numbers were calculated by Dr. W. J. Leigh.

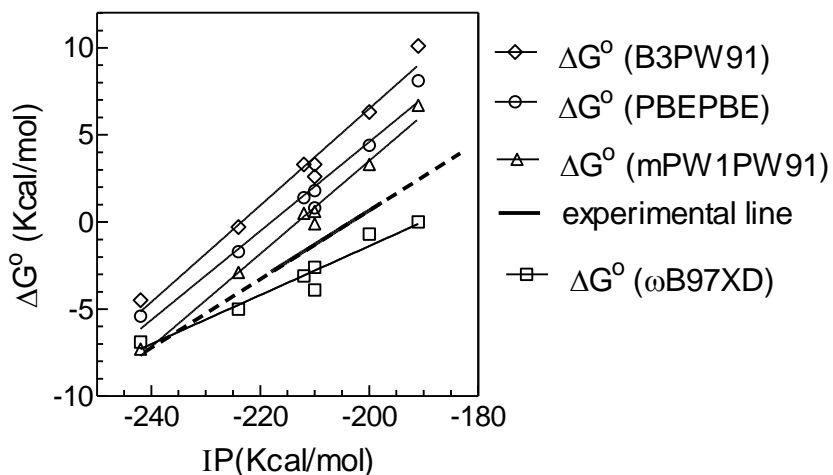
Unlike  $\text{GeMe}_2$ , the experimental results for the reaction of  $\text{GePh}_2$  with alkenes were available to be used as a benchmark. As it was concluded that the three most appropriate DFT methods for the reaction of  $\text{GeMe}_2$  with alkenes were PBEPBE, B3PW91 and mPW1PW91, calculations on  $\text{GePh}_2$  started with these three methods. Additionally, the long range dispersion-corrected functional,  $\omega\text{B97XD}$ , was employed after it came to our attention that this method gives very good results in a separate computational project on germanium compounds. Later, the effect of solvent (heptane)



was investigated at the PBE/PBE/6-311+G(d,p) level which showed slight difference with the results of PBE/PBE without solvent. Finally, a split basis set method was employed, in the hope of saving calculation time as  $\text{GePh}_2$  is bigger than  $\text{GeMe}_2$  and their calculations were expected to be computationally expensive. A large basis set (6-311G(2df,p)) was used for germanium and a smaller basis set (6-31G(d)) was applied for other atoms. It was found however that the time saved using this method was negligible.

Figure 3.8 compares the calculated and experimental  $\Delta G^\circ_r$  versus the IP values for the reaction of  $\text{GePh}_2$  with alkenes. It is apparent that the PBE/PBE, B3PW91 and mPW1PW91 methods all underestimate the stabilities of the germiranes (mPW1PW91 the least), while the  $\omega$ B97XD method overestimates them. The experimental line lies between the mPW1PW91 and  $\omega$ B97XD. The slope of this line is best reproduced using  $\omega$ B97XD, and was selected as the most appropriate DFT method examined.

Figure 3.8. Comparison between experimental and calculated  $\Delta G^\circ$  of the reactions versus experimental ionization potential of the involved alkene on the reaction of  $\text{GePh}_2$  with alkenes. The 6-311G+(d,p) basis set was employed in all cases. All IP values were obtained from NIST (National Institute of Standards and Technology of the United States).<sup>8</sup>



### 3.5. Summary

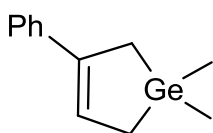
The reactions of GeH<sub>2</sub>, GeMe<sub>2</sub> and GePh<sub>2</sub> with a selection of alkenes were investigated computationally using several different DFT methods in conjunction with the 6-311+G(d,p) basis set. The results show that the reaction becomes less exergonic moving from GeH<sub>2</sub> to GeMe<sub>2</sub> and then to GePh<sub>2</sub>. In addition, plots of calculated  $\Delta G^\circ_r$  against IP for the (1+2) cycloaddition reaction of the respective alkenes with these germylenes showed a similar trend to that observed experimentally for GePh<sub>2</sub> in solution. It was also concluded that  $\omega$ B97XD and mPW1PW91 are the most reliable DFT methods to evaluate the stability of gemiranes, giving the closest results to experimental values. The  $\omega$ B97XD/6-31+G(d,p) comes the closest to matching the experimental established trend.

### 3.6. References:

- (1) Becerra, R.; Gaspar, P. P.; Harrington, C. R.; Leigh, W. J.; Vargas-Baca, I.; Walsh, R.; Zhou, D. *J. Am. Chem. Soc.* **2005**, *127*, 17469.
- (2) Birukov, A.; Faustov, V.; Egorov, M.; Nefedov, O. *Russ. Chem. Bull.* **2005**, *54*, 2003.
- (3) Inamoto, N.; Masuda, S. *Chemistry Letters* **1982**, *11*, 1003.
- (4) Leigh, W. J.; Lollmahomed, F.; Harrington, C. R. *Organometallics* **2006**, *25*, 2055.
- (5) Leigh, W. J.; Harrington, C. R. *J. Am. Chem. Soc.* **2005**, *127*, 5084.
- (6) Boganov, S.; Egorov, M.; Faustov, V.; Krylov, I.; Nefedov, O.; Becerra, R.; Walsh, R. *Russ. Chem. Bull.* **2005**, *54*, 483.
- (7) Walsh, R. *Pure Appl. Chem.* **1987**, *59*.
- (8) National Institute of Standards and Technology of the United States (NIST) chemwebook, June 8, **2011**, <http://webbook.nist.gov/chemistry>.

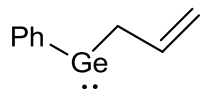
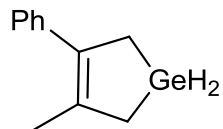
## Chapter 4 –Future Direction

The results of our kinetic studies of the reaction of  $\text{GePh}_2$  with alkenes (chapter 2) establish a reasonable correlation between the Gibbs free energy of the reaction and the ionization potential of the involved alkenes. This study can be extended to investigate the reaction of  $\text{GeMe}_2$  with alkenes to see whether similar behavior can be observed or not. It is known that  $\text{GeMe}_2$  yields more stable germiranes compared to  $\text{GePh}_2$ .<sup>1</sup> For example, the equilibrium constant of the reaction of  $\text{GeMe}_2$  with isoprene and DMP were both estimated to be about  $20000 \text{ M}^{-1}$  which are much higher than the equilibrium constant of the same reaction for  $\text{GePh}_2$  ( $6000$  and  $2500 \text{ M}^{-1}$  respectively).<sup>1</sup> This means that the reaction of  $\text{GeMe}_2$  with a given alkene is expected to be more exergonic than that of its phenylated counterpart. Therefore the Gibbs free energy-ionization potential correlation line for  $\text{GeMe}_2$  should fall below the  $\text{GePh}_2$  line. Knowing this, a series of laser flash photolysis studies of the reaction of  $\text{GeMe}_2$  with alkenes can be proposed as a logical extension of this thesis. For this purpose, the following compound was synthesized (experimental section, Chapter 5). However, the amount of compound obtained was insufficient for a meaningful laser flash photolysis study to be undertaken.



This study can also be extended by studying the temperature dependence of the equilibrium constants for reaction of  $\text{GePh}_2$  with alkenes. This would extend our knowledge about the thermochemistry and the effect of temperature on the stability of resulting germirane. The results presented in this thesis and the proposed follow up studies will complete an earlier unpublished study of the effects of aromatic substituents on the stability of the resulting germirane in the reaction of  $\text{GePh}_2$  with alkenes. With the results of these two studies, a broad understanding of electronic effect on the stability of germirane for the reaction of  $\text{GePh}_2$  with alkenes will be obtained.

The results presented in this thesis raises some questions: what will happen if germylene bear an alkene substituent (something like compound **51**)? How much the reactivity of germylene will be affected by the alkene chain? It is known that the photolysis of **52** results in just 30-40% extrusion of  $\text{GeH}_2$  due to the existence of an intramolecular germylene-alkene  $\pi$ -complex.<sup>2</sup> The complex appeared as a transient in laser flash photolysis studies and it was observed that solvent plays a significant role in the extrusion of free  $\text{GeH}_2$ . Knowing this, investigation of the chemistry of compound **51** could be an interesting research topic because **51** is able to show a similar intramolecular  $\pi$ -complex, in addition to a probable intra- or inter-molecular (1+2) cycloaddition reaction between germlyene and the alkene chain. The effect of germylene substituent, the length of alkene chain and the solvent should be studied as they are expected to be major factors which can potentially affect the complexation or (1+2) cycloaddition pathway.

**51****52**

## References

- (1) Leigh, W. J.; Lollmahomed, F.; Harrington, C. R. *Organometallics* **2006**, 25, 2055.
- (2) Billone, P. S.; Beleznyay, K.; Harrington, C. R.; Huck, L. A.; Leigh, W. J. *J. Am. Chem. Soc.* **2011**, 133, 10523.

## Chapter 5 - Experimental

### 5.1. Synthesis

#### 5.1.1. Chemicals

Column chromatography was performed using Silica Gel (acid washed, 230-400 mesh) (Silicycle) with hexanes as eluent, unless otherwise stated. All synthesized compounds were stored at -20 °C in vials which were purged with argon or nitrogen.

Pyridine (Caledon Reagent) was dried by fractional distillation over potassium hydroxide.<sup>1</sup> The following chemicals were used as received from the supplier: Germanium tetrachloride (**48**), tetramethyldisiloxane (Gelest, Inc), chloromethyltrimethylsilane (Gelest, Inc), benzaldehyde (Fisher Scientific), chromium oxide (Fisher Scientific), bromobenzene (Fisher Scientific), glacial acetic acid (Caledon Reagent), allylmagnesium chloride in THF (1.6 M) (Sigma-Aldrich), methylmagnesium bromide in diethyl ether (3 M) (Sigma-Aldrich), 1,4-dioxane (Sigma-Aldrich).

#### 5.1.2. Solvents

Hexanes and diethyl ether (both Caledon Reagent grade) were dried by passage through activated alumina under nitrogen using a Solv-Tek purification system (Solv-Tek, Inc). Tetrahydrofuran (Caledon Reagent) was refluxed over CaH<sub>2</sub> for two hours, distilled into a flask containing sodium and refluxed for four days. It was then freshly distilled under nitrogen prior to use. Dichloromethane (Caledon Reagent) was stirred over calcium hydride and distilled prior to use.

### 5.1.3. Equipment

$^1\text{H}$  NMR spectra were acquired with a Bruker AV600 spectrometer and were referenced to the residual solvent protons. NMR samples were prepared in deuterated solvents purchased from Cambridge Isotope Laboratories ( $\text{CDCl}_3$  unless otherwise stated). Static UV-Vis spectra were acquired by a Varian Cary 50 scan UV/Visible spectrometer. High-resolution mass spectra were obtained using a Micromass ToFSpec 2E (MALDI-TOF) Mass spectrometer. Gas chromatographic/mass (GC/MS) analysis were carried out using a Varian Saturn 2200 GC/MS/MS system equipped with a VF-5ms Capillary column (30 m x 0.25 mm; 0.25 mm; Varian, Inc).

### 5.1.4. Synthesis of 3,4-dimethyl-1,1-diphenyl-1-germacyclopent-3-ene (32)

Compound **32** was prepared by a modification of the procedures of Nefedov and coworkers.<sup>2,3</sup> The synthetic scheme is shown in Figure 5.1.

For the preparation of compound **54**, germanium tetrachloride (5.6 g, 0.026 mol), 1,1,3,3-tetramethyldisiloxane (3.6 g, 0.027 mol) and 1,4-dioxane (3.8 g, 0.043 mol) were mixed in a flame-dried 100 mL roundbottom flask equipped with a reflux condenser and nitrogen inlet. The reaction mixture was heated to 85 °C and then left at this temperature for 12 hours, whereby a suspension of colorless crystals in the reaction flask is formed. The reaction mixture was cooled to room temperature and the excess solution was decanted. The crystals were washed with pentane (3 x 25 mL), and then pumped under vacuum for 2 hours to yield  $\text{GeCl}_2$ -dioxane as colorless needles (3.6 g, 0.016 mol, 60%).

1,1-Dichloro-3,4-dimethyl-1-germacyclopent-3-ene (**55**): a solution of  $\text{GeCl}_2$ -dioxane (6.0 g, 0.026 mol) in dry THF (100 mL) was stirred under nitrogen and heated to reflux in a flame-dried reaction set up consisting of a two-neck round-bottom 250mL flask, reflux condenser, addition funnel, nitrogen inlet and magnetic stirrer. A solution of 2,3-dimethyl-1,3-butadiene (2.8 g, 0.034 mol) in dry THF (20 mL) was added dropwise over 30 minutes and the solution was stirred for 1 hour. The apparatus was reconfigured for distillation and the solvent was removed under nitrogen. Continued distillation under vacuum afforded **55** as a colorless liquid (5.0 g, 0.022mol, 85%, bp 56 °C) whose boiling point and  $^1\text{H}$  NMR spectrum is consistent with the literature data.<sup>4</sup>  $^1\text{H}$  NMR (600 MHz,  $\text{CDCl}_3$ ):  $\delta$  1.8 (s, 6H,  $\text{CH}_3$ ), 2.25 (s, 4H,  $\text{CH}_2$ ).

3,4-Dimethyl-1,1-diphenyl -1-germacyclopent-3-ene (**32**): For the preparation of **32** a modification of the procedure of Manuel and coworkers was followed.<sup>5</sup> First, a mixture of (**55**) (1.0 g, 0.0044mol) in anhydrous THF (20 mL) was placed in a flame-dried apparatus containing a 100mL two-neck round bottom flask, reflux condenser, addition funnel, and magnetic stirrer. The solution was cooled in an ice water bath (0 °C), and then a solution of phenyl magnesium bromide (10 mL of a 1.2 M solution in THF, 0.011mol) was added dropwise with stirring over 1 hour. The cooling bath was removed and the reaction mixture was allowed to stir at room temperature (22- 25 °C) for 24 hours. The resulting solution was treated with saturated aqueous ammonium chloride (25 mL) and transferred to a separatory funnel. The aqueous fraction was extracted with diethyl ether (2 X 75 mL), and then the combined ether fractions were washed with water (1 x 25mL), 5% aqueous sodium bicarbonate (1 x 25 mL), and distilled water (1 x 25 mL). The resulting organic layer was dried with anhydrous



magnesium sulfate and filtered. The solvent was removed on a rotary evaporator to yield a light yellow oil. **32** was obtained as a white solid after purification using column chromatography and slow recrystallization from hexanes. The results were checked with GC/MS spectroscopy and the purification continued until less than 0.01 % biphenyl remained. The final product was obtained as colorless crystals (0.89g, 0.0029mol, 85%, mp 48.4-49.5 °C) whose  $^1\text{H}$  NMR spectra and melting point are consistent with that previously reported<sup>4</sup>  $^1\text{H}$  NMR(600 MHz,  $\text{CDCl}_3$ ):  $\delta$  1.82 (s, 6H), 2.05 (s, 4H), 7.39 (m, 6H) , 7.56 (m, 4H).

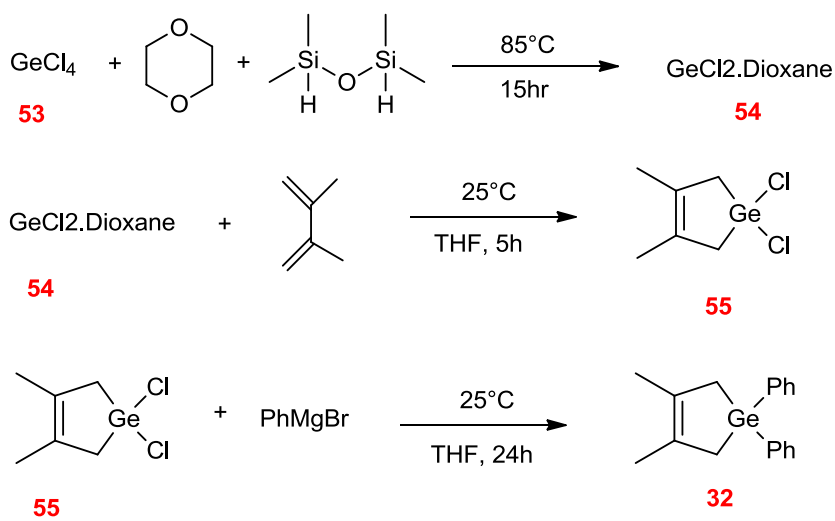


Figure 5.1. Overall scheme for the synthesis of 3,4-dimethyl-1,1-diphenyl-1-germacyclopent-3-ene (**32**).

### 5.1.5. Synthesis of 1,1-dimethyl-3-phenyl-1-germacyclopent-3-ene (**61**) :

The synthesis of (**61**) was adapted from Brown et al.<sup>6</sup> The synthetic scheme employed is shown in Figure 5.2:

Trimethylsilylmethylmagnesium chloride: 85 mL of dried diethyl ether was added to a flame-dried two-neck 250 mL roundbottom flask containing solid magnesium (13.0 g, 0.55 mol), a reflux condenser, nitrogen inlet and a 60 mL addition funnel. The solution was cooled in an ice bath and trimethylsilylmethyl chloride (14.0 g, 0.12 mol) was then added dropwise with stirring. The ice bath was removed, and the reaction was allowed to stir for an additional 24 h.

1-Phenyl-2-(trimethylsilyl)ethanol (**56**): A solution of benzaldehyde (8.9 g, 0.084 mol) in ether (70 mL) was prepared in a flame dried 500 mL two neck round bottom flask containing a condenser, a 60 mL addition funnel and nitrogen inlet. The addition funnel was filled with trimethylsilylmethylmagnesium chloride (80 mL of a 1.4 M solution in ether, 0.12 mmol) which was transferred by a cannula from the previous reaction mixture. The addition proceeded at room temperature (22-24 °C) under nitrogen. The mixture was heated under reflux for 2 hours and, after cooling, saturated aqueous ammonium chloride (100 mL) was added. After separation of the organic and aqueous layers, the latter was washed with diethyl ether (2 × 100 mL). The organic fractions were combined and washed with distilled water (150 mL), 5% aqueous sodium bicarbonate (100 mL), distilled water (100 mL), dried with anhydrous magnesium sulfate, and filtered. Evaporation of the solvent on a rotary evaporator afforded **56** (12.0 g, 0.60 mol, 72%) as a light yellow oil whose <sup>1</sup>H NMR is in good agreement with literature.<sup>6</sup> <sup>1</sup>H NMR δ(600 MHz, CDCl<sub>3</sub>): 0.00 (s, 9H), 1.25 (dd, 1H), 1.35 (dd, 1H), 1.82 (s, 1H), 4.95 (t, 1H) and 7.32-7.45 (m, 5 H).

1-Phenyl-2-(trimethylsilyl)ethanone (**57**) : To a one-neck 500 mL round bottom flask containing a stirred solution of pyridine (32.2 g, 0.41 mol) in dry dichloromethane

(350 mL), Celite<sup>®</sup> (34.0 g), and chromium(VI) oxide (34.6 g, 0.34 mol) were added, resulting in a color change to deep red within a few minutes. After stirring for 30 minutes, a solution of the alcohol **56** (9.8 g, 0.051 mol) in dichloromethane (30 mL) was added in one portion. The solution became brown immediately. After stirring for 1 minute, the reaction mixture was filtered through Buchner funnel containing ca. 5 g of silica gel, and the residues were washed with dichloromethane (100 mL). Removal of the solvent under reduced pressure (room temperature / 4mmHg) afforded the ketone (3.2 g, 0.17mol, 63%) as a light yellow oil whose <sup>1</sup>H NMR spectrum is in good agreement with the literature data.<sup>6</sup> <sup>1</sup>H NMR δ (600 MHz, CDCl<sub>3</sub>): 0.40 (s, 9H), 2.71 (s, 2H) and 7.32-7.94 (m, 5H).

1-Phenyl-2-(trimethylsilyl)but-3-en-2-ol (**58**): A flame-dried 250mL two necked round bottom flask was charged with a solution of ketone **53** (3.3 g, 0.017 mol) in THF (100 mL) and was equipped with a condenser, 60 mL addition funnel, nitrogen inlet and magnetic stir bar. The mixture was placed in an ice-water bath and a solution of vinylmagnesium chloride (14 mL, 1.6 M solution in TH, 0.022 mol) was added dropwise over 1 hour under nitrogen. The mixture was stirred for a further 12 hours, and then a saturated solution of ammonium chloride (50 mL) was added. After separation of the organic and aqueous layers, the latter was washed with diethyl ether (2 × 75 mL). The organic fractions were combined and washed with distilled water (50 mL), 5% aqueous sodium bicarbonate (50 mL), distilled water (50 mL), dried with anhydrous magnesium sulfate, and filtered. The solvent was removed on a rotary evaporator and the residue was pumped on for two hours under high vacuum, affording **58** as a yellow oil (3.4 g, 0.015mol, 88%), the <sup>1</sup>H NMR spectra was in agreement with the literature.<sup>6</sup> <sup>1</sup>H NMR δ

(600 MHz,  $\text{CDCl}_3$ ): 0.3 (s, 9H,  $\text{Me}_3\text{Si}$ ), 1.29-1.99 (m, 2H,  $\text{CH}_2\text{Si}$ ) , 3.25 (s, 1H, OH), 5.08-5.57 (m, 2H,  $\text{CH}=\text{CH}_2$ ), 6.40 (dd, 1H, J 17 and 11,  $\text{CH}=\text{CH}_2$ ) , 7.30-7.82 (m, 5H, ArH).

2-Phenyl-1,3-butadiene (**59**): the alcohol **58** (5.6 g, 0.015mol) was added to a 250 mL round bottom flask containing a 50 mL saturated solution of sodium acetate in glacial acetic acid. A condenser was fitted and the mixture was stirred for 3 hours at 60 °C. 200 mL of water was then added and the mixture was neutralized to pH 7 using a saturated solution of sodium bicarbonate. After washing with diethyl ether (3 × 100 mL), the combined organic fractions were washed once with distilled water (100 mL), dried with anhydrous magnesium sulfate, filtered, and the solvent was evaporated on a rotary evaporator. Compound **60** was collected as a yellow oil (2.4 g, 0.018 mol, 70%), the  $^1\text{H}$  NMR spectra matching that of the literature.<sup>6</sup>  $^1\text{H}$  NMR  $\delta$  (600 MHz,  $\text{CDCl}_3$ ): 5.15-5.29 (m, 4H, 2 x  $\text{CH}_2$ ), 6.61 (dd, 1H, J 17.1 and 11.2,  $\text{CH}=\text{CH}_2$ ), 7.20-7.39 (m, 5H, ArH).

1,1-Dimethyl-3-phenyl-1-germacyclopent-3-ene (**61**): For the preparation of **61** a modification of the procedure of Manuel and coworkers was followed.<sup>5</sup> A two neck round-bottom 250mL flask was fitted with a reflux condenser, addition funnel, nitrogen inlet and magnetic stirrer. The apparatus was flame dried under argon, charged with a solution of  $\text{GeCl}_2$ -dioxane (0.30 g, 1.3 mmol) in dry THF (20 mL) and heated to 70 °C. Afterwards, a solution of **59** (0.12 g, 0.85 mmol) in dry THF (5 mL) was added dropwise over 30 minutes and allowed to stir for 5 hours. Upon cooling, the addition funnel was charged with a solution of methyl magnesium bromide (1.5 mL of a 3 M solution in diethyl ether, 4.5 mmol), which was then added dropwise with stirring over 1 hour. The reaction mixture was then stirred at room temperature for a further 24 hours. The

resulting solution was treated with saturated aqueous ammonium chloride (25 mL) and the mixture was transferred to a separatory funnel. The aqueous fraction was extracted with diethyl ether (2 X 35 mL), the combined ether fractions were washed with water (1 x 25mL), 5% aqueous sodium bicarbonate (1 x 25 mL), and distilled water (1 x 25 mL). The resulting organic layer was dried with anhydrous magnesium sulfate and filtered. The solvent was removed on a rotary evaporator to yield a light yellow oil (0.17 g, 0.73 mmol, crude yield 85%) whose  $^1\text{H}$  NMR spectrum is consistent with the previously reported<sup>7</sup>:  $^1\text{H}$  NMR (600 MHz,  $\text{CDCl}_3$ ):  $\delta$  0.42 (s, 6H), 1.78 (s, 2H), 1.96 (m, 6H) , 6.48(m, 4H), 7.27 (m, 3H), 7.52 (m, 2H).

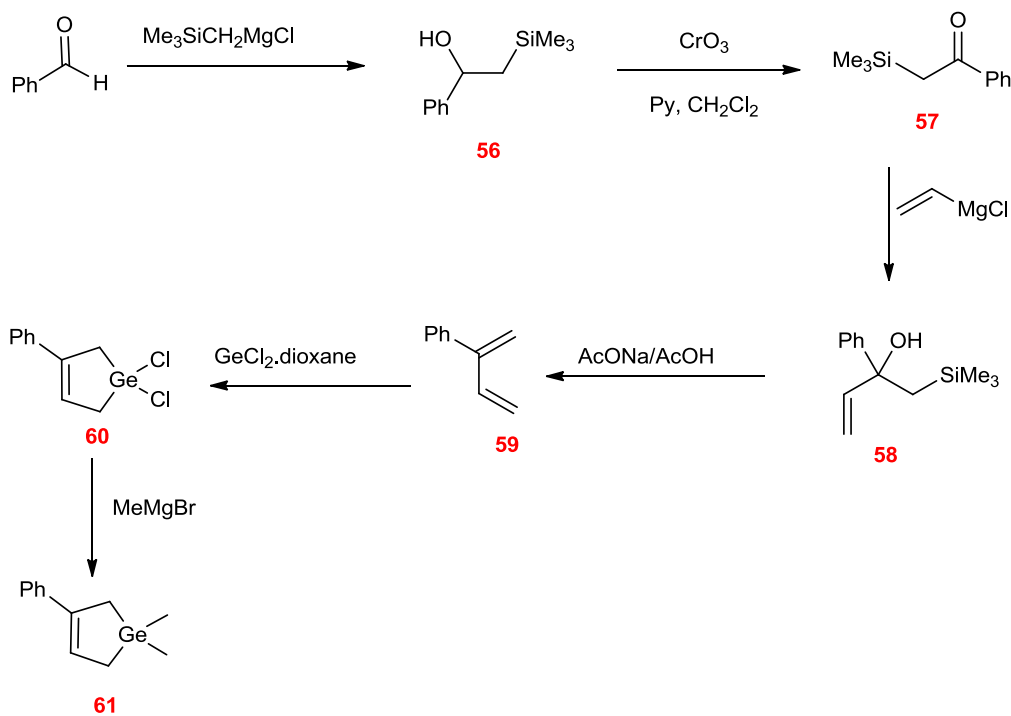


Figure 5.2. synthetic scheme for 1,1-dimethyl-3-phenyl-1-germacyclopent-3-ene (**61**).

## 5.2. Nanosecond Laser Flash Photolysis (LFP)<sup>4</sup>:

### 5.2.1. Chemicals

Precursor **32** was synthesized as described in section 5.1. All the alkenes used for laser experiments were purchased from Sigma-Aldrich and were dried prior to use according to known procedures as follows<sup>1</sup>: Cyclohexene was distilled from maleic anhydride and passed through a silica column. Methylcyclohexene was distilled from CaH<sub>2</sub> and passed through a silica column. 2-Methyl-2-pentene was distilled from CaH<sub>2</sub>. Cyclopentene and cis-cyclooctene were distilled from NaOH and passed through an alumina column. Cis-2-hexene was distilled from CaCl<sub>2</sub>. Trans-3-hexene was distilled from CaH<sub>2</sub> by vacuum bulb to bulb distillation and then passed through a silica column. 2-Methyl-1-pentene was distilled from LiAlH<sub>4</sub> by vacuum bulb to bulb distillation. Trans-3-methyl-2-pentene was distilled from CaH<sub>2</sub> by vacuum bulb to bulb distillation.

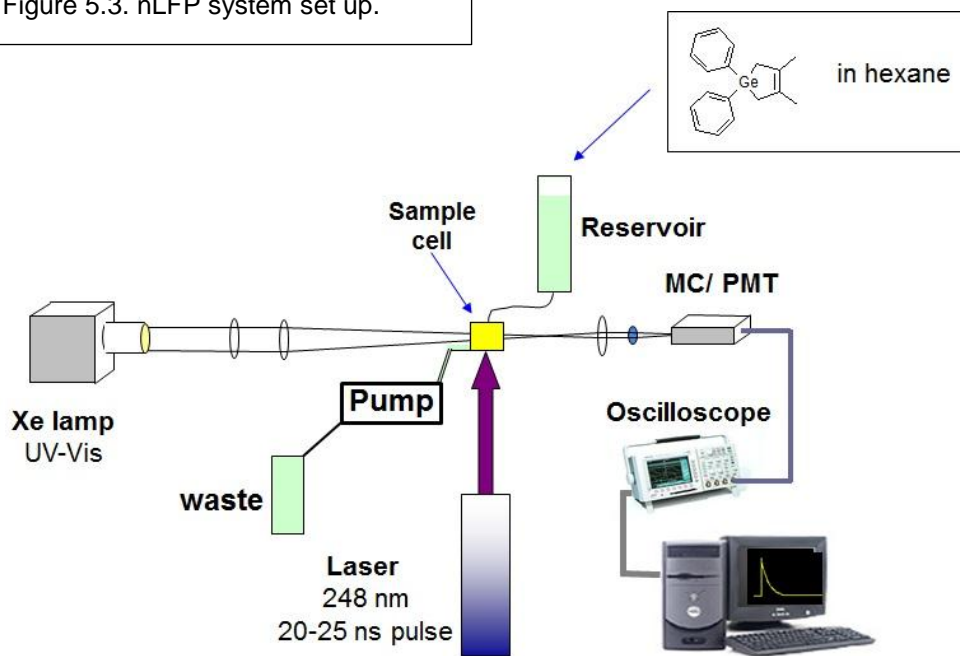
### 5.2.2. System Design<sup>4</sup>

Figure 5.3 shows a schematic representation of the laser flash photolysis system used in this study. It consists of a Lambda Physik Compex 120 excimer laser filled with Kr/F<sub>2</sub>/Ne (248 nm, ~20 ns pulse width, 100 ± 5 mJ pulse energies) and a Luzchem Research LFP-111 laser flash photolysis system. The beam emitted from a 150 W high pressure Xe lamp as monitoring source and is focused through the quartz sample cell. The detection system consists of a monochromator / photomultiplier tube (MC/PMT) combination and lenses. The system is set up to deliver the excitation beam at a 90 ° angle relative to the monitoring beam. The PMT output is converted to digital format using a digital oscilloscope and then transferred to a computer for subsequent

processing. The required acquisition setting as well as laser triggering is controlled by specially designed software on the computer.

In a typical experiment, a solution of precursor in dry hexane was prepared in a 100 mL reservoir at a concentration such that the absorbance at the excitation wavelength (248nm) was between 0.5 and 0.7. Extra care was taken to ensure that all glassware, lines and chemicals were dried because scavenging of the transient germylene by sub-millimolar concentrations of water effectively competes with the desired substrate. This reduces the concentration of free germylene present in solution and complicates the analysis of reaction kinetics.<sup>4</sup> Solutions were deoxygenated by continuously bubbling argon through the reservoir, as oxygen has also been shown to be an effective germylene scavenger.<sup>8</sup> The dry deoxygenated solution is then flowed through a 7 x 7 mm<sup>2</sup> cell.

Figure 5.3. nLFP system set up.



During the laser pulse, the precursor undergoes a photoreaction to yield transient germylene and 2,3-dimethyl-1,3-butadiene. Germylene then reacts to form other compounds which can be monitored as a function of time. The presence of a compound exhibiting an absorption band in the 270 - 650 nm wavelength range would change the intensity of light. These changes are recorded by the detector and the difference in intensity is converted to a change in optical density ( $\Delta OD$ ) or absorbance ( $\Delta A$ ). This change is proportional to the change in the concentration of the species in solution. Plotting  $\Delta A$  against time yield the decay/growth profiles which are the basis of kinetic measurement analysis.

### 5.2.3. Experimental Set up for the Determination of Rate/Equilibrium Constants

All glassware, sample cells, transfer lines, and reservoirs used for nLFP experiments were washed and placed in a 65 °C vacuum oven overnight. They were taken out of the oven just prior to assembling the system for the experiment.

In each laser experiment, dried hexane (as described in section 5.1.2) was added to a 100 mL reservoir fitted with a glass frit to allow argon bubbling. The reservoir was subsequently attached to an argon line, deoxygenated for 30 minutes prior to photolysis, and is continuously deoxygenated throughout the experiment. Afterward, **32** was added directly to the hexanes solution and the absorbance at 248 nm was checked by a static UV spectrophotometer to ensure  $\Delta A \sim 0.5 - 0.7$ . A low concentration of precursor leads to low signal intensity and consequently loss of resolution and precision. On the other hand, high concentration of precursor causes a non-uniform photoreaction.



The solution was then flowed through the thermostated cell, where it is irradiated with the Kr/F laser pulse leading to photocycloreversion of precursor **32**. The absorption spectra of the resulting solution was then monitored as a function of time for each selected wavelength (commonly 440 nm and 500 nm) which give decay/growth profiles of the transient species in the solution. Each profile is typically the average of 10 or more laser pulses in order to obtain a better signal to noise ratio. Then, the scavengers were added directly to the reservoir by microliter syringes from a previously prepared standard solution of alkene, and decay/growth profiles of the resulting solution were acquired at each concentration of the added alkenes. At the end of experiment, all acquired profiles were kinetically analyzed to give rate/equilibrium constants (Chapter 2). The solution temperature was measured during the experiment with a thermocouple around the flow cell.

Since the establishment of equilibrium between germlyenes and alkenes is measured as an apparent reduction in the optical yield of GePh<sub>2</sub> as a function of alkene concentration, analysis requires that the equilibrium reaction is the only contributor to this, so any trivial contributions to the transient absorbance must be eliminated. These include factors such as variation in the laser intensity and the systematic introduction of absorbing impurities or water during the run. Consequently, the alkenes used in this study were purified and their UV spectra were checked before each laser experiment to ensure the absorbance at 248nm is equal to or lower than hexanes absorbance (see Table 2.1). Figure 5.4 shows an example of the UV-visible spectrum of a stock solution of cyclohexene taken right before a laser experiment, along with the spectrum of hexane (reaction solvent) and unpurified cyclohexene.

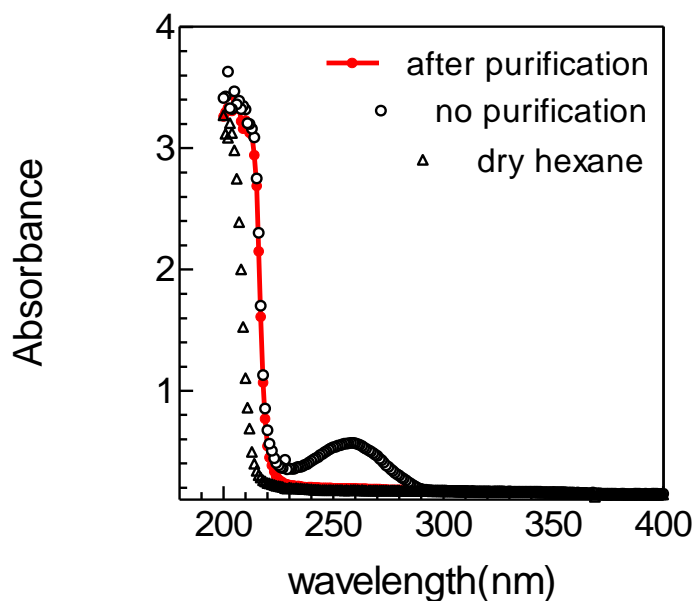


**Figure 5.4.** UV-visible spectrum of a 0.2 M cyclohexene stock solution before and after purification by distillation over maleic anhydride and passing through a silica column.

### 5.3. Steady State Photolysis Experiments.

#### 5.3.1. Chemicals

Cyclohexane- $d_{12}$  (Cambridge Isotope Laboratories), hexamethyldisilane (Gelest, Inc) and 4,4-dimethyl-1-pentene (Sigma-Aldrich) were used as received from the supplier. Acrylonitrile (Sigma-Aldrich) was washed with 5% sulfuric acid solution, 5% sodium carbonate solution, and then distilled from calcium chloride. It was stored at  $-20^{\circ}\text{C}$  in a vial and passed through a micropipette packed with alumina immediately before each experiment. Methanol (HPLC grade, Caledon Reagent) was distilled from a MeONa/MeOH solution immediately prior to the experiment.

### 5.3.2. General Procedure<sup>4</sup>

Steady-state photolysis experiments were carried out using a Rayonet photochemical reactor (Southern New England Ultraviolet Co.) equipped with a merry-go-round and low pressure mercury lamps (254 nm). Solutions were contained in quartz NMR tubes, which were sealed with a septum after transfer of the prepared reaction mixture. The progress of the reaction was monitored by 600 MHz <sup>1</sup>H-NMR spectroscopy. The reaction mixture was prepared in 1 mL of cyclohexane-d<sub>12</sub> as follows: the precursor **32** was added to a volumetric flask containing 1 mL of cyclohexane-d<sub>12</sub> and the flask was sealed with a septum and deoxygenated with a fine stream of dry argon for ca. 10 minutes. Then the purified volatile components (e.g. acrylonitrile or methanol) and ca. 1 μL of Si<sub>2</sub>Me<sub>6</sub> as an internal integration standard were added by microliter syringe to make the final solution. This solution was then transferred to a quartz NMR tube using a 10 μL microsyringe.

### 5.4. References

- (1) Armarego, W. L. F.; Li Lin Chai, C. *Purification of Laboratory Chemicals*; 5 ed.; Butterworth Heinemann, **2003**.
- (2) Kolesnikov, S. P.; Rogozhin, I. S.; Nefedov, O. M. *Akademiia nauk SSSR. Izvestiia. Seriiia khimicheskaiia*. **1974**, 2379.
- (3) Nefedov, O. M.; Kolesnikov, S. P.; Ioffe, A. I. *Akademiia nauk SSSR. Izvestiia. Seriiia khimicheskaiia*. **1976**.
- (4) Leigh, W. J.; Harrington, C. R.; Vargas-Baca, I. *J. Am. Chem. Soc.* **2004**, 126, 16105.
- (5) Mazerolles, P.; Manuel, G. *Bull. Soc. Chim. Fr.* **1965**, 56.
- (6) Brown, P. A.; Bonnert, R. V.; Jenkins, P. R.; Lawrence, N. J.; Selim, M. R. *J. Chem. Soc., Perkin Trans. 1* **1991**, 1893.
- (7) Leigh, W. J.; Lollmahomed, F.; Harrington, C. R. *Organometallics* **2006**, 25, 2055.
- (8) Leigh, W. J.; Harrington, C. R. *J. Am. Chem. Soc.* **2005**, 127, 5084